

Clemson University

TigerPrints

All Dissertations

Dissertations

8-2022

Development of a Reverse Engineered, Parameterized, and Structurally Validated Computational Model to Identify Design Parameters that Influence American Football Faceguard Performance

William Ferriell
wferrie@clemson.edu

Follow this and additional works at: https://tigerprints.clemson.edu/all_dissertations



Part of the [Biomechanical Engineering Commons](#), [Biomechanics and Biotransport Commons](#), [Computer-Aided Engineering and Design Commons](#), and the [Design of Experiments and Sample Surveys Commons](#)

Recommended Citation

Ferriell, William, "Development of a Reverse Engineered, Parameterized, and Structurally Validated Computational Model to Identify Design Parameters that Influence American Football Faceguard Performance" (2022). *All Dissertations*. 3086.

https://tigerprints.clemson.edu/all_dissertations/3086

This Dissertation is brought to you for free and open access by the Dissertations at TigerPrints. It has been accepted for inclusion in All Dissertations by an authorized administrator of TigerPrints. For more information, please contact kokeefe@clemson.edu.

DEVELOPMENT OF A REVERSE ENGINEERED, PARAMETERIZED, AND
STRUCTURALLY VALIDATED COMPUTATIONAL MODEL TO IDENTIFY
DESIGN PARAMETERS THAT INFLUENCE
AMERICAN FOOTBALL FACEGUARD PERFORMANCE

A Dissertation
Presented to
the Graduate School of
Clemson University

In Partial Fulfillment
of the Requirements for the Degree
Doctor of Philosophy
Biomechanical Engineering

by
William Davis Ferriell
August 2022

Accepted by:
Dr. John DesJardins, Committee Co-Chair
Dr. Gregory Batt, Co-Chair
Dr. William Richardson
Dr. Gang Li

ABSTRACT

Traumatic brain injury (TBI) continues to have the greatest incidence among athletes participating in American football. The headgear design research community has focused on developing accurate computational and experimental analysis techniques to better assess the ability of headgear technology to attenuate impacts and protect athletes from TBI. Despite efforts to innovate the headgear system, minimal progress has been made to innovate the faceguard. Although the faceguard is not the primary component of the headgear system that contributes to impact attenuation, faceguard performance metrics, such as weight, structural stiffness, and visual field occlusions, have been linked to athlete safety. To improve upon the understanding of the discrepancies in faceguard performance metrics, this research developed reverse engineered, structurally validated, and parameterized finite element (FE) simulations of common American football faceguards. The reverse engineered, FE simulation validation, and parametric analysis process was repeated for a total of nine common American football faceguards spanning four style categories, four helmet-compatible series, and three equipment manufacturers. The results comparing the faceguard models indicated measured responses—mass and stiffness—varied across faceguard styles and helmet-compatible series.

Additionally, this work developed the Central Visual Field – Occlusion (CVF-O) metric and the Peripheral Visual Field – Occlusion (PVF-O) metric which quantified the amount of occlusion from each faceguard in each of the hypothesized segments of the visual field. The comparison of the nine faceguards modeled indicated a large difference

in faceguard styles and helmet-compatible series; however, the results were not correlated to faceguard style, mass, or structural stiffness.

Leveraging the results from the parametric analysis, an “overbuilt” faceguard was reverse engineered and modeled. The metal wire cross-sections were parameterized as an ellipse, and the mass of the overbuilt faceguard was minimized subject to stress and stiffness constraints. When comparing the models of the original manufacturer’s designs with two materials, the masses and structural stiffnesses were directly proportional to the densities and elastic moduli of the two materials. Both innovating the metal wire cross section and changing material properties have demonstrated the potential to improve upon faceguard performance metrics.

DEDICATION

This work is dedicated to my wife for her love, selflessness, and unwavering support throughout my time at Clemson. Without her, the completion of this work would not have been possible.

ACKNOWLEDGMENTS

There are countless people to thank who have helped me in my education and throughout the completion of this work. First and foremost, I am grateful to my family and friends for supporting me. Their love and encouragement have been invaluable.

I would also like to thank my dissertation advisors, Dr. Gregory Batt and Dr. John DesJardins, and their families for all their support. My advisors have coached me to be a better researcher and educator, and I am very grateful that they have supported my efforts to train as an instructor. I am also very appreciative of the numerous other advisors that have supported me including Dr. Christine Buckley, Dr. Tyler Harvey, and Dr. Marian Kennedy. I am also grateful to have had the guidance of Dr. Martine LaBerge. Each of their mentorship has been a blessing, and I am grateful for their time and wisdom.

I am also very appreciative of each of the lab members that have supported this work. I would like to thank Noah Wright who has been a great friend and colleague since I started my graduate program. Additionally, thanks to the Bioengineering and Food, Nutrition, and Packaging Science Departments for their support.

Thanks to the Engineering and Science Education Department for their support in the certificate program. Thanks to the Clemson Makerspace for their support of the work in the CHIP Lab. Thanks to industry partners Green Gridiron, Schutt Sports, and Zuti Facemasks for their insight and efforts to support the work in the CHIP Lab. Thanks to the Clemson University Major Research Instrumentation program for their funding and support of the work in the CHIP Lab. Thanks to the SPECTRA program, EXPLORE Mobile Lab, and Trident Technical College for their support.

TABLE OF CONTENTS

	Page
TITLE PAGE	i
ABSTRACT.....	ii
DEDICATION	iv
ACKNOWLEDGMENTS	v
LIST OF TABLES	viii
LIST OF FIGURES	x
LIST OF EQUATIONS	xii
CHAPTER	
I. INTRODUCTION	1
References	3
II. FINITE ELEMENT VALIDATION OF 3D AMERICAN FOOTBALL FACEGUARD STRUCTURAL STIFFNESS MODELS	8
Introduction.....	8
Methods.....	11
Results.....	20
Discussion	22
Conclusion	29
References.....	30
III. PARAMETRIC DESIGN METHODS DEVELOPMENT FOR THE COMPARISON OF AMERICAN FOOTBALL FACEGUARDS USING VALIDATED STRUCTURAL STIFFNESS MODELS.....	34
Introduction.....	34
Methods.....	38
Results.....	45
Discussion	49
Conclusion	52

Table of Contents (Continued)	Page
References	52
IV. COMPARISON OF PARAMETER EFFECT ON PERFORMANCE RESPONSES IN AMERICAN FOOTBALL FACEGUARD MODELS ...	56
Introduction.....	56
Methods.....	59
Results.....	66
Discussion	71
Conclusion	75
References.....	76
V. ANALYSIS OF PARAMETRIC DESIGN METHODS TO AFFECT PERFORMANCE RESPONSES IN VALIDATED AMERICAN FOOTBALL FACEGUARD STRUCTURAL STIFFNESS MODELS	80
Introduction.....	80
Methods.....	83
Results.....	88
Discussion	94
Conclusion	97
References.....	98
VI. CONCLUSION.....	101
Summary	101
Future Work	103
APPENDICES	106
A: Riddell SpeedFlex SF-2BD-SW Results	107
B: Riddell SpeedFlex SF-2BD Results.....	109
C: Riddell SpeedFlex SF-3BD Results.....	111
D: Schutt Q11 ROPO-SW Results.....	113
E: Schutt F7 ROPO-SW-NB-VC Results.....	115
F: Schutt F7 ROPO-NB-VC Results.....	117
G: Vicis Zero1 SO-212-LP Results	119
H: Vicis Zero1 SO-213-E-LP Results.....	121
I: Vicis Zero1 SO-223-LP Results	123
J: Visibility Calculations Documentation.....	125

LIST OF TABLES

Table	Page
2.1 Mesh metrics for each faceguard style.....	15
2.2 Summarized boundary conditions applied to the model. Boundary condition titles and corresponding letters are annotated in Figs. 2.4-2.6.....	17
2.3 Constraint reaction magnitudes recorded at the “Nose” position for each faceguard.....	22
3.1 Categories for the SpeedFlex Helmet-compatible faceguards.....	40
3.2 Parameter names and initial values for the SF-2BD-SW, ROPO-SW, and SF-2BD faceguard styles	41
3.3 Comparison of the correlations between mass and structural stiffness responses for each of the faceguards	46
3.4 Comparison of the correlations between large diameter parameter and the structural stiffness response for each of the faceguards.....	46
3.5 Comparison of the correlations between the large diameter parameter and the mass response for each of the faceguards	46
3.6 Summary of results specifying the three parameters for each faceguard that contributed most to the structural stiffness	47
3.7 Percent changes from maximum response to minimum response for viable designs from each faceguard.....	47
3.8 Comparison of two viable designs with similar Structural Stiffnesses and different masses	48
3.9 Comparison of two viable designs with similar masses and different Structural Stiffnesses	49
4.1 Faceguards analyzed in this study with respective manufacturers and compatible helmets	61
4.2 Correlations between Structural Stiffness and the larger diameter parameter from results of the design of experiments for each faceguard style	70

List of Tables (Continued)

Table	Page
5.1 The parameter values for the baseline reverse engineered model and the bounds on the parameters used in the optimization approach	86
5.2 Comparison of two viable designs to the original reverse engineered model of the BrickhouZe faceguard.....	90

LIST OF FIGURES

Figure	Page
2.1 The SF-3BD faceguard model in the coronal plane.....	14
2.2 The SF-3BD faceguard model in the sagittal plane rotated at 0° (Nose), 20° (Mouth), and 30° (Chin) with corresponding compression locations....	14
2.3 The SF-3BD mesh with 1.5 mm element size assigned for the entire body.	16
2.4 Annotated SF-3BD model in the coronal plane detailing boundary conditions and the geometry on which each was applied for the “Nose” compression location.....	18
2.5 Detail from Fig. 2.4 of the annotated SF-3BD model detailing midline (A) and prescribed compression (C) boundary conditions with the geometry on which each was applied for the “Nose” compression location	18
2.6 Annotated SF-3BD model in the sagittal plane detailing boundary conditions with the geometry on which each was applied for the “Nose” compression location.....	19
2.7 Linear regression model detailing statistically significant correlation between experimental and computational stiffness. Note: Error bars represent a single experimental standard deviation.....	20
2.8 Bar chart comparison of computational results and experimental averages with standard deviations.....	21
3.1 The design space—outlined by the dashed line—superimposed on the Riddell SpeedFlex-compatible (Left) and Schutt Q11-compatible (Right) faceguard frame	39
3.2 Framework summarizing approach to verifying the models used for parametric analyses in this study	43
3.3 All viable designs plotted to compare two responses: Mass and Structural Stiffness for the SF-2BD faceguard experiment	48
4.1 The manufacturers, faceguard models, and compatible helmet (in parentheses) analyzed in this study	60

List of Figures (Continued)

Figure	Page
4.2 (a) Median plane view of a football helmet with the inferior-superior central visual field boundaries overlayed, (b) Transverse plane view of a football helmet with the medial-lateral central, peripheral, and far peripheral visual field boundaries overlayed.....	63
4.3 Comparison of mass and structural stiffness responses from the models of the original manufacturer's designs	67
4.4 Comparison of the CVF-O metric and the PVF-O metric for the original manufacturer's designs.	68
4.5 Percent changes from maximum responses of viable designs for each faceguard.....	69
5.1 Reverse engineered model of the BrickhouZe faceguard manufactured by Zuti Facemasks	84
5.2 Evolution of designs from the minimization approach used in this study demonstrating the decrease in mass	89
5.3 Evolution of designs from the minimization approach used in this study demonstrating the decrease in structural stiffness converging around the minimum stiffness constraint (70 N/mm)	90
5.4 Mass and stiffness responses for two viable BrickhouZe designs plotted against results previously reported of original reverse engineered models of manufacturer's designs	91
5.5 Mass and structural stiffness responses for two viable BrickhouZe designs plotted against a gray diagonally striped field representing the ranges for mass and structural stiffness of the legal faceguards analyzed previously in Chapter 4	92
5.6 Mass responses comparing two materials (stainless steel and titanium alloy) for faceguard models previously reported and the BrickhouZe overbuilt faceguard.....	93
5.7 Structural stiffness responses comparing two materials (stainless steel and titanium alloy) for faceguard models previously reported and the BrickhouZe overbuilt faceguard	93

LIST OF EQUATIONS

Equation	Page
4.1 The Central Visual Field Occlusion (CVF-O) Metric	64
4.2 Vertical angle of occlusion	64
4.3 Horizontal angle of occlusion within the central visual field	64
4.4 Distance from approximate location of the eyes to the superior occlusion within the Central Visual Field by the faceguard as a function of parameters	64
4.5 Distance from approximate location of the eyes to the lateral occlusion within the Central Visual Field by the faceguard as a function of parameters .	64
4.6 Distance from approximate location of the eyes to the anterior occlusion within the Central Visual Field by the faceguard as a function of parameters	64
4.7 The Peripheral Visual Field Occlusion (PVF-O) Metric	65
4.8 Vertical occlusion in the periphery as a function of parameters.....	65
4.9 Vertical occlusion of eye guards as a function of parameters	65
5.1 Mass minimization function of input parameters	86
5.2 Structural stiffness constraint.....	86
5.3 Stress constraint	86
5.4 Row vector of major axis parameters	86
5.5 Row vector of minor axis parameters	86
5.6 Row vector of angle parameters measured from a reference position.....	86

CHAPTER ONE

INTRODUCTION

Of all youth sports, American football remains one of the most popular; however, participation has been declining precipitously in recent years [1-5]. It is possible that increased awareness of traumatic brain injury and risks associated with contact sports—football, in particular—have led to decreased participation. The immediate risks of traumatic brain injury are well understood; however, the long-term effects from repetitive impacts are not as clear [6]. Research has shown long-term effects of repetitive, low-severity impacts may lead to dementia, personality changes, and Alzheimer's later in life [7-12]. In recent years, research has improved the community's understanding of the pathophysiology of traumatic brain injury [13-16]. This has led to more appropriate impact reconstructions in the laboratory which has resulted in improved headgear designs and methods for headgear analysis [13, 17-22].

Despite recent innovations to the helmet shell and headgear system, the faceguard has not been subjected to similar degrees of scrutiny. Although each new helmet system has its own compatible faceguard series, the primary design components have changed little between helmet systems [23]. As advancements in manufacturing technologies, like investment casting, are developed, the parameters that affect faceguard design performance should be better understood.

Computational methods, particularly finite element analysis, have been widely used to evaluate headgear performance and inform headgear design in many industries [24-28], particularly in American football [23, 29-34]. To inform the community of

faceguard design variables pertinent to athlete performance and safety, parameterized computational models should be developed to iterate between design variables while assessing faceguard performance metrics for improved design.

In Chapter 2, the reverse engineering and computational method for structurally validating three American football faceguards is detailed. Experimental data from a structural stiffness test on a materials testing machine [35] is used to validate the finite element simulation. Percent difference, statistically significant correlation, and a linear regression model are used to evaluate the reverse engineered models for validation.

In Chapter 3, the structural validation of the reverse engineered models and finite element simulations are leveraged to detail the parameterization of three American football faceguards. The design of experiments and parameter definitions are discussed, and the correlation between input parameters is used to evaluate the performance of the design of experiments. The responses are used to inform modelling and parameterization approaches employed in future chapters.

In Chapter 4, the reverse engineering, finite element modelling, and parametric analyses are repeated for nine total faceguards spanning four faceguard categories across four helmet-compatible series and three headgear manufacturers. In addition to the structural stiffness and mass responses investigated in previous chapters, three visibility metrics are proposed as important responses to evaluate for athlete safety and performance. The models of the original manufacturer's designs are used to compare the responses of the legal faceguards currently in use. Additionally, the parametric analyses are used to identify the parameters that influence faceguard performance responses.

In Chapter 5, a critical approach to the blanket ban of overbuilt faceguards utilizes the results from Chapter 4 to inform a focused parametric analysis of an overbuilt faceguard. The cross sections of the heavier and stiffer faceguards are parametrized as an ellipse and a mass minimization approach is employed using the validated structural stiffness finite element simulation. To evaluate the blanket ban of overbuilt faceguards, the results from the model of the original manufacturer's design are compared to legal faceguards currently in use. Additionally, two viable designs resulting from the mass minimization approach employed are compared to the ranges of structural stiffness and mass of the faceguard models investigated in Chapter 4. Lastly, the material assumed in the validated simulations is altered for each of the nine faceguards analyzed in Chapter 4. These results are compared to the overbuilt faceguard model with the same materials to elucidate the degree to which material can affect mass and stiffness responses.

Collectively, these studies will inform the American football headgear design community of modelling methods that can be used to affect faceguard performance responses that may improve athlete safety and performance. The summary of results is detailed in Chapter 6 along with suggestions for future work.

References

- [1] The National Federation of State High School Associations, "2018-19 High School Athletics Participation Survey," 2019. [Online]. Available: <https://www.nfhs.org/sports-resource-content/high-school-participation-survey-archive/>. [Accessed 21 February 2020].
- [2] The National Federation of State High School Associations, "2017-18 High School Athletics Participation Survey," 2018. [Online]. Available: <http://www.nfhs.org/ParticipationStatistics/PDF/2017-18%20High%20School%20Athletics%20Participation%20Survey.pdf>. [Accessed 23 10 2018].

- [3] The National Federation of State High School Associations, "2016-17 High School Participation Survey," 2017. [Online]. Available: <https://www.nfhs.org/sports-resource-content/high-school-participation-survey-archive/>. [Accessed 21 February 2020].
- [4] The National Federation of State High School Associations, "2015-16 High School Athletics Participation Survey," 2016. [Online]. Available: <https://www.nfhs.org/sports-resource-content/high-school-participation-survey-archive/>. [Accessed 21 February 2020].
- [5] The National Federation of State High School Associations, "High School Athletics Participation Survey (1969-2008)," 2000. [Online]. Available: <https://www.nfhs.org/sports-resource-content/high-school-participation-survey-archive/>. [Accessed 21 February 2020].
- [6] G. Martin, "Acute Brain Trauma," *Annals of The Royal College of Surgeons of England*, vol. 98, no. 1, pp. 6-10, 2016.
- [7] S. M. Gysland, J. P. Mihalik, J. K. Register-Mihalik, S. C. Trulock, E. W. Shields and K. M. Guskiewicz, "The Relationship Between Subconcussive Impacts and Concussion History on clinical Measures of Neurologic Function in Collegiate Football Players," *Annals of Biomedical Engineering*, vol. 40, no. 1, pp. 14-22, 2012.
- [8] N. Sayed, C. Culver, K. Darns-O'Connor, F. Hammond and R. Diaz-Arrastia, "Clinical Phenotype of Dementia after Traumatic Brain Injury," *Journal of Neurotrauma*, vol. 30, pp. 1117-1122, 2013.
- [9] A. A. Hirad, J. J. Bazarian, K. Merchant-Borna, F. E. Garcea, S. Heilbronner, D. Paul, E. B. Hintz, E. v. Wijngarnden, G. Schifitto, D. W. Wright, T. R. Espinoza and B. Z. Mahon, "A common neural signature of brain injury in concussion and subconcussion," *Science Advances*, vol. 5, pp. 1-11, 2019.
- [10] A. C. McKee, R. C. Cantu, C. J. Nowinski, T. Hedley-Whyte, B. E. Gavett, A. E. Budson, V. E. Santini, H.-S. Lee, C. A. Kubilus and R. A. Stern, "Chronic Traumatic Encephalopathy in Athletes: Progressive Tauopathy After Repetitive Head Injury," *Journal of Neuropathology and Experimental Neurology*, vol. 68, no. 7, pp. 709-735, 2009.
- [11] P. H. Montenegro, M. L. Alosco, B. M. Martin, D. H. Daneshvar, J. Mez, C. E. Chaisson, C. J. Nowinski, R. Au, A. C. McKee, R. C. Canut, M. D. McClean, R. A. Stern and Y. Tripodis, "Cumulative Head Impact Exposure Predicts Later-Life Depression, Apathy, Executive Dysfunction, and Cognitive Impairment in Former High School and College Football Players," *Journal of Neurotrauma*, vol. 34, pp. 228-340, 2017.

- [12] T. M. Talavage, E. A. Nauman, E. L. Breedlove, U. Yoruk, A. E. Dye, K. E. Morigaki, H. Feuer and L. J. Leverenz, "Functionally-Detected Cognitive Impairment in High School Football Players without Clinically-Diagnosed Concussion," *Journal of Neurotrauma*, vol. 31, pp. 327-338, 2014.
- [13] S. T. DeKosky, M. D. Ikonovic and S. Gandy, "Traumatic Brain Injury--Football, Warfare, and Long-Term Effects," *The New England Journal of Medicine*, vol. 363, no. 14, pp. 1293-1296, 2010.
- [14] T. L. Spires-Jones, W. H. Stoothoff, A. d. Calignon, P. B. Jones and B. T. Hyman, "Tau Pathophysiology in Neurodegeneration: A tangled Issue," *Trends in Neurosciences*, vol. 32, no. 3, pp. 150-159, 2009.
- [15] R. J. Castellani and G. Perry, "Tau Biology, Tauopathy, Traumatic Brain Injury, and Diagnostic Challenges," *Journal of Alzheimer's Disease*, vol. 67, pp. 447-467, 2019.
- [16] M. Prins, T. Greco, D. Alexander and C. C. Giza, "The pathophysiology of traumatic brain injury at a glance," *Disease Models and Mechanisms*, vol. 6, pp. 1307-1315, 2013.
- [17] V. Ivancevic, "New Mechanics of Traumatic Brain Injury," *Cognitive Neurodynamics*, vol. 3, pp. 281-293, 2009.
- [18] H. Kimpara and M. Iwamoto, "Mild Traumatic Brain Injury Predictors Based on Angular Accelerations During Impacts," *Annals of Biomedical Engineering*, vol. 40, no. 1, pp. 114-126, 2012.
- [19] A. M. Bailey, E. J. Sanchez, G. Park, L. F. Gabler, J. R. Funk, J. R. Crandall, M. Wonnacott, C. Withnall, B. S. Myers and K. B. Arbogast, "Development and Evaluation of a Test Method for Assessing the Performance of American Football Helmets," *Annals of Biomedical Engineering*, vol. 48, no. 11, pp. 2566-2579, 2020.
- [20] L. F. Gabler, J. R. Crandall and M. B. Panzer, "Development of a Second-Order System for Rapid Estimation of Maximum Brain Strain," *Annals of Biomedical Engineering*, vol. 47, no. 9, pp. 1971-1981, 2019.
- [21] National Football League, "The NFL Engineering Roadmap," in *Head Health Tech Challenge Symposium*, Youngstown, OH, 2019.
- [22] National Football League, "The NFL Helmet Challenge," in *HeadHealthTech Challenge Symposium*, Youngstown, OH, 2019.

- [23] K. L. Johnson, S. Chowdhury, W. B. Lawrimore, Y. Mao, A. Mehmani, R. Prabhu, G. Rush and M. F. Horstemeyer, "Constrained Topological Optimization of a Football Helmet Facemask based on Brain Response," *Materials and Design*, vol. 111, pp. 108-118, 2016.
- [24] N. J. Mills and A. Gilchrist, "Finite-element analysis of bicycle helmet oblique impacts," *International Journal of Impact Engineering*, vol. 35, pp. 1087-1101, 2008.
- [25] M. A. Forero Rueda, L. Cui and M. D. Gilchrist, "Finite element modelling of equestrian helmet impacts exposes the need to address rotational kinematics in future helmet designs," *Computer Methods in Biomechanics and Biomedical Engineering*, vol. 14, no. 12, pp. 1021-1031, 2011.
- [26] L. B. Tan, K. M. Tse, H. P. Lee, V. B. C. Tan and S. P. Lim, "Performance of an advanced combat helmet with different interior cushioning systems in ballistic impact: Experiments and finite element simulations," *International Journal of Impact Engineering*, vol. 50, pp. 99-112, 2012.
- [27] F. M. Shuaeib, A. M. S. Hamouda, S. V. Wong, R. S. Radin Umar and M. M. H. Megat Ahmed, "A new motorcycle helmet liner material: The finite element simulation and design of experiment optimization," *Materials and Design*, vol. 28, pp. 182-195, 2007.
- [28] P. Schwizer, M. Demierre and L. V. Smith, "An experimental and numerical study of softball to facemask impacts," *Journal of Sports Engineering and Technology*, vol. 23, no. 4, pp. 336-343, 2017.
- [29] J. G. Beckwith, W. Zhao, S. Ji, A. G. Ajamil, R. P. Bolander, J. J. Chu, T. W. McAllister, J. J. Crisco, S. M. Duma, S. Rowson, S. P. Broglio, K. M. Guskiewicz, J. P. Mihalik, S. Anderson, B. Schnebel, P. G. Brolinson, M. W. Collins and R. M. Greenwald, "Estimated Brain Tissue Response Following Impacts Associated with and without Diagnosed Concussion," *Annals of Biomedical Engineering*, vol. 46, no. 6, pp. 819-830, 2018.
- [30] F. Hernandez, L. C. Wu, M. C. Yip, K. Laksari, A. R. Hoffman, J. R. Lopez, G. A. Grant, S. Kleiven and D. B. Camarillo, "Six Degree-of-Freedom Measurements of Human Mild Traumatic Brain Injury," *Annals of Biomedical Engineering*, vol. 43, no. 8, pp. 1918-1934, 2015.
- [31] L. E. Miller, J. E. Urban, M. E. Kelley, A. K. Powers, C. T. Whitlow, J. A. Maldjian, S. Rowson and J. D. Stitzel, "Evaluation of Brain Response during Head Impact in Youth Athletes Using an Anatomically Accurate Finite Element Model," *Journal of Neurotrauma*, vol. 36, pp. 1561-1570, 2019.

- [32] M. A. Corrales, D. Gierczycka, J. Barker, D. Bruneau, M. C. Bustamante and D. S. Cronin, "Validation of a Football Helmet Finite Element Model and Quantification of Impact Energy Distribution," *Annals of Biomedical Engineering*, vol. 48, no. 1, pp. 121-132, 2020.
- [33] W. Decker, A. Baker, X. Ye, P. Brown, J. Stitzel and F. S. Gayzik, "Development and Multi-Scale Validation of a Finite Element Football Helmet Model," *Annals of Biomedical Engineering*, vol. 48, no. 1, pp. 258-270, 2020.
- [34] D. C. Viano, I. R. Casson, E. J. Pellman, L. Zhang, A. I. King and K. H. Yang, "Concussion in Professional Football: Brain Responses by Finite Element Analysis: Part 9," *Neurosurgery*, vol. 57, no. 5, pp. 891-916, 2005.
- [35] A. Bina, G. S. Batt and J. DesJardins, "Development of a Non-destructive Method to Measure Football Facemask Stiffness," *Journal of Sports Engineering and Technology*, vol. 233, no. 2, pp. 175-185, 2019.

CHAPTER TWO

FINITE ELEMENT VALIDATION OF 3D AMERICAN FOOTBALL FACEGUARD STRUCTURAL STIFFNESS MODELS

Introduction

American football has an enduring role in the culture of the United States of America. Of all youth sports, football remains one of the most popular; however, participation has been decreasing by tens of thousands in each of the past four years, with 2019 totaling the least participation since 1999-2000 [1-5]. One reason for this decrease might be as a result of the heightened media attention and growing awareness of traumatic brain injury and the risks associated with participating in contact sports, specifically football. The challenges parents, players, coaches, and healthcare professionals face in weighing the benefits and risks of playing football cannot be overstated [6, 7]. Although the immediate risks of concussion are well understood [8], the long-term effects from repetitive impacts are not as clear. Research shows repetitive, sub-concussive impacts may lead to conditions such as dementia, personality changes, and Alzheimer's that develop later in life [9-14]. In recent years, our understanding of the pathophysiology of traumatic brain injury has improved [15-18]; however, the challenge remains on how to translate this new information into rule changes and improved outcomes for athletes [15].

In the laboratory setting, research findings have improved headgear performance analysis. For example, it has been found that rotational accelerations applied to the head (or headform) more closely correlate to concussion and diffuse axonal injury than linear

accelerations [15, 19, 20]. The Helmet Performance Score (HPS), a summation of the Head Acceleration Response Metric (HARM) results from 18 impacts, was recently developed for the National Football League (NFL) Helmet Challenge. This metric weights rotational accelerations from the Diffuse Axonal Multiaxial General Evaluation (DAMAGE) score more heavily than linear accelerations from the Head Injury Criterion (HIC) score, which allows headgear design researchers a better standard for assessing equipment, thus allowing more information to be shared with the community regarding headgear performance [21, 22]. Although companies like Vicis (Seattle, WA) and HitGard (Asheville, NC) have innovated helmet structure to improve performance, minimal quantitatively informed changes have been made to overall headgear design. Despite continued efforts from programs like the NFL HeadHealth Tech Challenge and other groups devoted to improving headgear technology, only minor improvements have been made to laboratory injury metrics [23, 24].

The lack of design innovation in headgear is especially true for structural changes to the faceguard design in the past 20 years [25]. Although each new helmet system has its own compatible faceguard series, the primary design components have changed little between helmet systems. Furthermore, little is known about how individual faceguards structurally perform with respect to each other or in the absence of a helmet. It has been shown that the inclusion of the faceguard changes measured helmet values, such as HIC and Severity Index, when impacted using the National Operating Committee on Standards for Athletic Equipment (NOCSAE) drop tower [24], but results were inconclusive when using a linear impactor [26]. Although it is well documented that the

faceguard will stiffen the structure of the overall headgear system [24, 26], a problem arises when attempting to assess the performance contributions of individual faceguards using current laboratory measurement devices. The main problem is the lack of control for testing. The effect of variation in helmet placement, chin strap placement, and strap tension, for example, can compound greatly. This affects the ability of researchers to assess differences in faceguards based upon performance within the entire helmet system.

Recently, a novel testing procedure was developed to analyze the structural stiffness of faceguards independent of the helmet system [27]. This testing methodology has demonstrated the ability to statistically differentiate performance-relevant stiffness measures between faceguard designs. Faceguard stiffness is a result of its material and geometry; however, little is known about which specific design parameters most influence faceguard structural stiffness. As companies like Zuti Facemasks (Mayfield Athletics, Shelby Township, MI) use advancements in additive manufacturing technologies to develop increasingly complex faceguard designs, the parameters that influence faceguard structural stiffness and performance should be better understood.

To inform the community of faceguard design variables pertinent to structural performance, parameterized computational models should be developed to iterate between design variables while assessing faceguard performance for improved structural design. Initial work performed by Johnson et al. sought to assess the topology of faceguards within the entire helmet system [25], stressing the importance of simulation-based analysis and illustrating the usefulness of computational models to improve faceguard performance. Furthermore, the headgear design community has embraced

computational modeling and parametric analysis for improving design. Specifically, the presenters at the 2019 NFL Head Health Tech Challenge Symposium held in Youngstown, Ohio stressed the importance of utilizing computational analyses to elucidate design variables and combinations of design variables to achieve preferred headgear performance [22].

The goal of this study is two-fold: to validate the reverse engineering method for developing a library of validated faceguard models; and to validate the finite element simulation of three common American football faceguards subject to a quasi-static structural stiffness test [27]. This study will result in a validated method for model generation and validated models to be used in parametric design analysis and computational optimization. Collectively, these new tools can be used to conduct further work that will assist football athletes, coaches, parents, equipment managers, and headgear manufacturers in the understanding of design variables essential to faceguard performance.

Methods

In the experiment described by Bina et al., ten faceguard specimens in each of 17 faceguard styles were assessed for compressive stiffness using a materials testing system and custom-fabricated alignment platform. In the study, the faceguards were held at the clip attachment location using the alignment platform. The platen compressed each faceguard at a rate of 100 mm/sec in three orientations: nose, mouth, and chin. Displacement and force were monitored to determine structural stiffness, and the elastic and plastic regions of the facemask deformation were determined. The study had three

major findings: the test method was non-destructive at 5 mm of vertical compression, the test method could quantify differences in faceguard structural stiffness, and the test method was consistent as determined by the low coefficient of variation for each faceguard style. Of the 17 faceguard styles, three common Riddell® (Des Plaines, IL) SpeedFlex™ faceguard styles were selected to validate the computational model. The SF-2BD-SW, SF-2BD, and SF-3BD faceguard styles were selected for model validation because the experimental results for each faceguard style were available; they are commonly used at all levels of football; they span a range of stiffness values reported by Bina et al.; and they have a theoretically preferred lower stiffness for impact attenuation [27]. These reasons are important to prove that advancements can be made to already well-performing faceguards currently used in most leagues, and that the modelling methodology is validated across a range of stiffness values to be applied to other faceguards. Prior to testing, each faceguard was reconditioned according to NOCSAE standards [28], which included a structural inspection and re-coating with polyethylene powder. One faceguard specimen of each of the three faceguard styles was modeled as discussed below.

To develop accurate faceguard models, a reverse-engineering approach was used. According to a novel protocol similar to that found in the literature [29], each faceguard was imaged using an Eva 3D handheld scanner (Artec, Santa Clara, CA), which has a 3D point accuracy of 0.1 mm. A 3D model was developed from the scanned images in Artec Studio Professional and visually inspected to ensure sufficient geometry was captured.

The final image was then exported to SOLIDWORKS® (Dassault Systèmes SolidWorks Corporation, Waltham, MA) software in .stl file format.

Within the SOLIDWORKS software, a 3D point-cloud was manually developed to capture pertinent design geometry. Each point was inspected to ensure the points had been placed in the center of the bar at each pertinent design location. Through an iterative process, geometrically accurate models were developed using 50-70 points at pertinent design locations, defined as junctions, bends, and arcs. The weld geometry and polyethylene coating were not included in the models. From this point-cloud, a parameterized 3D model was developed.

To simulate the compression locations and directions described in the study by Bina et al., custom coordinate systems were used. A coordinate system was created for each faceguard at the “Nose” compression location to correspond to the anatomical planes of the body. In Figs. 2.1 and 2.2 below, the xy, yz, and xz planes correspond to the coronal, midsagittal, and transverse planes, respectively. Furthermore, each plane is rotated 20° and 30° about the x-axis for the “Mouth” and “Chin” compression locations, respectively, in accordance with the experimental protocol. Figure 2.2 illustrates this transformation for each compression location.

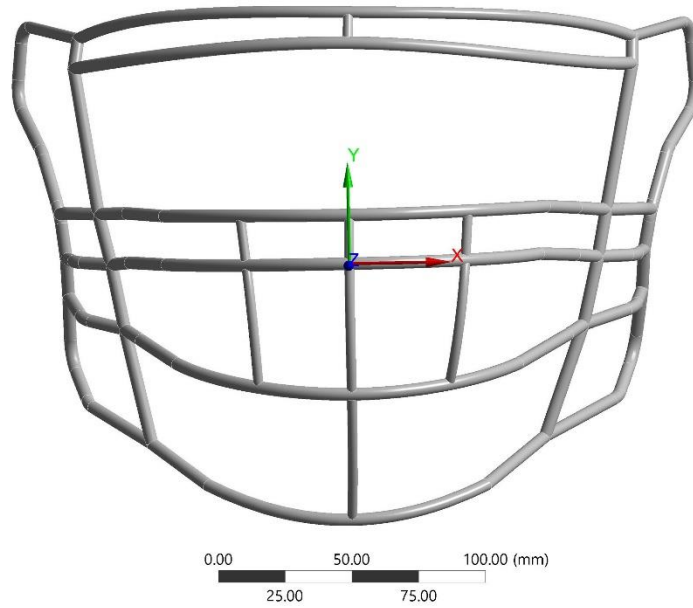


Figure 2.1. The SF-3BD faceguard model in the coronal plane.

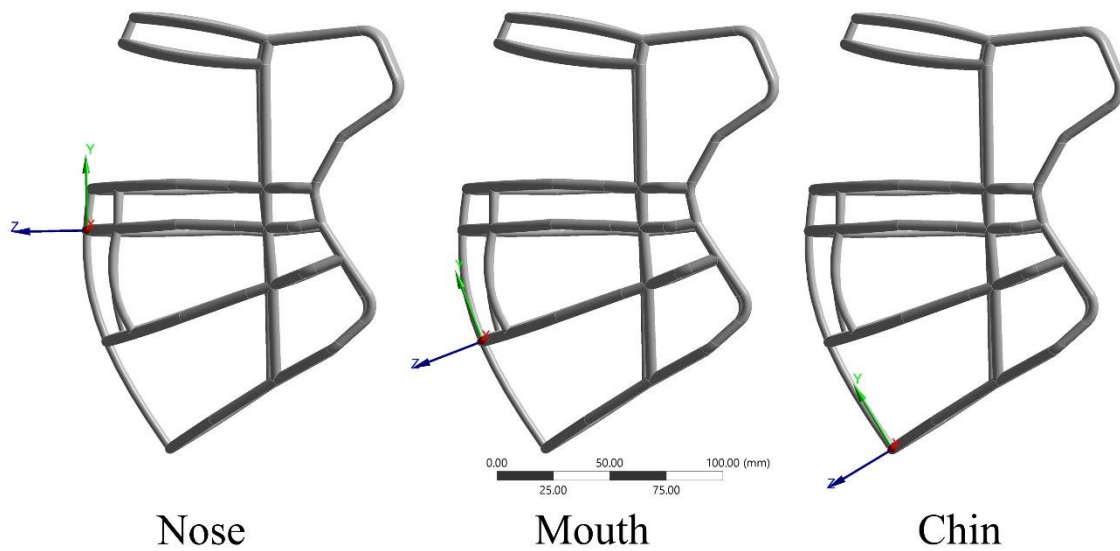


Figure 2.2. The SF-3BD faceguard model in the sagittal plane rotated at 0° (Nose), 20° (Mouth), and 30° (Chin) with corresponding compression locations.

The model was exported into ANSYS® Workbench™ 17.2 (ANSYS, Inc., Canonsburg, PA) using static structural analysis. Each imported faceguard was opened in ANSYS DesignModeler™ (ANSYS, Inc., Canonsburg, PA) and manipulated using planes from the custom coordinate systems discussed above and the slice tool to accommodate boundary and loading conditions.

The standard Riddell SpeedFlex faceguard is a proprietary high strength steel [30]. Some faceguards are made of a low carbon steel [25], while others are made from stainless steel. Therefore, the SpeedFlex faceguards were estimated to have an elastic modulus (E) between 189 GPa - 215 GPa. These values encompass the low-range of stainless steel and the high-range of low carbon steel for elastic moduli found in the literature [31]. Thus, an isotropic general stainless steel from Workbench (E=193 GPa, Poisson's ratio=0.31) was used to approximate the material properties of the faceguard.

To improve the ability of each element to accurately simulate the rounded surface, each faceguard was meshed with quadratic tetrahedral elements. A standard mesh control sizing of 1.5 mm was used for all faceguards. This resulted in a mesh convergence of 0.2% or less, compared to 2 mm sizing control, and a reasonable computational time for parametric analysis. The mesh elements, nodes, and element aspect ratios are detailed in Table 2.1. The SF-3BD faceguard mesh used for analyses is shown in Fig. 2.3.

Table 2.1. Mesh metrics for each faceguard style.

Faceguard	No. of Nodes	No. of Elements	Average Aspect Ratio	Aspect Ratio Standard Deviation
SF-2BD-SW	153381	90959	1.89	0.52
SF-2BD	181953	107553	1.89	0.52
SF-3BD	197236	116162	1.90	0.54

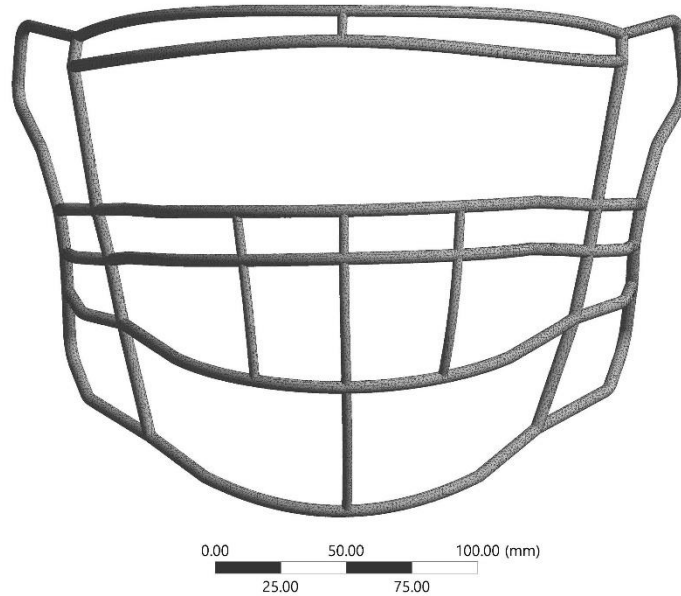


Figure 2.3. The SF-3BD mesh with 1.5 mm element size assigned for the entire body.

The quasi-static structural stiffness test, described by Bina et al., was simulated in ANSYS Mechanical™ (ANSYS, Inc., Canonsburg, PA). The experimental test compresses faceguards 5 mm at a rate of 100 mm/min. To simulate these conditions, the analysis was prescribed to take place over a singular step lasting 3 seconds. A displacement of 5 mm was prescribed in the posterior (z) direction to an edge consistent with the contact location from the experimental protocol. The exact displacement was taken from raw experimental data and is summarized in Table 2.2. The experimental test allows for coronal plane translation of the Clip (B, B') geometry; thus, the corresponding geometry and boundary conditions, Table 2.2, were applied as shown in Figs. 2.4-2.6. To prevent rigid body motion, two boundary conditions were applied: the midline face (annotated A in Figs. 2.4 and 2.5) was constrained to the midsagittal plane and program

controlled weak springs were applied to the entire model. Although these constraints were not prescribed in the experiment, it was assumed they would not affect the computational stiffness of the faceguard significantly. To assess this assumption, constraint reaction force and moment magnitudes were used to ensure each additional boundary condition did not significantly stiffen the faceguard model.

Table 2.2. Summarized boundary conditions applied to the model. Boundary condition titles and corresponding letters are annotated in Figs. 2.4-2.6.

	Mask	Boundary Condition				
		Midline (A)		Clip (B, B')		Prescribed Compression (C)
Anatomical Directions	SF-2BD-SW	Linear	Rotation	Linear	Rotation	Linear
	Lateral/Medial	0	Free	Free	0°	Free
	Superior/Inferior	Free	0°	Free	Free	Free
	Anterior/Posterior	Free	0°	0	0°	5.042 mm
	SF-2BD					
	Lateral/Medial	0	Free	Free	0°	Free
Anatomical Directions	Superior/Inferior	Free	Free	Free	Free	Free
	Anterior/Posterior	Free	0°	0	0°	5.043 mm
	SF-3BD					
	Lateral/Medial	0	Free	Free	0°	Free
	Superior/Inferior	Free	Free	Free	Free	Free
	Anterior/Posterior	Free	0°	0	0°	5.043 mm

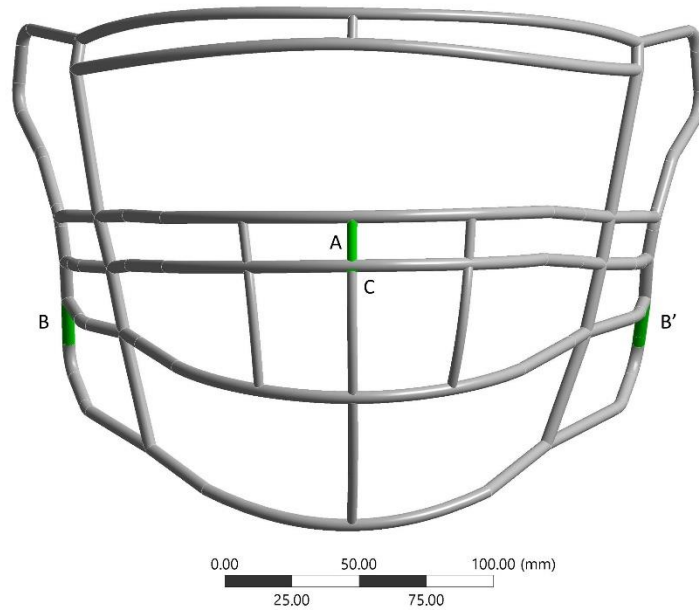


Figure 2.4. Annotated SF-3BD model in the coronal plane detailing boundary conditions and the geometry on which each was applied for the “Nose” compression location.

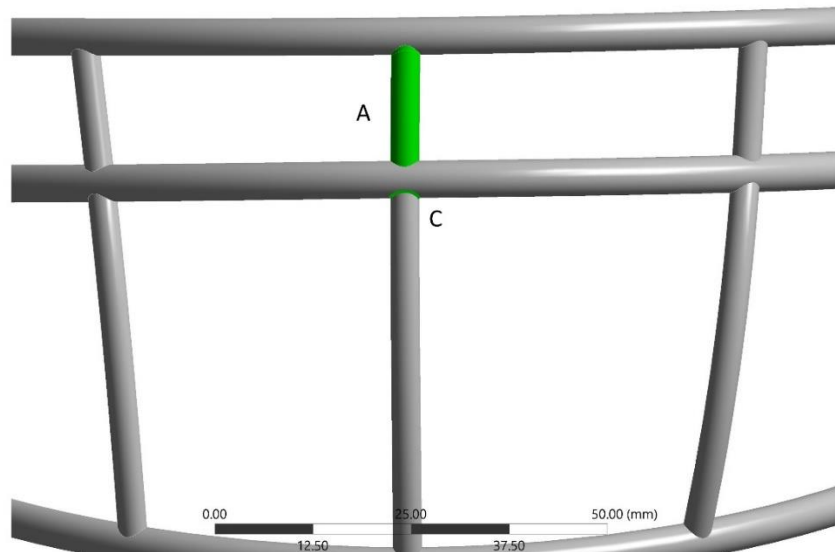


Figure 2.5. Detail from Fig. 2.4 of the annotated SF-3BD model detailing midline (A) and prescribed compression (C) boundary conditions with the geometry on which each was applied for the “Nose” compression location.

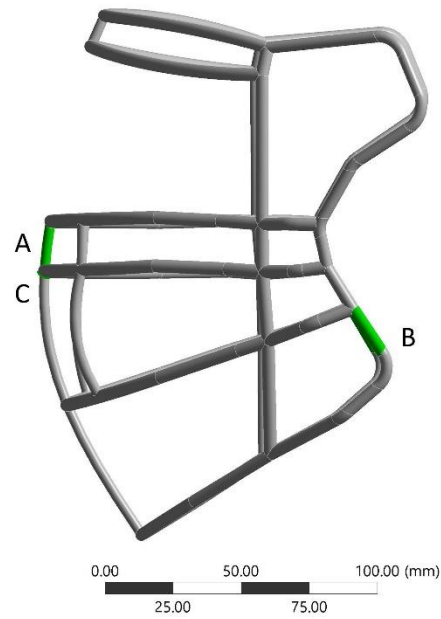


Figure 2.6. Annotated SF-3BD model in the sagittal plane detailing boundary conditions with the geometry on which each was applied for the “Nose” compression location.

To calculate stiffness of the faceguard, the force reaction from the prescribed 5 mm displacement constraint was divided by the displacement. This stiffness value was then compared to the experimental averages and standard deviations from the work by Bina et al. The experimental results from Bina et al. were obtained by permission of the author and used for comparison with the computational models. Validation was determined using a Pearson Correlation test with a 95% confidence interval ($\alpha=0.05$). A linear regression model was used to further assess the correlation of the experimental and computational data. The slope, representing the ratio of computational to experimental results, was analyzed for proximity to one. The y-intercept, representing an offset in stiffness between computational and experimental results, was analyzed for proximity to zero.

Results

The computational results correlate to the experimental results with statistical significance (p-value=0.001). The Pearson's Correlation coefficient of 0.912 demonstrates an acceptable degree of correlation to indicate model validation. Furthermore, a linear regression model, shown in Fig. 2.7, illustrates the near 1:1 comparison between computational (y-axis) and experimental (x-axis) results with minimal offset. Specifically, the ratio between computational and experimental results is 0.98:1, meaning the computational results are 98% of the experimental results. The offset between computational and experimental results is -0.07 N/mm.

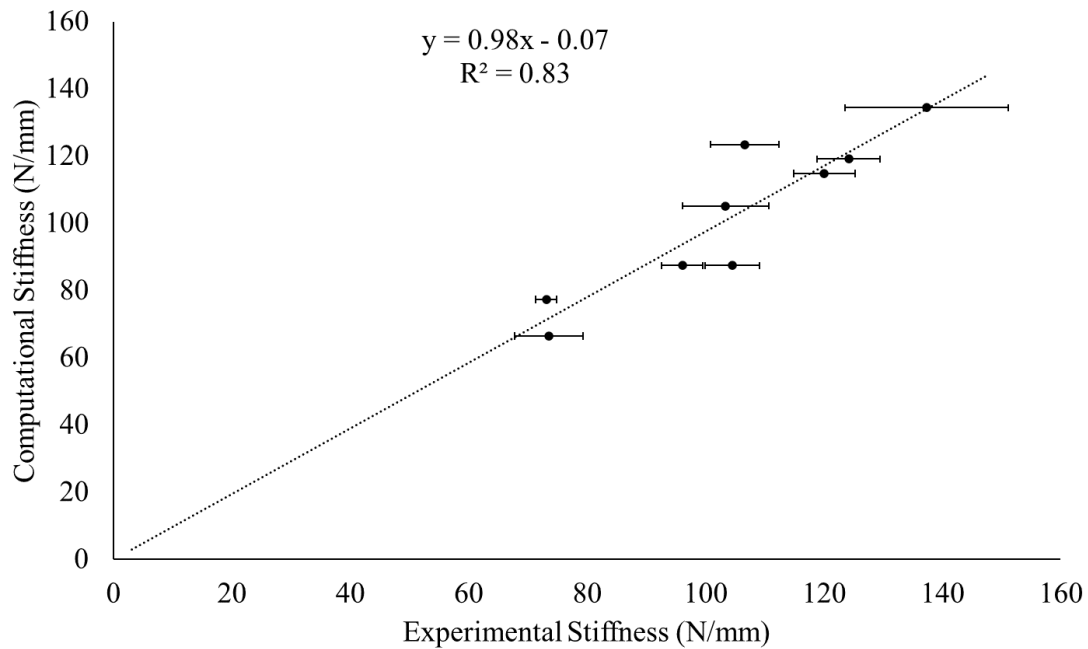


Figure 2.7. Linear regression model detailing statistically significant correlation between experimental and computational stiffness. Note: Error bars represent a single experimental standard deviation.

Figure 2.8 depicts the direct comparison of each computational result with the corresponding experimental averages and standard deviations. Additionally, the constraint reaction force and moment magnitudes for each faceguard model at the “Nose” position are detailed in Table 2.3. These results are representative of the “Mouth” and “Chin” positions; thus, only the “Nose” is reported below.

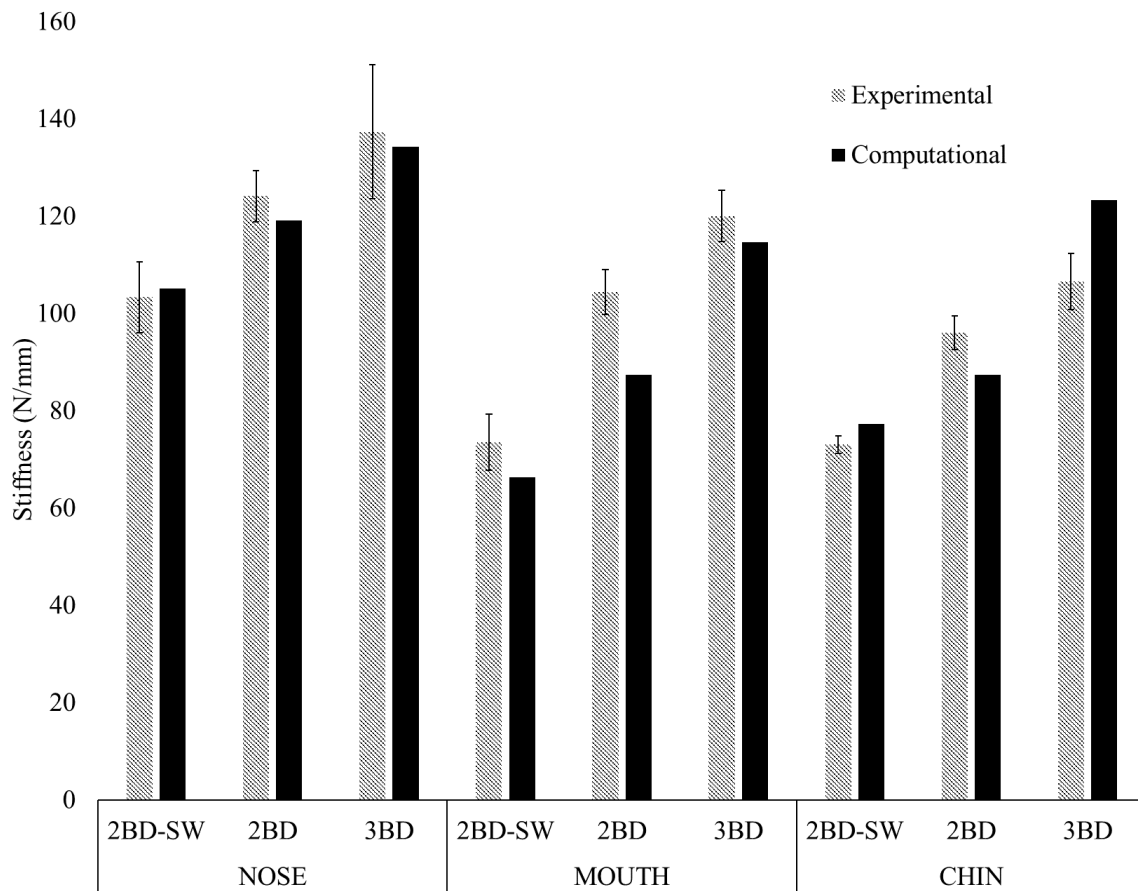


Figure 2.8. Bar chart comparison of computational results and experimental averages with standard deviations.

Table 2.3. Constraint reaction magnitudes recorded at the “Nose” position for each faceguard.

Faceguard	Axis	Force Reaction (N)				Moment Reaction (N-mm)		
		Weak Springs	Midline	Clip	Prescribed Compression	Midline	Clip	Prescribed Compression
SF-2BD-SW	Lateral/Medial	0.000	0.009	0.000	0.000	0.000	713.7	3108
	Superior/Inferior	0.000	0.000	0.000	0.000	581.0	0.000	0.000
	Anterior/Posterior	0.006	0.000	530.4	530.4	151.7	0.000	153.9
SF-2BD	Lateral/Medial	0.003	0.004	0.000	0.000	0.000	4453	1023
	Superior/Inferior	0.000	0.000	0.000	0.000	0.000	0.000	4822
	Anterior/Posterior	0.002	0.000	648.3	600.9	965.9	3286	0.000
SF-3BD	Lateral/Medial	0.002	0.002	0.000	0.000	0.000	631.2	397.8
	Superior/Inferior	0.000	0.000	0.000	0.000	0.000	0.000	3484
	Anterior/Posterior	0.004	0.000	677.8	677.8	1686	953.5	0.000

Discussion

Model Validation

An outcome-based approach, as opposed to point-by-point approach, was used to determine model validation. The maximum force reaction on the prescribed compression constraint was used to calculate the stiffness. This outcome-based approach is common and discussed at length in the literature [32]. Similar to many validated finite element simulations in the literature, statistically significant correlation [20, 33-35], a linear regression model [20, 23, 26], and percent difference [25, 32, 37-40] to experimental results were all used for validating the model in this study. Both the experimental and computational data sets are normally distributed with $p\text{-value} > 0.05$ for a 95% confidence interval; thus, the use of Pearson’s correlation coefficient as a measure of model validation is appropriate. The Pearson’s correlation coefficient of 0.913 with

statistical significance ($p\text{-value}=0.001$) indicates correlation between experimental and computational results, suggesting a validated model. In the literature, correlation with coefficients of determination (R^2) greater than 0.8 has been accepted as proof of a validated computational model [20], a threshold which has been achieved and depicted in Fig. 2.7. Additionally, the linear fit between experimental and computational results suggests model validation with proximity to $y=x$. This metric has been discussed in the literature to support model validation [41].

Percent difference is commonly used to support the claim of a validated model; however, little consensus exists as to appropriate percent differences. This is largely dependent on the context in which each model is used. Although it can be challenging to justify what percent differences are acceptable, this method of comparison between experimental and computational results can be appropriate to illustrate model validation. A difference of 5% or less between computational and experimental results has been used to conclude model validation [32, 36]. In other cases, as much as 10% or more may be accepted [25, 32, 36-40]. As shown in Fig. 2.8, the “Nose” location is the most accurate across the faceguards used in this study with an average percent difference of 2.7%. In contrast, the “Mouth” and “Chin” locations had average percent differences of 10.8% and 9.9%, respectively. Further analysis shows the computational result of each faceguard at the “Nose” location is within the experimental standard deviation; comparatively, neither the “Mouth” nor “Chin” locations are within the experimental standard deviations. This is illustrated in Fig. 2.8. The lack of agreement between experimental results and computational models at the “Mouth” and “Chin” locations is likely due to the 20° and

30° rotation, respectively, about a remote point. The rotation in the experimental procedure is performed on the custom-fabricated alignment platform. Computationally, this rotation was prescribed with respect to a remote point, approximately the same distance from contact to the center of rotation of the alignment platform. Although measurements were taken to best approximate the location of this remote point, error in remote point location likely affected the agreement between the computational model and experimental results at the “Mouth” and “Chin” locations. It is possible that a more accurate description of the rotation in the experimental setup would yield improved agreement between the computational model and experimental results at the “Mouth” and “Chin” locations. This is important for future studies as the “Nose” location models should be used with greater confidence than the “Mouth” or “Chin” locations. This conclusion is supplemented by a study in which a comprehensive video analysis found the predominant location of impact to be at the “Nose” location or higher [42]. Although more accurate results at the “Mouth” and “Chin” locations would validate the faceguard structural stiffness at additional impact locations, the accuracy at the “Nose” location is most important for use in future computational models when simulating on-field impacts.

In attempting to engineer the best protective headgear, little work has been done to improve the faceguard. Johnson et al. used topological optimization at two impact locations to optimize the performance of the faceguard with respect to multiple injury metrics, primarily shear strain on the brain [25]. The current study did not use a finite element model of the human head to validate the faceguard. Instead, the faceguards discussed in this study have been validated structurally and independent of the headgear

system. This isolation is important for using accurate faceguard models in future parametric analyses and complex computational models. With increased model complexity, errors in modeling can increase; therefore, it is important to validate components of more complex models individually [35, 41]. Three studies in the literature performed initial work in this area by validating individual components of a football helmet model prior to implementation in a holistic headgear simulation [35, 43, 44]. The faceguard validation procedures discussed in the studies compressed a faceguard similarly to Bina et al.; however, the validation metric reported was lateral faceguard structural stiffness. The current study has validated the structural stiffness of the faceguard when compressed in the anterior-posterior direction, similar to common, on-field impacts [42]. This is important for improving the structural performance of the faceguard in directions of compression commonly seen on the field to improve the applicability of the computational models. Additionally, the models validated in this study are parameterized to elucidate variables that influence structural stiffness and improve faceguard design.

A common method for developing geometrically accurate models of headgear reported in the literature is Computed Tomography (CT) scan data. While this is a preferred method for model generation, it was not available for this study. To verify the modelling method used in this study, each faceguard was visually inspected for pertinent design geometry. Minor imperfections in the model, such as a lack of symmetry on either side of the midsagittal plane, were considered acceptable. A point-cloud method would be required to produce a parameterized model; thus, many of the inaccuracies in the

model geometry would persist, regardless of the method for model geometry generation. Despite this, automatic point-cloud methods, similar to common automatic approaches found in the literature [45], should be used if CT scan data becomes viable in future studies. Should CT scanning not be viable, this study has validated the reverse engineering approach used.

The geometry from CT scan data is widely accepted to be accurate, but most studies utilizing CT scan data do not report validation of the model geometry or structural properties. Although a standardized approach for validating computational models doesn't exist, addressing applicability of the model reported is important [36, 46, 47]. For example, in the present study, the “Nose” compression location is more accurate than the “Mouth” or “Chin” locations; therefore, to apply the “Nose” location in a parametric analysis is supported by the data. In contrast, the “Mouth” and “Chin” locations should be used more cautiously. Using the reverse engineering method, this study has structurally validated three common faceguard models using finite element analysis. These faceguards can now be used with confidence in future parametric analyses and more complex computational models.

Model Assumptions

Four primary modeling assumptions were made to obtain a computational solution. First, the material of the faceguards was modeled as a general stainless steel using the materials database in ANSYS Workbench 17.2. The decision to model these faceguards as stainless steel, as opposed to a low carbon steel or a titanium alloy as noted in the literature [25], was based upon information found in an online catalog from

Riddell, Inc. (Des Plaines, IL) [30]. Regardless of material selected to approximate the proprietary high strength steel, it is important to note that changing the material properties corresponds to a proportional change in structural stiffness. For example, preliminary analyses illustrated that a 3.6% change in elastic modulus (193 GPa to 200 GPa) corresponded to a similar change in structural stiffness; therefore, this expected behavior further verifies model performance.

Second, the constraints used do not artificially stiffen the faceguard models as to affect the validation. This is proven in Table 2.3 in which minimal force and moment reactions indicate little effect each constraint has on the results. The large constraint reactions (greater than 1 N or 1 N-mm) were analyzed further by prescribing reactions at each location to see if each would affect the stiffness result. The stiffness for each faceguard is not sensitive to constraint reaction forces and moments. Different constraint reaction results exist between the SF-2BD-SW and other faceguard styles as a result of the model geometry. The SF-2BD and SF-3BD faceguard styles have a bar along the midsagittal plane extending from the nose to the chin, whereas the SF-2BD-SW faceguard does not have a bar. To apply the midline constraint to the SF-2BD-SW faceguard, a slice and merged topology tool was used in ANSYS DesignModeler to apply the midline constraint to an edge on the midsagittal plane; comparatively, the midline constraint was applied to the face of the midsagittal bar on both the SF-2BD and SF-3BD faceguards as highlighted in Fig. 2.5. FEA theory suggests that the application of artificial boundary conditions may stiffen computational models; however, these constraints were necessary to achieve a solution and had physical justification for

application. Considering the stiffness results of each model are not sensitive to the constraint reactions and the constraint reactions are minimal, the modeling assumptions used to justify the constraint applications are considered valid.

Third, the polyethylene powder coating was not modeled. Although the theoretical justification for not modeling the coating is sound, realizing that the elastic modulus of stainless steel is approximately two orders of magnitude greater than polyethylene [31], it was not clear how the area of application of displacement would be affected. To assess this, Hertzian contact theory was used to approximate the area to prescribe the displacement. The calculated contact area was small enough, approximately 0.1% of the primary bar cross sectional area, to suggest the application of displacement to an edge is acceptable.

Fourth, welds were not included in the model. Although welds would likely stiffen the faceguards, the additional stiffness was assumed to be negligible. Preliminary computational models resulted in less than 1% increase in faceguard stiffness. This modeling assumption was further justified due to the added model complexity each would introduce in future attempts at creating a more comprehensive library of validated faceguard models.

Additional research in this area should include the further development of validated computational models of faceguards to create a comprehensive library for complete headgear computational models. Furthermore, faceguards compatible with other helmets should be validated to develop a complete library of faceguards. This library of faceguards can then be used in complex headgear computational models with improved

confidence of faceguard model accuracy. Additional experimental and computational analyses should include the dynamic response of faceguards to characterize faceguard performance in more realistic, on-field impact conditions. More in-depth analysis is needed in the design of faceguards to continue to inform headgear manufacturers of ways to improve their headgear technology for improved athlete safety.

Conclusion

This study serves as a validation of a faceguard modelling methodology and finite element simulation to be used for comprehensive parametric analysis. This method of model generation and faceguard validation is important for ensuring accuracy of individual components of headgear systems to improve the accuracy of complex headgear computational models. As advancements in additive manufacturing technologies become increasingly utilized, specific design variables should be understood to better protect football athletes. With the models validated in this study, parameterized faceguard models should be used to iterate between design variables and assess the contribution of each variable on faceguard structural stiffness. It is the goal of this future study to influence faceguard design by informing headgear manufacturers of the specific variables that affect faceguard stiffness to advance headgear technologies for improved athlete safety. Furthermore, this study should inform athletes, parents, coaches, and equipment managers of the faceguard specifications pertinent for improved headgear performance to influence faceguard selection and improve the industry standard.

References

- [1] The National Federation of State High School Associations. 2018-19 High School Athletics Participation Survey, <https://www.nfhs.org/sports-resource-content/high-school-participation-survey-archive/> (2019, accessed 21 February 2020).
- [2] The National Federation of State High School Associations. 2017-18 High School Athletics Participation Survey, <http://www.nfhs.org/ParticipationStatistics/PDF/2017-18%20High%20School%20Athletics%20Participation%20Survey.pdf> (2018, accessed 21 February 2020).
- [3] The National Federation of State High School Associations. 2016-17 High School Participation Survey, <https://www.nfhs.org/sports-resource-content/high-school-participation-survey-archive/> (2017, accessed 21 February 2020).
- [4] The National Federation of State High School Associations. 2015-16 High School Athletics Participation Survey, <https://www.nfhs.org/sports-resource-content/high-school-participation-survey-archive/> (2016, accessed 21 February 2020).
- [5] The National Federation of State High School Associations. High School Athletics Participation Survey (1969-2008), <https://www.nfhs.org/sports-resource-content/high-school-participation-survey-archive/> (2000, accessed 21 February 2020).
- [6] Maroon JC. Should you allow your child to play football? Update on concussion management, prevention, and treatment. In: Anti-Aging Ther. 2013 Conf. Year, Las Vegas, Nevada, 12 December-15 December 2013, paper no. __, pp.125-139. Boca Raton: AAAAM
- [7] Laker SR, Greiss C, Finnoff JT, et al. Football participation and chronic traumatic encephalopathy. *Am Acad of Phys Med Rehabil* 2018; 12(6):655-660.
- [8] Martin GT. Acute brain trauma—A review. *Ann R Coll Surg Engl* 2016; 98:6-10.
- [9] Gysland SM, Mihalik JP, Register-Mihalik JK, et al. The relationship between subconcussive impacts and concussion history on clinical measures of neurologic function in collegiate football players. *Ann Biomed Eng* 2012; 40(1): 14-22.
- [10] Sayed N, Culver C, Darns-O'Connor K, et al. Clinical phenotype of dementia after traumatic brain injury. *J Neurotrauma* 2013; 30: 1117-1122.
- [11] Hirad AA, Bazarian JJ, Merchant-Borna K, et al. A common neural signature of brain injury in concussion and subconcussion. *Sci Adv* 2019; 5: 1-11.

- [12] McKee AC, Cantu RC, Nowinski CJ, et al. Chronic traumatic encephalopathy in athletes: Progressive tauopathy after repetitive head injury. *J Neuropathol Exp Neurol* 2009; 68(7): 709-735.
- [13] Montenigro PH, Alosco ML, Martin BM, et al. Cumulative head impact exposure predicts later-life depression, apathy, executive dysfunction, and cognitive impairment in former high school and college football players. *J Neurotrauma* 2017; 34: 228-340.
- [14] Talavage TM, Nauman EA, Breedlove EL, et al. Functionally-detected cognitive impairment in high school football players without clinically-diagnosed concussion. *J Neurotrauma* 2014; 31(4): 327-338.
- [15] DeKosky ST, Ikonomic MD and Gandy S. Traumatic brain injury—Football, warfare, and long-term effects. *N Engl J Med* 2010; 363(14):1293-1296.
- [16] Spires-Jones TL, Stoothoff WH, de Calignon A, et al. Tau pathophysiology in neurodegeneration: A tangled issue. *Trends Neurosci* 2009; 32(3): 150-159.
- [17] Castellani RJ and Perry G. Tau biology, tauopathy, traumatic brain injury, and diagnostic challenges. *J Alzheimer Dis* 2019; 67:447-467.
- [18] Prins M, Greco T, Alexander D, et al. The pathophysiology of traumatic brain injury at a glance. *Dis Models Mech* 2013; 6: 1307-1315.
- [19] Ivancevic V. New mechanics of traumatic brain injury. *Cogn Neurodyn* 3: 281-293.
- [20] Kimpara H and Iwamoto M. Mild traumatic brain injury predictors based on angular accelerations during impacts. *Ann of Biomed Eng* 2012; 40(1): 114-126.
- [21] National Football League. The NFL Engineering Roadmap, <https://www.playsmartplaysafe.com/nfl-helmet-challenge-symposium/> (2019, accessed 4 April 2020).
- [22] National Football League. The NFL Helmet Challenge, <https://www.playsmartplaysafe.com/nfl-helmet-challenge-symposium/> (2019, accessed 4 April 2020).
- [23] Viano DC, Withnall C and Halstead D. Impact performance of modern football helmets. *Ann of Biomed Eng* 2012; 40(1): 160-174.
- [24] Rush GA, Alston GA III, Sbravati N, et al. Comparison of shell-facemask responses in American football helmets during NOCSAE drop tower tests. *Sports Eng* 2017; 20: 199-211.

- [25] Johnson KL, Chowdhury S, Lawrimore WB, et al. Constrained topological optimization of a football helmet facemask based on brain response. *Mater Des* 2016; 111: 108-118.
- [26] Rowson B, Terrell EJ and Rowson S. Quantifying the effect of the facemask on helmet performance. *J Sports Engineering and Technology* 2018; 232(2): 94-101.
- [27] Bina A, Batt GS and DesJardins J. Development of a non-destructive method to measure football facemask stiffness. *J Sports Engineering and Technology* 2019; 233(2): 175-185.
- [28] NOCSAE ND087—18m18. Standard method of impact test and performance requirements for football faceguards.
- [29] Zhang L, Ramesh D, Yang KH, et al. Effectiveness of the football helmet assessed by finite element modeling and impact testing. In: *Proc. 2003 IRCOBI Conference, Lisbon, Portugal, 25 September-26 September 2003*.
- [30] Riddell, Inc. Team Catalog, <http://www.riddell.com/team-catalog/> (2020, accessed 21 April 2020).
- [31] Ashby MF. Appendix C Data and Information for Engineering Materials. In: *Materials Selection in Mechanical Design*. 4th ed. Amsterdam: Butterworth-Heinemann, 2005, pp. 513-535.
- [32] Mann JA III, Yost B, Westwater G, et al. Validating FEA simulations of structural collapse of a complex vessel geometry. In: *ASME 2016 Pressure Vessels and Piping Conference, Vancouver, British Columbia, 17 July-21 July 2016*.
- [33] Takhounts EG, Craig MJ, Moorhouse K, et al. Development of Brain Injury Criteria (BrIC). *Stapp Car Crash Journal* 2013; 57: 243-266.
- [34] Viano DC, Casson IR, Pellman EJ, et al. Concussion in professional football: brain responses by finite element analysis: part 9. *Neurosurgery* 2005; 57(5): 891-916.
- [35] Bustamante MC, Bruneau D, Barker JB, et al. Component-level finite element model and validation for a modern American football helmet. *J of Dynamic Behavior of Mater* 2019; 5: 117-131.
- [36] Durand LB, Guimaraes JC, Monteiro S Jr, et al. Modeling and validation of a 3D premolar for finite element analysis. *Rev Odontol UNESP* 2016; 45(1): 21-26.

- [37] Lin CL, Chang YH and Liu PR. Multi-factorial analysis of a cusp-replacing adhesive premolar restoration: a finite element study. *J Dent* 2008; 36:194-203.
- [38] Wang W, Cao X and Cheng S. Structural failure analysis of a sport utility vehicle chassis. In: 2018 International Conference on Mechatronic Systems and Robotics, Singapore, 25 May-27 May 2018.
- [39] Sutradhar A, Park J, Carrau D, et al. Experimental validation of 3D printed patient-specific implants using digital image correlation and finite element analysis. *Comput Biol Med* 2014; 52: 8-17.
- [40] Willinger R, Kang HS and Diaw B. Three-dimensional human head finite element model validation against two experimental impacts. *Ann Biomed Eng* 1999; 27: 403-410.
- [41] Anderson AE, Ellis BJ and Weiss JA. Verification, validation, and sensitivity studies in computational biomechanics. *Comput Methods Biomech Biomed Engin* 2007; 10(3): 171-184.
- [42] Pellman EJ, Viano DC, Tucker AM, et al. Concussion in professional football: location and direction of helmet impacts—part 2. *Neurosurgery* 2003; 53(6): 1328-1341.
- [43] Corrales MA, Gierczycka D, Barker J, et al. Validation of a football helmet finite element model and quantification of impact energy distribution. *Ann Biomed Eng* 2020; 48(1): 121-132.
- [44] Decker W, Baker A, Ye X, et al. Development and multi-scale validation of a finite element football helmet model. *Ann Biomed Eng* 2020; 48(1): 258-270.
- [45] Chen LC and Lin GCI. A vision-aided reverse engineering approach to reconstructing free-form surfaces. *Robot CIM-Int Manuf* 1997; 13(4): 323-336.
- [46] Dumont E, Grosse I and Slater G. Requirements for comparing the performance of finite element models of biological structures. *J Theor Biol* 2009; 256:96-103.
- [47] Erdemir A, Guess TM, Halloran J, et al. Considerations for reporting finite element analysis studies in biomechanics. *J Biomech* 2012; 45: 625-633.

CHAPTER THREE

PARAMETRIC DESIGN METHODS DEVELOPMENT FOR THE COMPARISON OF AMERICAN FOOTBALL FACEGUARDS USING VALIDATED STRUCTURAL STIFFNESS MODELS

Introduction

Research focusing on American football headgear performance and design has seen increased attention from manufacturers, researchers, sports organizations, and media in the past decade. Despite this continued emphasis on improving protective headgear technologies, sports related concussions continue to have the greatest incidence in American tackle football [1]. A majority of research efforts have investigated the helmet or entire headgear system [2-5]. Recent efforts from the National Football League (NFL) and partnered researchers have developed a Helmet Performance Score (HPS) [6] similar to the Summation of Tests for the Analysis of Risk (STAR) rating system [7]. Both rankings attempt to inform the athletes—as well as the design and research community—of the headgear that best attenuate simulated impacts in a laboratory setting. These laboratory reconstructions and published results have provided athletes with greater agency in their safety related decisions. In contrast, little quantitatively informed comparisons exist for athletes to select faceguards based upon safety and performance metrics, as manufacturers typically suggest athletes of specific positions to use certain faceguard designs [8]. In addition to improving researchers' and manufacturers' understanding of faceguard design performance, faceguard designs should be more thoroughly explored to improve athlete agency in their safety and performance related decisions.

Faceguard Design Research

It is logical that a stiffer faceguard might be preferred to protect the athlete from catastrophic injury to the face; however, a desire for a stiffer material or geometry is in conflict with the theoretical perspective that a less stiff structure will improve energy absorption properties [9]. Faceguards have been shown to stiffen the mechanical response in laboratory reconstructions of on-field impacts [10]. Additionally, recent work has demonstrated an ability to discern between faceguard designs by measuring the structural stiffness [11]. Despite the ability to compare the structural stiffness of faceguards, it is not clear which faceguard design parameters contribute to these differences; therefore, athletes have minimal quantitative data to inform faceguard design selection.

Additionally, protecting the face is not the only safety metric to consider. For instance, it has been reported that a greater weight of the faceguard may lead to athletes leading with the crown of their helmet—leading to injury [12]. Additionally, visibility has been reported as being important to athlete reaction—which can contribute to both athlete safety and performance [12, 13]. The degree to which each contributes to athlete safety has not been explored.

As manufacturers consider developing new faceguards to improve performance metrics, it is clear a consistent method for defining and measuring faceguard design parameters in the laboratory is not easily available due to complex geometry.

Additionally, developing a consistent measurement technique across all faceguards may also be challenging. Although some faceguard performance metrics—such as weight and structural stiffness—are repeatable and objectively measured in the laboratory, the

challenge of comparing these faceguard performance metrics as a function of faceguard design parameters remains; thus, computational modelling is one approach to consistently define and measure faceguard parameters and performance metrics to objectively compare faceguard designs.

Computational Design Methodology

Recent efforts in the headgear design community have emphasized computational methods to improve headgear design [14-17]. Computational methods, particularly finite element analysis, have been widely used to evaluate headgear performance and inform headgear design [18-22], particularly in American football [23-26]. Many of these studies investigated the effects of different headgear designs on impact performance; however, few have used parametric analysis to assess headgear designs [27], likely due to the duration of performing multiple analyses of computationally expensive simulations. Although a mixed methods approach of utilizing laboratory reconstructions and computational methods have been employed, primary focus has been on the helmet system including helmet structure, helmet linings and foam, helmet component materials, and personalized fit [15]. Some recognize the need to validate each individual component for computational analyses, but few have investigated the faceguard directly [14, 16, 23]. Johnson et al. proved categorically different faceguard designs could improve the shear strain on the brain by nearly 40%. The topological optimization and surrogate modeling performed in this study demonstrated an ability to improve headgear performance by changing the faceguard design [23]. Another study demonstrated the ability to distinguish between faceguard 3D models by comparing structural stiffnesses using finite element

simulations of laboratory procedures [28]. Despite these improvements in computational faceguard design research, little is known about the faceguard design parameters that can improve brain injury metrics or affect structural stiffness.

Faceguard Design

Currently, manufacturers categorize their faceguards based upon their material, helmet-compatible series, and visual geometry. Typical faceguard materials include stainless steel [28, 29], carbon steel [14], and titanium [23]; however, the specific alloy compositions used are not disclosed. Faceguards are designed to configure with each new helmet. This is accomplished with a unique outer frame that fixes to the helmet shell. Traditionally, each helmet-compatible faceguard series has a prefix that corresponds to the helmet with which each faceguard attaches. For example, the Riddell Speed and SpeedFlex compatible faceguard series include prefixes of “S” and “SF”, respectively. Lastly, manufacturers and sports equipment retailers typically suggest certain faceguard geometry to athletes of specific positions [8]. For example, a faceguard with more bars and less visibility may be considered a faceguard for linemen, whereas a faceguard with less bars and more visibility may be preferred by “skill” players such as wide receivers and quarterbacks. Although the visual differences between faceguard designs enable athletes to compare faceguard designs, minimal quantitative data exists to compare faceguard design performance metrics. Differences between faceguard design parameters including bar diameters, angles, lengths, and locations have not been quantified.

To address the lack of understanding of faceguard design parameters influencing measured performance metrics, this study seeks to: develop methods for parameter

definitions that can be consistently defined across faceguard styles and helmet-compatible faceguard series; and analyze this parameterization method with three faceguards using an appropriate design of experiments. The results from this study will enable researchers to compare manufacturer's original faceguard designs and the parameters that most affect performance metrics across a range of faceguards.

Methods

Leveraging the same reverse engineering approach discussed in the literature [28], parametric models were developed to compare how different parametric analysis techniques performed. Three popular faceguard models—the Riddell® (Des Plaines, IL) SpeedFlex™ SF-2BD, SpeedFlex SF-2BD-SW, and the Schutt (Schutt Sports, Litchfield, IL) Q11 ROPO-SW—were used in this method development study. These faceguards were chosen to elucidate differences between categorically similar faceguards of different helmet series (i.e. the SpeedFlex SF2BD-SW and the Q11 ROPO-SW faceguards are both in the single wire—SW—category but from different helmets—SpeedFlex and Q11) and differences between categorically different faceguards of the same helmet series (i.e. the SF2BD has two horizontal design bars and three vertical design bars whereas the SF2BD-SW has a single horizontal design bar and two vertical design bars). This comparison was important for the parametric method development stage so that parameters could be consistently defined across helmet types and faceguard categories.

The design space is defined as the volume between the frame of the faceguard that configures with the specific helmet for which the faceguard is designed. In Fig. 3.1, representative frames for the SpeedFlex and Q11 helmet-compatible series are compared.

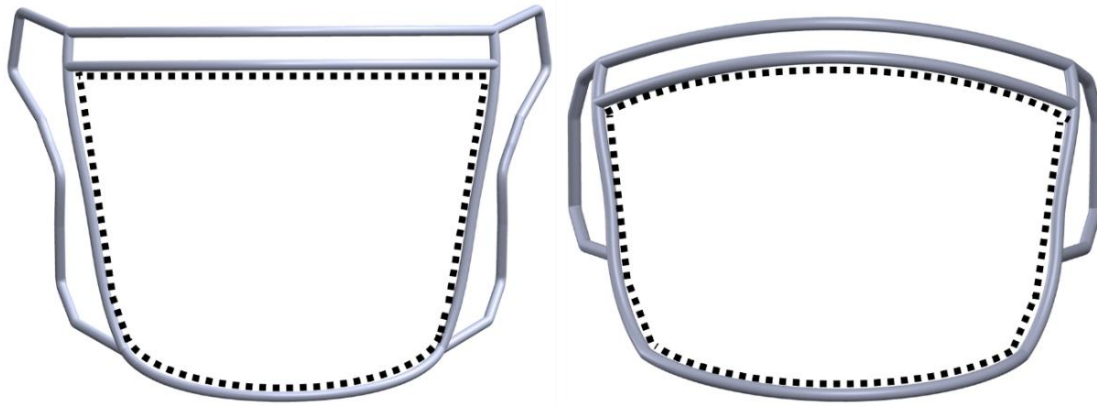


Figure 3.1. The design space—outlined by the dashed line—superimposed on the Riddell SpeedFlex-compatible (Left) and Schutt Q11-compatible (Right) faceguard frame.

Using these helmet-compatible frames, parameters can be consistently defined across faceguards of different helmet-compatible series and of different categories. This design space is limited to 70mm anterior to the nose and 70mm to the chin. This is defined by NOCSAE limits to faceguard design [30]. The design space is also limited to the upper frame of each faceguard as this is typically in contact with the helmet and can be an attachment location—depending on the helmet. Since it is a part of the frame for some faceguards, it was considered to be a part of the frame for all faceguards so that parameters could be more appropriately compared across all faceguards. Lastly, the design space is limited side to side by the vertical frame bar that exists for all faceguards. It is important to note that on some faceguards, the design space may be larger due to the bottom, sides, and tops of the faceguard frame being different. Although this could be a design parameter, the frame cannot be consistently quantified with parameters to appropriately compare across faceguards of different helmet series. The approach of using the upper and lower frames as the definition of the design space is supported in the







literature in which the design space was defined for topological optimization [23].

Despite this limitation, comparisons can be made across similar designs with different outer frames to suggest the effects that frame design may have on responses. For this work, the frame is not a part of the study; however, this could be an important design consideration in future studies.

Parametric Definitions

To define parameters, a single faceguard was qualitatively compared to similar faceguards of different helmets and different faceguard styles from all helmets. It was found that similar categories of faceguard styles exist from different helmet-compatible series. For example, most helmets have a faceguard option with a single wire across the design space and two vertical bars connecting the bottom of the frame to the single horizontal wire. Example categories and common Riddell SpeedFlex compatible faceguards are listed in Table 3.1.

Table 3.1. Categories for the SpeedFlex Helmet-compatible faceguards.

Faceguard Categorization		Riddell SpeedFlex					
		SF-2BD-SW	SF-2EG-SW	SF-2BD	SF-2EG	SF-2BDC	SF-3BD
One horizontal Bar	Two Vertical Bars						
Two Horizontal Bars	Two Vertical Bars						
Three Horizontal Bars	Three Vertical Bars						

In addition to the categories that faceguards can be defined by, there were consistent variations in the designs across faceguards of the same category and

faceguards of different categories but the same helmet compatible series. Initial values of parameters and parameter descriptions for the three faceguards used in this methods development study are detailed in Table 3.2.

Table 3.2. Parameter names and initial values for the SF-2BD-SW, ROPO-SW, and SF-2BD faceguard styles.

Parameter Name	Unit	Baseline Values			Description
		SF-2BD	SF-2BD-SW	ROPO-SW	
ANS_D1	mm	47.7	17.7	44.1	Nose Visibility (Translation of Nose Bar)
ANS_D2	deg	90	90	90	Nose Visibility (Rotation of Nose Bar)
ANS_D3	mm	82.3	77.0	76.6	Nose Protection
ANS_D4	mm	40.9	39.0	41.5	Cheek Bone Protection
ANS_D5	mm	14.2	12.8	8.6	Nose Sharpness Index
ANS_D6	mm	40.9	39.0	41.5	Upper Mouth Protection
ANS_D7	mm	28.6	27.9	32.2	Lower Mouth Protection
ANS_D8	deg	90	90	90	Left Side Vertical Bar Angle
ANS_D9	deg	90	90	90	Right Side Vertical Bar Angle
ANS_D10	mm	30.6	38.0	19.9	Left Side Vertical Bar Apex Length
ANS_D11	mm	5.7	9.5	7.8	Left Side Vertical Bar Apex Height
ANS_D12	mm	30.6	38.0	19.9	Right Side Vertical Bar Apex Length
ANS_D13	mm	5.7	9.5	7.8	Right Side Vertical Bar Apex Height
ANS_D14	mm	31.6	N/A	N/A	Mid Vertical Bar Apex Length
ANS_D15	mm	5.2	N/A	N/A	Mid Vertical Bar Apex Height
ANS_D16	mm	17.7	N/A	N/A	Secondary Horizontal Bar Offset Distance
ANS_D17	deg	90	N/A	N/A	Secondary Horizontal Bar Offset Angle
ANS_DiaS	mm	4.8	4.8	5.6	Frame/Horizontal Bar Diameter
ANS_DiaL	mm	3.7	3.7	4.8	Vertical Bar Diameter

Although there are virtually infinite possibilities for defining and measuring parameters of a faceguard, two main approaches were used throughout the parameter definition phase of this study. First, the method of parameter definitions had to be

consistently defined. For example, measuring the Nose Protection (D3) parameter was measured perpendicular to a line coincident with the frame attachment locations. This allowed for a consistent measurement technique that did not bias results across faceguard styles or helmet-compatible series due to the measurement from a consistent and objective location. Secondly, the parameter definitions had to be physical. For example, a change of a parameter should result in the same change to the geometry. This is best illustrated in the following discussion regarding the definitions of the splines parameterizing the main horizontal arcs used in this study.

Splines as opposed to Bezier curves were used to define the curvature of the horizontal bars for a few reasons. First, the Bezier curve definition method would have resulted in definitions for parameters that were not physical. For instance, to define the curve using a Bezier control point (or control vertices), the value would be approximately 115 mm as opposed to D3 (in Table 3.2 above) which is 77 mm. The apex of the arc of the SF2BDSW is 77 mm from the attachment frame. The definition of the parameter that has physical context enables direct comparisons to the geometry (i.e., a difference in variable D3 of 5 mm translates to a primary horizontal design arc of 5 mm difference in apex length. The same cannot be said for defining these variables using the Bezier curve method). Secondly, to define the Bezier curve, an extra parameter is needed to completely constrain the curve. Bezier curve parametric definitions for the primary horizontal arcs could have been used to define the curvature of the arc more precisely; however, agreement with the original manufacturer's designs was found from using the generic spline definitions of D3, D4, and D5 which fully defined the spline.

Model Verification

To ensure the parameter definitions, modeling constraints, and geometric relationships were appropriately modeled, an iterative process of model review verified the models. The framework used for this approach is summarized in Fig. 3.2.

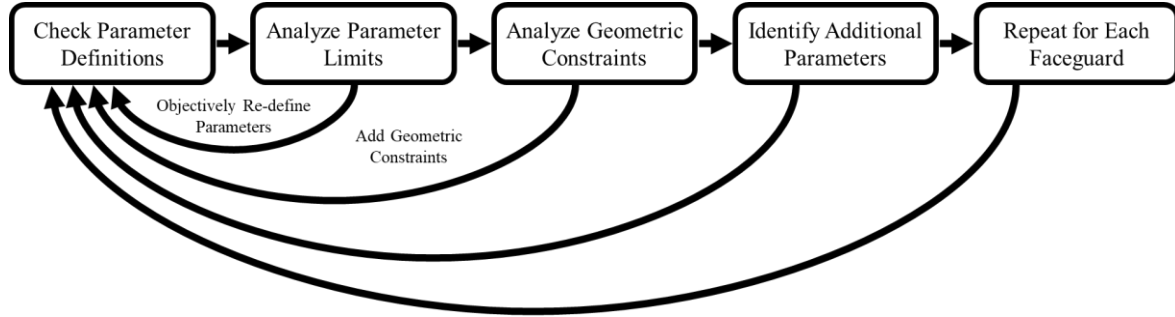


Figure 3.2. Framework summarizing approach to verifying the models used for parametric analyses in this study.

Following each step in the iterative process, the initial parameter definitions and bounds had to be reassessed to ensure proper model performance. For example, under constrained geometry resulted in unrealistic models at the limits of single parameters and at the limits of two or more parameters. To address these issues, additional geometric constraints were added or the bounds for parameters were limited.

Verified parametric models from SOLIDWORKS were imported into ANSYS® Workbench™ 19.0 (ANSYS, Inc., Canonsburg, PA) for Static Structural Analysis—similar to the methods discussed in the literature [28]. Upon validation of the structural stiffness models from the experimental values [11], the finite element simulations were configured with ModeFrontier 2020 (ESTECO, Trieste).

Design of Experiments

Many algorithms exist to sample the design space, but common approaches include factorial, Monte Carlo, Sobol, completely random, and Uniform Latin Hypercube. The Uniform Latin Hypercube (ULH) algorithm was selected as the preferred method for filling the design space with samples. This decision was made based upon the performance of the algorithm to sample the design space such that the input variables were minimally correlated [31]. Minimally correlated input variables and the uniform distribution of design points in the design space was important in this study as there was no objective function for the responses [32]. Although this algorithm may be preferred for sampling the entire design space, it may lead to correlated variables when greater than 3 dimensions are used [33]; therefore, it was determined the correlations of input parameters should be monitored due to the high dimensionality of the parameterized faceguards. The sample size of each design of experiments (DOE) for the ROPO-SW, SF-2BD-SW, and SF-2BD, faceguards were 130, 130, and 150, respectively. With each of the faceguards used in this study, the maximum correlation value was 0.018. Using a commonly accepted range for degrees of correlation, the ULH algorithm produced a DOE that had negligible correlation [34]. The decision to use the ULH is supported in the literature.³²

Additionally, preliminary investigations revealed that previously uncorrelated parameters may be correlated following the failure of some designs to solve during the analyses. Failed designs could occur when a combination of parameter values resulted in invalid geometry in SOLIDWORKS® (Dassault Systèmes SolidWorks Corporation,

Waltham, MA) or failed mesh in ANSYS. Failed designs were omitted, and the Pearson's Correlation coefficients were recalculated at the completion of the analyses.

Results

Following the completion of all simulations, the ROPO-SW, SF-2BD-SW, and the SF-2BD had 34, 44, and 85 designs, respectively, that failed to solve. Despite these omissions from the design space, the subsequent correlations were all less than 0.2 which is still widely accepted as negligibly correlated [34]; thus, it can be concluded that the parameter definitions, bounds, and constraints are robust enough to consistently sample the entire design space sufficiently. Additionally, the ULH design of experiments can produce a DOE with negligible correlation amongst the designs of the input parameters. No designs exceeded the yield strength; therefore, all designs that solved were included in the design analyses.

As shown in the Tables 3.3-3.5, expected outcomes for changes in the large diameter were achieved. From the results, it is clear that: the increases in mass were also reflected as increases in structural stiffness; a larger diameter will increase the structural stiffness; and a larger diameter will increase the mass. In other words, more material—greater mass—will lead to a stiffer faceguard. Although intuitive, these results increase confidence in the model performance.

Table 3.3. Comparison of the correlations between mass and structural stiffness responses for each of the faceguards.

Correlation between Mass and Stiffness	
Faceguard	Pearson's Correlation Coefficient
SF-2BD	0.942
SF-2BD-SW	0.912
ROPO-SW	0.908

Table 3.4. Comparison of the correlations between large diameter parameter and the structural stiffness response for each of the faceguards.

Correlation between DiaL and Stiffness	
Faceguard	Pearson's Correlation Coefficient
SF2BD	0.938
SF2BDSW	0.898
ROPOSW	0.879

Table 3.5. Comparison of the correlations between the large diameter parameter and the mass response for each of the faceguards.

Correlation between DiaL and Mass	
Faceguard	Pearson's Correlation Coefficient
SF2BD	0.982
SF2BDSW	0.989
ROPOSW	0.984

A sensitivity analysis was performed that included all parameters. The results for each faceguard are summarized in Table 3.6.

Table 3.6. Summary of results specifying the three parameters for each faceguard that contributed most to the structural stiffness.

Parameter Effects on Stiffness		
Faceguard	Parameter	Percent Effect
ROPO-SW	DiaL	78%
	D3	16%
	D2	4%
SF-2BD-SW	DiaL	86%
	D3	11%
	D2	2%
SF-2BD	DiaL	92%
	D3	5%
	D17	1%

Although the large diameter design parameter has the greatest effect on structural stiffness, the arc length and angle of the primary horizontal bar can contribute to the structural stiffness of a faceguard for the same large diameter. Additionally, large changes in both the mass and structural stiffness response were achieved among viable designs. The percent ranges of the maximum response value of all viable designs are detailed in Table 3.7. In contrast, the results from each faceguard demonstrated an ability to change some parameters such that minimal changes of responses were made in viable faceguard designs. Counter

Table 3.7. Percent changes from maximum response to minimum response for viable designs from each faceguard.

	Percent Change in Response Among Viable Designs	
Faceguard	Structural Stiffness	Mass
SF2BD	77%	48%
SF2BDSW	90%	58%
ROPOSW	73%	47%

Two responses for each individual design in the SF-2BD faceguard experiment are compared in Fig. 3.3. This illustrates an ability to change the mass without changing the structural stiffness as indicated by comparing designs on a similar horizontal line. Similarly, the structural stiffness can vary without changing the mass which is visualized by comparing designs on a similar vertical line. An example of this for each response is detailed in Tables 3.8 and 3.9.

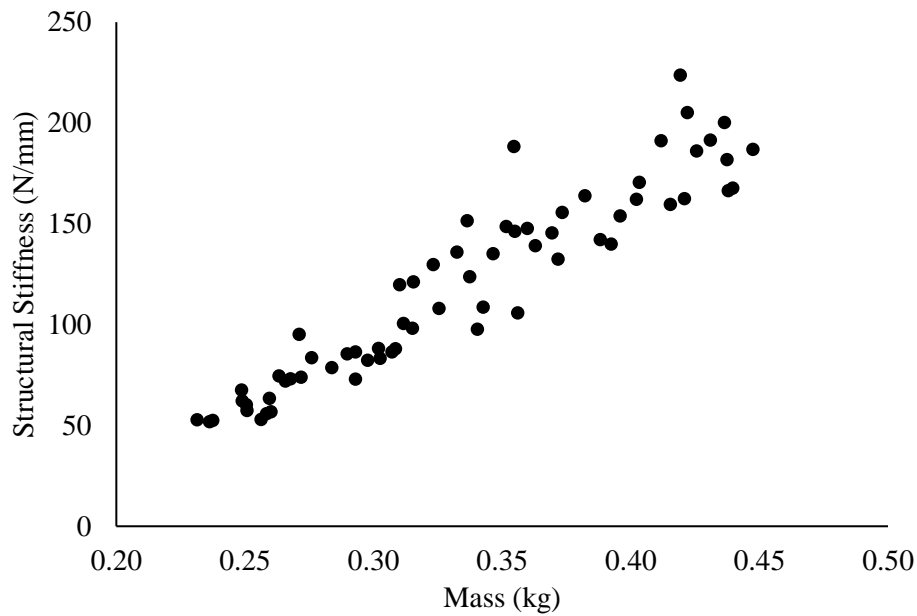


Figure 3.3. All viable designs plotted to compare two responses: Mass and Structural Stiffness for the SF-2BD faceguard experiment.

Table 3.8. Comparison of two viable designs with similar Structural Stiffnesses and different masses.

	SF-2BD Viable Designs		
	Design 1	Design 2	Percent Difference
Mass (kg)	0.35	0.45	20.8%
Stiffness (N/mm)	188	187	0.8%

Table 3.9. Comparison of two viable designs with similar masses and different Structural Stiffnesses.

	SF-2BD Viable Designs		
	Design 1	Design 3	Percent Difference
Mass (kg)	0.35	0.36	0.4%
Stiffness (N/mm)	188	106	43.8%

Discussion

This study sought to utilize the reverse engineered and structurally validated models of three common American football faceguards to develop a framework for parametric methods development that can be applied to similar faceguards of different faceguard categories and helmet-compatible series. This was accomplished by testing this framework on two faceguards of different helmet compatible series—the ROPO-SW and SF-2BD-SW that are compatible with the Schutt Q11 and Riddell SpeedFlex, respectively—and on two faceguards of different categories—the SF-2BD and SF-2BD-SW have different number of horizontal and vertical bars.

Using data available from the literature and by permission of the authors [11, 28], the computational results from Ferriell et al. and experimental results from Bina et al. are in agreement with the models of the original manufacturers' designs analyzed in this study. Furthermore, changes in structural stiffness and mass were highly correlated with changes in the large diameter parameter for all three experiments. Although intuitive, these results improve confidence in the computational models. Despite these correlations, the experiments elucidated the possibility of changing the stiffness of a faceguard by over 40% while maintaining similar mass. The opposite is similarly true, although similar

stiffnesses could have up to a 20% change in mass. These results are important for both athletes and faceguard manufacturers as preferred stiffnesses can be maintained given different masses. Since the literature points to a lack of safety for faceguards with a greater weight due to the potential for athletes to lead with the crown of the helmet [35], these results indicate the possibility of reducing the weight (mass) while still maintaining similar stiffnesses.

The ability of the framework to produce large changes in responses for different faceguard designs is similar to the results found by Johnson et al. in which a 39.5% decrease in shear strain on the brain for a front impact was found in their optimal design. Furthermore, their results suggest that the faceguard design can have a significant effect on the mechanical response of the brain. Coupled with comparisons to laboratory reconstructions that elucidate the effects of faceguard structural stiffness on measured responses like rotational acceleration, future work using this framework should include approximate designs from the Johnson et al. work to provide context for the results to shear strain on the brain [23]. In turn, the importance of faceguard parameters on the mechanical response of the brain can be more appropriately determined.

The data suggests that a large faceguard diameter is the most critical parameter to consider when assessing mass and structural stiffness; however, the large diameter may not be the most important parameter when considering other responses not considered in this methods development study. For example, it has been shown that visibility can be a critical parameter of interest in athlete performance and safety [12]. Given the bounds on the large diameter used in this study, it is unlikely that the large diameter is the primary

parameter of interest to affect responses related to visibility. This means that although there are many parameters included in this study that did not affect the structural stiffness or mass of the faceguard, these same parameters may influence other responses not directly investigated for this study. It is important to consider these parameters in future faceguard analyses, because seemingly unimportant parameters may significantly influence responses not directly investigated in this study.

Bina et al. demonstrated an ability to distinguish faceguards based upon the structural stiffness [11]. Similarly, this study has sought to understand the parameters that influence the differences in structural response. Although more faceguards should be investigated before making conclusions for all faceguards, it appears the inclusion of different categorical variables such as number of horizontal or vertical bars can influence the impact certain parameters have on the structural performance of a faceguard. For example, the structural stiffness of the single-wire faceguards investigated in this study—SF-2BD-SW and the ROPO-SW—were greatly affected by the length of the main horizontal design arc (D3). This contrasts to the structural stiffness results of the SF-2BD faceguard—which has two horizontal bars and three vertical bars—which was less so affected by the angle of the middle horizontal bar (D17). Although the sensitivity analysis for all three faceguards were performed with negligibly correlated parameters, these results need to be compared across more faceguards to ensure consistency. It is also important to note that the structural stiffness of the single-wire faceguards were over three times more affected by the length of the main horizontal arc (D3), whereas the

structural stiffness of the SF-2BD faceguard was slightly more affected by the angle of the middle horizontal bar (D17) than the length of the main horizontal arc (D3).

Conclusion

This study has demonstrated an ability to consistently define parameters for faceguards of different qualitative conformations and of different helmet-compatible series. The framework used to make these comparisons can now be used to compare additional faceguards ranging more categories and helmet-compatible series to provide athletes with greater agency when making their headgear decisions. The ability to alter some faceguard performance metrics, such as stiffness, while maintaining the same mass suggests that manufacturers may be able to make changes to current designs while maintaining certain specifications like weight. Future work should investigate novel faceguard models to compare to manufacturers' original designs. Additional faceguard performance metrics should also be defined to compare how the parameters defined in this study affect other measures.

References

- [1] Dymek M, Ptak M, Fernandes FAO. Design and Virtual Testing of American Football Helmets-A Review. *Arch Comput Method E* 2021.
- [2] Bailey AM, McMurry TL, Cormier JM, et al. Comparison of Laboratory and On-Field Performance of American Football Helmets. *Ann Biomed Eng* 2020; 48 (11): 2531-2541.
- [3] Gabler LF, Crandall JR, Panzer MB. Development of a Second-Order System for Rapid Estimation of Maximum Brain Strain. *Ann Biomed Eng* 2019; 47 (9): 1971-1981.
- [4] Rowson S, Duma SM, Greenwald RM, et al. Can helmet design reduce the risk of concussion in football? *J Neurosurg* 2014; 120: 919-922.

- [5] Viano DC, Withnall C and Halstead D. Impact performance of modern football helmets. *Ann of Biomed Eng* 2012; 40(1): 160-174.
- [6] Bailey AM, Sanchez EJ, Park G, et al. Development and Evaluation of a Test Method for Assessing the Performance of American Football Helmets. *Ann Biomed Eng* 2020; 48 (11): 2566-2579.
- [7] Rowson S, Duma SM. Development of the STAR Evaluation System for Football Helmets: Integrating Player Head Impact Exposure and Risk of Concussion. *Ann Biomed Eng* 2011; 39 (8): 2130-2140.
- [8] Rush GA, Alston GA III, Sbravati N, et al. Comparison of shell-facemask responses in American football helmets during NOCSAE drop tower tests. *Sports Eng* 2017; 20: 199-211.
- [9] Ziejewski M, Goettler HJ. Effect of Structural Stiffness and Kinetic Energy on Impact Force. SAE Technical Paper, vol. No. 961852, 1996.
- [10] Rowson B, Terrell EJ and Rowson S. Quantifying the effect of the facemask on helmet performance. *J Sports Engineering and Technology* 2018; 232(2): 94-101.
- [11] Bina A, Batt GS and DesJardins J. Development of a non-destructive method to measure football facemask stiffness. *J Sports Engineering and Technology* 2019; 233(2): 175-185.
- [12] Creamer JL, Rogers RR, Benjamin CL, et al. The Influence of Overbuilt Versus Game-Permitted American Football Facemasks on Peripheral Visuomotor Ability in NCAA Division I Football Athletes. *Top Exercise Sci Kinesiology* 2021; 2 (1): 1-8.
- [13] Miller RA, Rogers RR, Williams TD, et al. Effects of Protective American Football Headgear on Peripheral Vision Reaction Time and Visual Target Detection in Division I NCAA Football Players. *Sports* 2019; 7 (213): 1-8.
- [14] Bustamante MC, Bruneau D, Barker JB, et al. Component-level finite element model and validation for a modern American football helmet. *J of Dynamic Behavior of Mater* 2019; 5: 117-131.
- [15] Corrales MA, Gierczycka D, Barker J, et al. Validation of a football helmet finite element model and quantification of impact energy distribution. *Ann Biomed Eng* 2020; 48(1): 121-132.
- [16] Decker W, Baker A, Ye X, et al. Development and multi-scale validation of a finite element football helmet model. *Ann Biomed Eng* 2020; 48(1): 258-270.

- [17] National Football League. The NFL Helmet Challenge, <https://www.playsmartplaysafe.com/nfl-helmet-challenge-symposium/> (2019, accessed 19 March 2022).
- [18] Mills NJ, Gilchrist A. Finite-element analysis of bicycle helmet oblique impacts. *Int J Impact Eng* 2008; 35: 1087-1101.
- [19] Forero Rueda MA, Cui L, Gilchrist MD. Finite element modelling of equestrian helmet impacts exposes the need to address rotational kinematics in future helmet designs. *Comput Method Biomec* 2011; 14 (12): 1021-1031.
- [20] Tan LB, Tse KM, Lee HP, et al. Performance of an advanced combat helmet with different interior cushioning systems in ballistic impact: Experiments and finite element simulations. *Int J Impact Eng* 2012; 50: 99-112.
- [21] Shuaeib FM, Hamouda AMS, Wong SV, et al. A new motorcycle helmet liner material: The finite element simulation and design of experiment optimization. *Mater Des* 2007; 28: 182-195.
- [22] Schwizer P, Demierre M, Smith LV. An experimental and numerical study of softball to facemask impacts. *J Sports Engineering and Technology* 2017; 23 (4): 336-343.
- [23] Johnson KL, Chowdhury S, Lawrimore WB, et al. Constrained topological optimization of a football helmet facemask based on brain response. *Mater Des* 2016; 111: 108-118.
- [24] Hernandez F, Wu LC, Yip MC, et al. Six Degree-of-Freedom Measurements of Human Mild Traumatic Brain Injury. *Ann Biomed Eng* 2015; 43 (8): 1918-1934.
- [25] Miller LE, Urban JE, Kelley ME, et al. Evaluation of Brain Response during Head Impact in Youth Athletes Using an Anatomically Accurate Finite Element Model. *J Neurotraum* 2019; 36: 1561-1570.
- [26] Viano DC, Casson IR, Pellman EJ, et al. Concussion in professional football: brain responses by finite element analysis: part 9. *Neurosurgery* 2005; 57(5): 891-916.
- [27] Taha Z, Arif Hassan MH. Parametric analysis of the influence of elastomeric foam on the head response during soccer heading maneuver. *Procedia Engineer* 2016; 47: 139-144.
- [28] Ferriell WD, Batt GS, DesJardins JD. Finite element validation of 3D American football faceguard structural stiffness models. *J Sports Engineering and Technology* 2021; 235 (3): 201-211.

- [29] Riddell, Inc., "Team Catalog," 2020. [Online]. Available: <http://www.riddell.com/team-catalog/>. [Accessed 21 4 2020].
- [30] National Operating Committee on Standards for Athletic Equipment, "Standard Method of Impact Test and Performance Requirements for Football Faceguards - NOCSAE DOC ND087 - 18m18," February 2018. [Online]. Available: <https://nocsae.org/wp-content/uploads/2018/05/1521576803ND08718m18FootballFGStandard.pdf>. [Accessed 4 March 2020].
- [31] Joseph VR. Space-filling designs for computer experiments: A review. *Qual Eng* 2016; 28 (1): 28-35.
- [32] Sobester A, Leary SJ, Keane AJ. On the Design of Optimization Strategies Based on Global Response Surface Approximation Models. *J Global Optim* 2005; 33: 31-59.
- [33] McKay MD, Beckman RJ, Conover WJ. A comparison of three methods for selecting Values of Input Variables in the Analysis of Output from a Computer Code. *Technometrics* 1979; 21 (2): 239-245.
- [34] Mukaka MM. Statistics Corner: A guide to appropriate use of Correlation coefficient in medical research. *Malawi Med J* 2012; 23 (3): 69-71.
- [35] Schmidt JD, Phan TT, Courson RW, et al. The Influence of Heavier Football Helmet Faceguards on Head Impact Location and Severity. *Clin J Sport Med* 2018; 28 (2): 106-110.

CHAPTER FOUR

COMPARISON OF PARAMETER EFFECT ON PERFORMANCE RESPONSES IN AMERICAN FOOTBALL FACEGUARD MODELS

Introduction

The American football headgear design community—consisting of researchers, equipment manufacturers, and equipment managers, among others—has continued to develop novel testing methodologies [1-4], as well as novel designs [5], to improve athlete safety and performance. Tools like the Summation of Tests for the Analysis of Risk (STAR) helmet rating system [6] and the National Football League (NFL) Helmet Challenge [7] have sought to rank headgear designs based upon critical safety metrics. These rankings give athletes, parents, and equipment managers the safety-related information necessary to make an informed decision about the headgear they may choose to wear or advise their athletes to wear. This improved agency for athletes should continue to be developed, so athletes can make informed decisions about the headgear technology they choose to wear.

Although the headgear design community has made great improvements in headgear technology, minimal design changes have been made to the faceguard. This could be, in part, due to the lack of performance and safety-related metrics that may be used to evaluate a faceguard—rendering potential design changes speculative. One method that has been demonstrated to differentiate between faceguard designs is a structural stiffness measurement [3]. Although this metric is capable of quantifying structural differences between faceguard designs, the preference to a particular stiffness is unclear. For example, a less stiff faceguard may improve impact attenuation [Ferriell

2022] while the original intent of a faceguard was to protect facial structures from catastrophic injury [8]. Additionally, research has shown the faceguard to affect the structure of the helmet by stiffening the entire headgear system which may be detrimental to impact performance [9]. Despite this, other research has found that head injury metrics are not greatly affected by changes in faceguard selection—especially when compared to the effects of the helmet [10].

Another metric that may be used to distinguish between faceguard designs is weight. Research has hypothesized that added weight from a faceguard may lead to athletes leading with the crown of their helmet [8]. The rule established by the National Football League (NFL) in 2014 banned the use of “overbuilt” faceguards. “Overbuilt” is a colloquial term used to categorize faceguards with a large number of bars in the design space. This can intuitively lead to a heavier faceguard. Although the safety of athletes is critical, a heavier faceguard may also affect athlete performance. Since athletes’ safety and performance may be affected by the weight of their faceguards, this performance metric should be reported and compared across faceguards currently available to improve athlete agency—especially considering the weight of specific faceguards are challenging to find on manufacturers’ websites.

A performance metric also discussed in the literature is visibility. Visibility has been shown to be an important consideration for athlete performance and safety [11-16]. Additionally, players lack quantitative comparisons of faceguard visibility metrics. Like weight and structural stiffness, each athlete—or each position—may have a particular preference for the degree of visual obstruction caused by the faceguard. Different metrics

should be developed to allow each athlete the ability to compare the different degrees of visibility within different visual field boundaries.

When comparing different degrees of occlusion caused by faceguards, the physiology that determines visual acuity should be considered. The human visual field is limited to 60 degrees superiorly, 75 degrees inferiorly, and 200 degrees laterally [17]. The physiological basis for types of vision—like in-focus or peripheral—is based upon the concentration of two different types of cells in the retina: cones and rods [18]. Cones are the cells that perceive color and allow for humans to see clearly with high acuity. The portion of the visual field attributed to the high concentration of cones at the center of the retina is called foveal vision. It is widely accepted that foveal vision extends 2 degrees both laterally/medially and superiorly/inferiorly from the line of sight. Conversely, the boundary for when foveal vision becomes peripheral vision is not as consistently defined. For example, the following have been used as the boundary for peripheral vision: anything outside of foveal vision [18, 19]; anything outside of parafoveal and perifoveal vision [19]; anything outside of the central visual field [11, 15, 16, 19]; and anything outside of binocular vision [17]. The degree to which the visual field is occluded is important to player safety [15, 16]. Additionally, the football faceguard has been identified as an obstruction to the visual field [14, 16]; however, an analysis that identifies the contributions of parameters to the occlusion of the visual field has not been done. Furthermore, comparisons between faceguards currently available to athletes has not been reported; therefore, the quantification of the visual occlusion from headgear—

and the faceguard specifically—could be of importance to improving athlete agency in player safety and performance decisions.

Given the considerable lack of faceguard performance data available to athletes to make informed decisions regarding performance and safety related headgear choices, this study seeks to: define new visibility metrics that may be used to evaluate the differences in visibility for faceguard designs; elucidate the differences in three performance metrics—stiffness, mass, and visibility—of reverse-engineered and structurally validated faceguard models of manufacturer’s original designs; and compare the parameters that most influence the performance metrics for different faceguard categories and helmet compatible series. The results from this study will: improve athlete agency in performance- and safety-related protective equipment decisions; inform manufacturers and innovators in the headgear design community of visibility metrics that may be used to further evaluate headgear designs; and explain performance results given differences in parameters and categorical variables of faceguard designs.

Methods

Original Manufacturer’s Design Comparison

Utilizing the methods discussed in Chapter 3, the same reverse engineering, finite element validation, and parametric modeling process was implemented with nine total faceguards from four helmet series spanning four faceguard categories. The nine faceguard models analyzed in this study, shown in Fig. 4.1, were manufactured by Riddell® (Des Plaines, IL), Schutt Sports (Litchfield, IL), or Vicis (Seattle, WA).

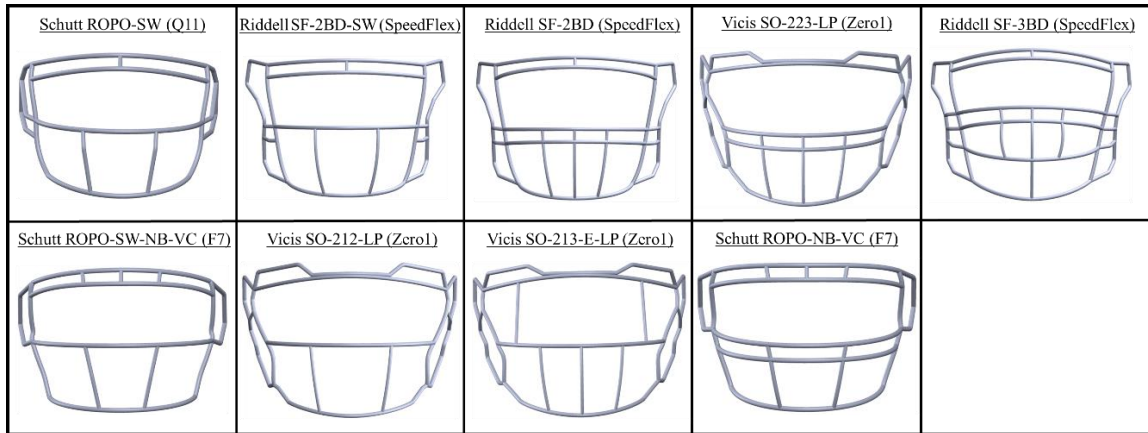


Figure 4.1. The manufacturers, faceguard models, and compatible helmet (in parentheses) analyzed in this study.

The reverse engineering approach was conducted by importing a 3D scanned .stl file image into SOLIDWORKS® (Dassault Systèmes SolidWorks Corporation, Waltham, MA) where the parameter definitions and geometric constraints were defined. The solid model that approximated the geometry of the 3D scan was then imported into ANSYS® Workbench™ 19.0 (ANSYS, Inc., Canonsburg, PA) with appropriate integration of parameters. Upon validation, a parametric approach was defined in a ModeFrontier 2020 (ESTECO, Trieste) workspace using the Uniform Latin Hypercube (ULH) algorithm [21, 22]. The design space was constrained to the designs that did not exceed yield strength of a general stainless steel (207 MPa). This material was applied to each of the faceguards to analyze the differences in the structure. It is unlikely this is the exact material used for the faceguards in this study; however, the proprietary materials used are not known. The decision to model the faceguards as stainless steel structures—when validated against an experimental result—is supported in the literature [22]. Additionally, the bounds on the parameters were selected through an iterative process to ensure the sufficient sampling of

viable designs and to obtain viable geometry per the methods discussed in Chapter 3. The selection for the faceguards in this work, detailed in Table 4.1, was determined by the availability for an experimental study being concurrently performed in the laboratory; however, the selection of the faceguards from the partner study was based upon common faceguards used in the industry. Additionally, the faceguards were selected based upon a sufficient sampling of each of two broad faceguard categories: skill and linemen. These represent an accepted delineation in the preferences of certain positions that can be found on sporting goods websites, is commonly accepted by players, equipment managers, and industry professionals, and is also found in the literature [11]. Lastly, these faceguards selected from the partner study are all commonly available and used at all levels of football including junior, collegiate, and professional.

Table 4.1. Faceguards analyzed in this study with respective manufacturers and compatible helmets.

Manufacturer	Helmet-Compatible	Faceguard Style
Riddell	SpeedFlex	SF-2BD-SW
		SF-2BD
		SF-3BD
Schutt	Q11	ROPO-SW
	F7	ROPO-SW-NB-VC
		ROPO-NB-VC
Vicis	Zero1	SO-212-LP
		SO-223-LP
		SO-213-E-LP

Parametric and Response Analysis

To analyze the effects of the parameters on responses for each of the faceguards, similar approaches to Chapter 3 were followed. For example, the Pearson's Correlation between parameters for the design of experiments was used as verification that the design space was sampled sufficiently [23]. Additionally, the Pearson's Correlation coefficient was used to compare the relationship between parameters and responses.

Visibility Response Definition

Using the Hybrid III 50th percentile male anthropomorphic testing device and image processing to approximate the position of the eyes, visibility metrics were calculated from this reference position for each faceguard. The total visual field considered in this study was defined as $180^{\circ} \times 76^{\circ}$ based upon 180 degrees horizontally measured from the center of the faceguard laterally and 23 degrees superiorly and 53 degrees inferiorly. Although each helmet compatible series has a unique total visual field due to the structure of the helmet-interfacing frame, the visibility metrics developed for this study were designed to objectively compare the design space. The visibility metrics proposed include the central visual field occlusion (CVF-O), peripheral visual field occlusion (PVF-O), and far peripheral field occlusion (FPVF-O) metrics. These visual field categories are illustrated in Fig. 4.2.

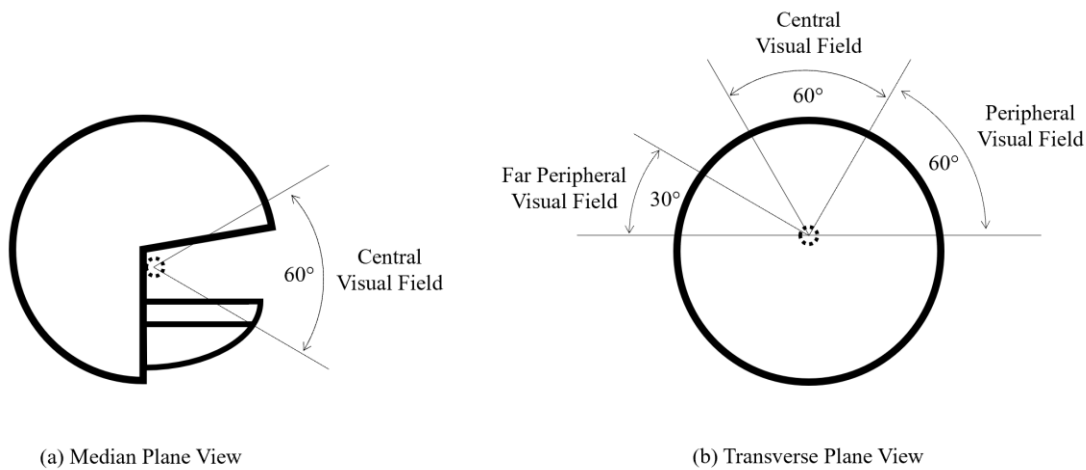


Figure 4.2. (a) Median plane view of a football helmet with the inferior-superior central visual field boundaries overlayed, (b) Transverse plane view of a football helmet with the medial-lateral central, peripheral, and far peripheral visual field boundaries overlayed.

Occlusions to the central visual field are defined by any portion of the faceguard within the central visual field. It is possible this metric will be chiefly important to athletes as this is the portion of vision that is directly in front of the eyes. Occlusions to the peripheral visual field are defined by any portion of the faceguard within the design space but outside of the central visual field. Occlusions to the far peripheral field are defined by any portion of the faceguard that occludes the portion of the visual field limited to monocular view laterally on both sides; thus, this would be the outer 30 degrees on either side of the 180° design space.

The dimension used to define the visual field was the approximate radius of the main (superior) horizontal design bar, D3, which has previously been defined in Chapter 3. This dimension creates a three-dimensional surface that can be considered a cylindrical approximation of the visual field, which is supported in the literature [20]. Horizontal, or

nearly horizontal, occlusions to the visual field were measured using the approximated radius away from the eyes and the radii of each bar. For example, a bar 70 mm away measuring 3 mm in diameter that spans the entire horizontal visual field is going to occlude the visual field by $\theta_1 \times \theta_2$, where $\theta_1 = \tan^{-1}(3/70)^\circ$ and $\theta_2 = 180^\circ$. Similar approaches were used for vertical, or nearly vertical, bars. Oblique bars were analyzed individually, since oblique structures pertinent to the visibility metrics calculated in this study were only found for a single faceguard—the SO-213-E-LP which was parameterized to potentially have oblique eye guards.

The Central Visual Field – Occlusion (CVF-O) metric (4.1) was calculated using an analytical equation of the form:

$$CVF - O = \theta_1 * \alpha \quad (4.1)$$

Where:

$$\theta_1 = \tan^{-1}(DiaL/D3)^\circ \quad (4.2)$$

$$\alpha = 2 * \tan^{-1}\left(x/\sqrt{y^2 + z^2}\right)^\circ \quad (4.3)$$

$$y(D1, D2, D3) \quad (4.4)$$

$$x(y) \quad (4.5)$$

$$z(D3) \quad (4.6)$$

D1 measures the distance from a reference position to the attachment location of the main horizontal design bar on the frame, and D2 measures the angle of the main horizontal design bar—as defined in Chapter 3. DiaL represents the large diameter parameter. These equations calculate the geometric obstruction of the uppermost

horizontal design bar that enters into the central visual field. Additionally, the metric assumes that the central visual field will be occluded completely below the uppermost horizontal bar. This assumption was made as an attempt to quantify the loss of quality of visual field below the faceguard (i.e., during game play, there may be less information below the main horizontal bar that is important to athlete safety and performance). Additionally, this assumption simplified analyses so that an analytical calculation could be more appropriately formulated; however, the measure remains consistent and objective across all faceguards included in the present study by controlling for the location of the reference positions.

The Peripheral Visual Field – Occlusion (PVF-O) metric was calculated by subtracting the occlusions of the horizontal bars, eye guards, and vertical bars from the total design space outside of the central visual field using analytical equations of the form:

$$PVF - O = (180^\circ - 60^\circ) * \beta + \theta_1 * \gamma \quad (4.7)$$

Where:

$$\beta(D1, DiaL) \quad (4.8)$$

$$\gamma(D1) \quad (4.9)$$

In (4.7), β quantifies the obstruction due to the uppermost horizontal bar, whereas γ quantifies vertical bar obstructions like eye guards. Each vertical obstruction was manually added for each vertical obstruction. In this study, only one vertical bar obstructed the peripheral visual field on either side of the median plane (SO-213-E-LP); therefore, only this faceguard included the γ term in the PFV-O metric calculation. It was

assumed that the peripheral visual field is anything outside the CVF but within the design space. Although portions of the horizontal bar and some of the vertical bars may occlude the CVF, the amount of the bar in the CVF was considered to be negligible compared to the occlusion of the PVF. Similar to the CVF-O metric, the peripheral visual field was assumed to be occluded below the obstruction from the uppermost horizontal bar. Furthermore, the effect of D2—the angle of the uppermost horizontal bar—was considered to be negligible in the periphery. Although β was not a function of D3, it still accounted for the lateral distance from the frame to the approximate location of the eyes. Since the frames were not parameterized in this study, these values were manually measured for each faceguard frame and considered to be constants throughout the parametric experiment for each individual faceguard frame.

The Far Peripheral Visual Field – Occlusion (FPVF-O) metric was calculated using the outer 30 degrees of the design space where binocular view is limited and monocular view occurs using analytical equations similar to the PVF-O metric; however, the horizontal obstruction calculation was limited to 180° - 120° . It is important to note that some frames may extend beyond the 180° limit used in this study. Since monocular view can extend 10° on both sides of the 180° limit used in this study, the faceguard frames that limit obstructions in the far peripheral visual field may not be measured appropriately with the FPVF-O metric.

Results

Original Manufacturer's Comparison

The results from this study elucidate quantitative differences between faceguard designs currently available to athletes when comparing multiple metrics. The results displayed in Fig. 4.3 compare the structural stiffness and mass of the original manufacturer's designs. This demonstrates the potential to vary stiffness while maintaining similar mass, as well as vary mass while maintaining similar structural stiffness. Furthermore, this can be achieved across faceguards of different helmet compatible series and styles.

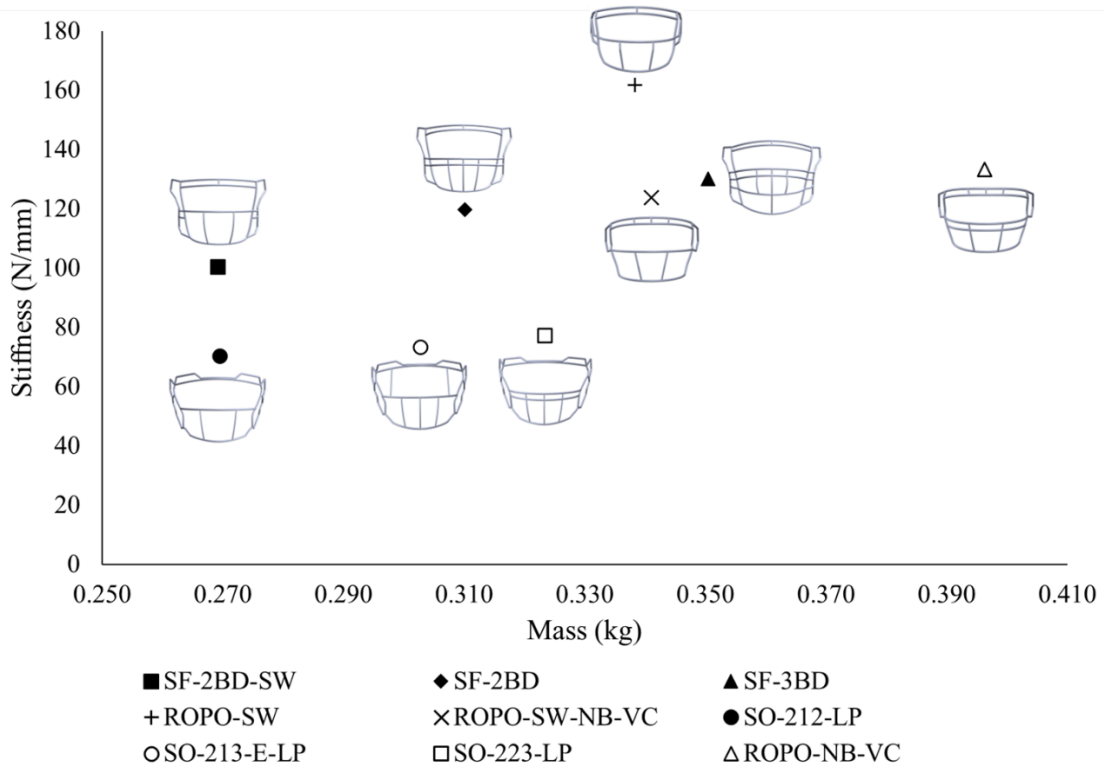


Figure 4.3. Comparison of mass and structural stiffness responses from the models of the original manufacturer's designs.

The results were varied for each of the visibility metrics analyzed, except the peripheral visual field and the far peripheral visual field. The far peripheral visual field – occlusion (FPVF-O) metric was not analyzed further due to the lack of information gained by analyzing in the far peripheral visual field; however, given the inclusion of an eye guard, the results could be more different because a greater percentage of the far peripheral visual field would be occluded. This was made clear by analyzing the PVF-O and FPVF-O metrics for the SO213-E-LP faceguard which has eye guards. The CVF-O and PVF-O metrics for each of the faceguards analyzed in this study are shown in Fig. 4.4.

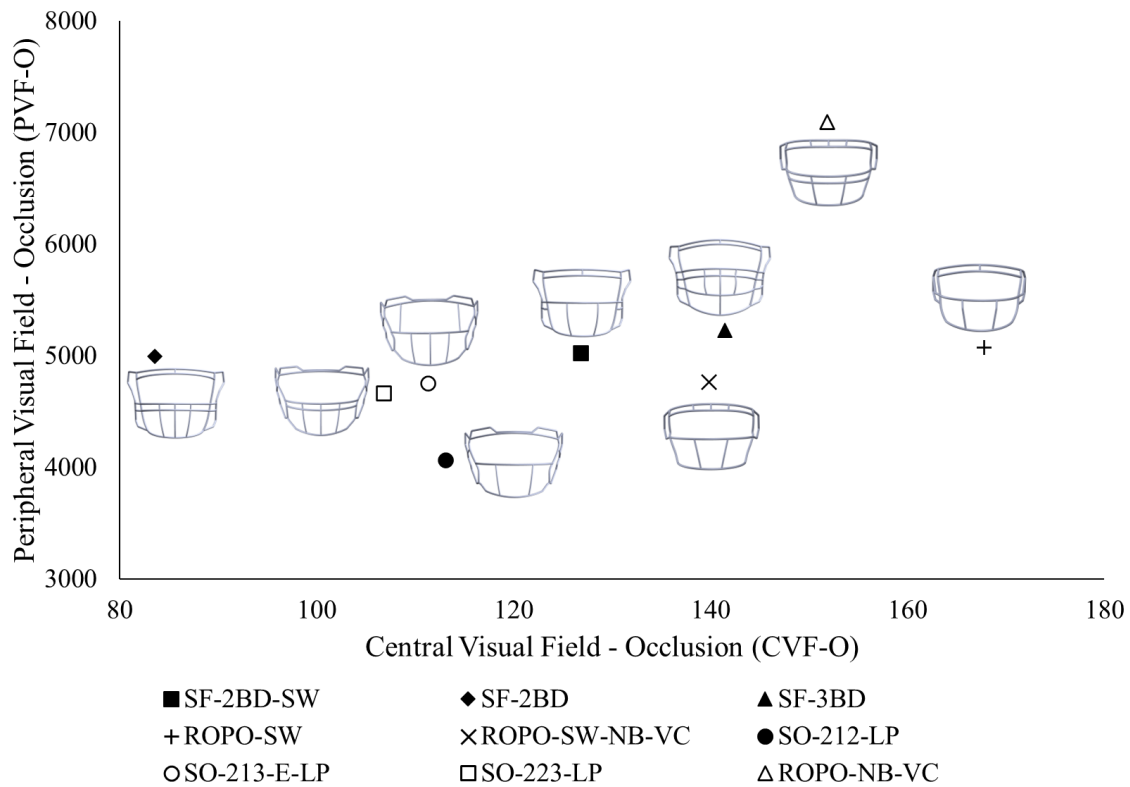


Figure 4.4. Comparison of the CVF-O metric and the PVF-O metric for the original manufacturer’s designs.

The percent difference between the most occluded faceguard in the central visual field (ROPO-SW) and the least occluded faceguard (SO-213-E-LP) was 21%. The percent difference between most occluded and least occluded faceguards in the peripheral visual field was 22%.

Parametric Comparisons

For all faceguards, the greatest predictor of structural stiffness and mass was the larger diameter parameter which defines most of the bar diameters in the frame and design space. For some faceguards, this parameter defines all the bars except the vertical bars in the design space. Large percent changes of mass and stiffness responses, shown in Fig. 4.5, were achieved in viable designs for all faceguards.

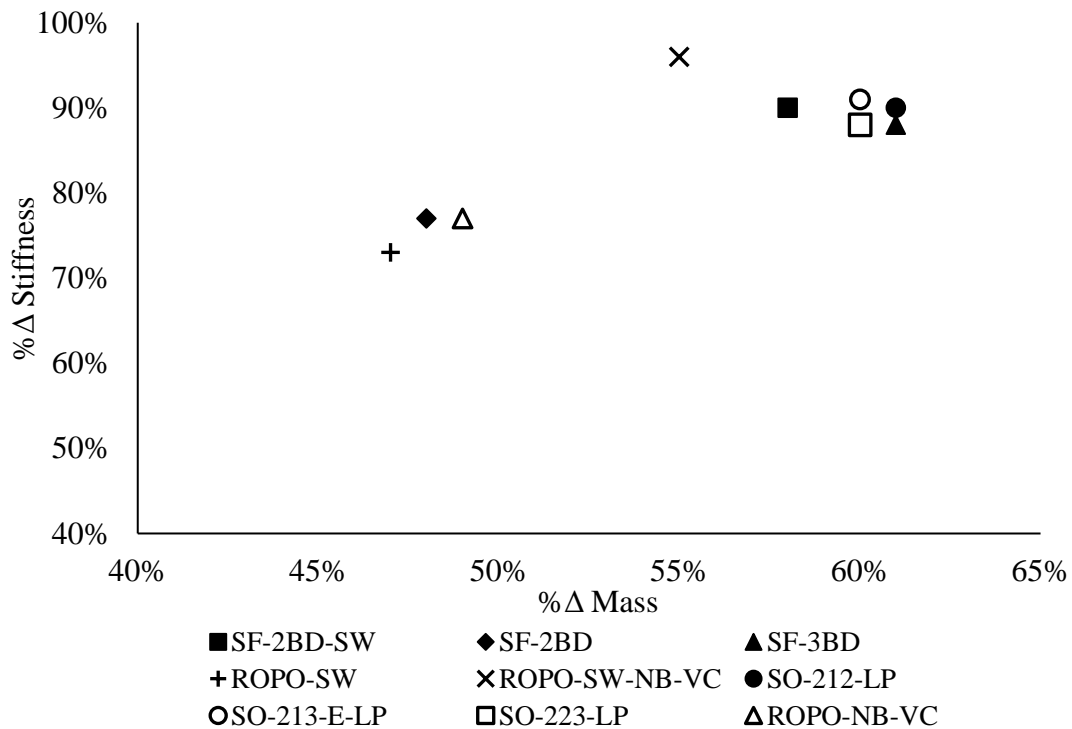


Figure 4.5. Percent changes from maximum responses of viable designs for each faceguard.

Table 4.3 details the values of the Pearson's Correlation Coefficient between the large diameter parameter and structural stiffness for all viable designs of each faceguard. Due to the high degree of correlation between the large diameter parameter and mass for all viable designs of each faceguard, the specific values are not detailed below. All Pearson's Correlation Coefficients between the large diameter parameter and mass were greater than 0.979.

Table 4.3. Correlations between Structural Stiffness and the larger diameter parameter from results of the design of experiments for each faceguard style.

Correlation between Large Diameter Parameters and Structural Stiffness	
Faceguard Style	Pearson's Correlation Coefficient
SF2BD	0.938
SF-3BD	0.928
ROPO-NB-VC	0.916
SF2BDSW	0.898
SO-223-LP	0.883
ROPOSW	0.879
SO-212-LP	0.873
SO-213-E-LP	0.871
ROPO-SW-NB-VC	0.83

Due to the definition and analytical equations used to calculate visibility in this study, the parameters that affect visibility were known prior to analysis. The arc length, large diameter, angle of the primary horizontal bar, and the vertical location along the frame where the horizontal design bar attaches are the parameters that contribute to the occlusion of the central visual field from a faceguard. The large diameter and vertical

location along the frame where the horizontal design bar attaches are the parameters that contribute to the occlusion of the peripheral visual field from a faceguard; however, the occlusion to the peripheral visual field—to a greater extent than the CVF-O metric—was dependent on values measured with respect to each unique frame.

The Pearson's Correlation Coefficient was greater than 0.8 between Mass and Structural Stiffness; greater than 0.7 for stress and structural stiffness; and negligible for visibility and all other performance metrics; thus, the visibility metrics for each faceguard were not predicted by other metrics.

Discussion

These results are the first of their kind to elucidate the parameters most influential to pertinent performance metrics in faceguard design. Faceguard categories can be organized based upon the degree of correlation between large diameter parameter and structural stiffness, as shown in Table 4.3. Additionally, the high degree of correlation between mass and the large diameter parameter for all faceguards suggests the interrelated nature of the mass, structural stiffness, and large diameter parameter. Despite this, the visibility metrics were either weakly or negligibly correlated to the structural stiffness, mass, and large diameter; therefore, the visibility may be altered independent from mass and stiffness which may be important for athletes seeking to maintain stiffness, decrease mass, and decrease visual field obstructions—as an example.

The methods detailed in Chapter 3 and the results presented in this study may afford manufacturers the opportunity to alter their own parameters to influence responses like stiffness, mass, and visibility. Some in the literature have attempted to quantify the

visibility of faceguards [14], but this is the first parametric approach to quantifying the relationship between faceguard performance metrics, parameters, and multiple visibility metrics. The results of the original manufacturer's designs indicate increased visibility in Vicis faceguards when compared to the categorically comparable faceguards from Riddell and Schutt; however, the results may be sensitive to modelling errors.

Considering the validated reverse engineering approach used in this study does not perfectly capture the structural performance of the faceguard [22], these errors could affect the discrepancies in visibility metrics for the faceguard designs. Despite this, inspection of Fig. 4.1 and images from manufacturers' websites will likely confirm the congruity between the computational models used in this study and actual faceguards.

There is a high degree of confidence in the parametric analyses considering the minimal correlations between input variables for most specimen; however, the heavier faceguards (i.e., SF-3BD) did have higher degrees of correlation between input parameters. This means the design space was not uniformly sampled when considering only viable designs. Decisions made from these results should be used cautiously as they may not indicate a sufficient sampling of the entire design space; however, the parameters that were correlated were not influential in any other faceguard design experiment. It is doubtful the results would be affected by the inclusion of more samples to reduce correlations of these non-influential parameters.

It is important to note the limitations of this study. First, the choice of material for each of these experiments were kept the same. Since each faceguard series has a proprietary material—typically a stainless steel, although titanium alloys and aluminum

hollow tubes have also been used—the selection of a standard stainless steel was intended to compare the influence of each faceguard structure on mass and structural stiffness. Future work should attempt to address the ways in which material selection can affect the responses because making design decisions with these models would not be advised until the specific materials and material properties are known; however, a preliminary investigation demonstrated expected results when selecting a material with a decreased elastic modulus (decreased structural stiffness) and decreased density (decreased mass). Second, the approximations for the visibility calculations could be refined to improve their accuracy. Although the computational values were manually validated, other computational measurement techniques and the inclusion of a parameterized frame may more accurately reflect the visibility values from the parametric analyses. Although the Von Mises stress was used to compare to the constraint of the yield strength of the material, the quasi-static loading condition is not indicative of the loading conditions imposed on faceguards during use; thus, to assess the viability of these designs for manufacture more appropriately, a dynamic loading simulation indicative of the loading conditions during use may be able to elucidate the limits of varying the design more clearly.

The human limits of the visual field are entirely within the faceguard design area. There is no portion of the faceguard design area that is limited by human physiology. Thus, these values, while based in physiology, are limited in their use as conceptualizations for objective comparison. These results should not be used as exact

measurements due to the use of cylindrical coordinates to approximate the measurements, which is supported in the literature [20].

The parametric approach used in this study has limitations. Research has demonstrated the limitations of using a parametric approach that does not accommodate for categorical structural changes [25]. Since the parametric approach used in the present study was limited to dimensional parameters, using a method like the approach discussed in the literature could illicit a more robust design tool. Topological optimization, for example, has been used to analyze the effects of structural variables on pertinent brain injury metrics [5]; however, the constraints imposed for this topological optimization did not accommodate for the design possibilities enabled by investment casting. Oblique bars, for example, were excluded from the experiment, and some original manufacturers' faceguards included in this present study have oblique bars. The decision to compare faceguards based upon the dimensional parameters defined in Chapter 3 attempts to inform faceguard manufacturers of the specific dimensions they can alter to improve faceguard performance metrics.

The analysis shows that the primary contribution to mass and structural stiffness is the large diameter parameter. This is critical to improving faceguard design, as future investigations of faceguard design should attempt to innovate the cross section of the bars. An elliptical cross section with parameterized major axis, minor axis, and angle orientation of these axes are one approach that could completely parameterize the cross section. Should innovations arise from the results presented in this study, compliance

with National Operating Committee on Standards for Athletic Equipment (NOCSAE)—specifically, ND087, a standard for evaluating faceguard safety—should be ensured [30].

Especially given the faceguard innovations seen recently from Zuti Facemask and Riddell (see Axiom helmet-compatible faceguards and integration within the helmet system), the need remains to develop testing methodologies and design comparison techniques to better inform athletes, parents, equipment managers, and manufacturers of the parameters pertinent to performance. Future work should continue to compare the latest technology to faceguards currently available. Future work should also attempt to parameterize the frame of the faceguards while monitoring both the changes to the PVF-O metric and the FPVF-O metric. Although this would be a critical step to perform early in the design process for the entire headgear system—given the integration of the faceguard to the helmet shell or other integration method—elucidating the effects different frame parameters may have on visibility could improve these athlete safety and performance metrics.

Conclusion

This study investigated the parameters that affect faceguard performance metrics for common American football faceguards. Nine faceguard styles from four helmet manufacturers were reverse engineered, parameterized, and computationally analyzed for structural stiffness, weight, and visibility to elucidate the variables pertinent to the respective performance metrics. The results indicated the original manufacturers' designs varied greatly. The most critical design parameter for each faceguard analyzed in this study was the large diameter parameter. The stiffness and mass were highly correlated for

each faceguard. The most critical design parameter for visibility was varied; however, the influence of the helmet-compatible frames was not investigated and is hypothesized to influence the peripheral visual field obstruction greatly. The results suggest that manufacturers should investigate the diameter of the bars more thoroughly to innovate to decrease weight and alter structural stiffness to enhance athlete performance while maintaining their safety. Since the visibility metrics were negligibly correlated to structural stiffness and mass, it is possible future studies may be able to alter visibility without affecting structural stiffness or mass. Future studies should investigate the ways in which the cross sections of the bars used for the frame and design space can be innovated. For example, using an elliptical cross section may reduce weight while maintaining stiffness within the stress constraints. A parametric approach to designing the cross sections would improve upon the sport equipment design communities understanding of the ways in which the design of faceguards can improve athlete performance and safety.

References

- [1] Dymek M, Ptak M, Fernandes FAO. Design and Virtual Testing of American Football Helmets-A Review. *Arch Comput Method E* 2021.
- [2] Bailey AM, McMurry TL, Cormier JM, et al. Comparison of Laboratory and On-Field Performance of American Football Helmets. *Ann Biomed Eng* 2020; 48 (11): 2531-2541.
- [3] Gabler LF, Crandall JR, Panzer MB. Development of a Second-Order System for Rapid Estimation of Maximum Brain Strain. *Ann Biomed Eng* 2019; 47 (9): 1971-1981.
- [4] Rowson S, Duma SM, Greenwald RM, et al. Can helmet design reduce the risk of concussion in football? *J Neurosurg* 2014; 120: 919-922.

- [5] Viano DC, Withnall C and Halstead D. Impact performance of modern football helmets. *Ann of Biomed Eng* 2012; 40(1): 160-174.
- [6] Bailey AM, Sanchez EJ, Park G, et al. Development and Evaluation of a Test Method for Assessing the Performance of American Football Helmets. *Ann Biomed Eng* 2020; 48 (11): 2566-2579.
- [7] Rowson S, Duma SM. Development of the STAR Evaluation System for Football Helmets: Integrating Player Head Impact Exposure and Risk of Concussion. *Ann Biomed Eng* 2011; 39 (8): 2130-2140.
- [8] Rush GA, Alston GA III, Sbravati N, et al. Comparison of shell-facemask responses in American football helmets during NOCSAE drop tower tests. *Sports Eng* 2017; 20: 199-211.
- [9] Ziejewski M, Goettler HJ. Effect of Structural Stiffness and Kinetic Energy on Impact Force. SAE Technical Paper, vol. No. 961852, 1996.
- [10] Rowson B, Terrell EJ and Rowson S. Quantifying the effect of the facemask on helmet performance. *J Sports Engineering and Technology* 2018; 232(2): 94-101.
- [11] Bina A, Batt GS and DesJardins J. Development of a non-destructive method to measure football facemask stiffness. *J Sports Engineering and Technology* 2019; 233(2): 175-185.
- [12] Creamer JL, Rogers RR, Benjamin CL, et al. The Influence of Overbuilt Versus Game-Permitted American Football Facemasks on Peripheral Visuomotor Ability in NCAA Division I Football Athletes. *Top Exercise Sci Kinesiology* 2021; 2 (1): 1-8.
- [13] Miller RA, Rogers RR, Williams TD, et al. Effects of Protective American Football Headgear on Peripheral Vision Reaction Time and Visual Target Detection in Division I NCAA Football Players. *Sports* 2019; 7 (213): 1-8.
- [14] Bustamante MC, Bruneau D, Barker JB, et al. Component-level finite element model and validation for a modern American football helmet. *J of Dynamic Behavior of Mater* 2019; 5: 117-131.
- [15] Corrales MA, Gierczycka D, Barker J, et al. Validation of a football helmet finite element model and quantification of impact energy distribution. *Ann Biomed Eng* 2020; 48(1): 121-132.
- [16] Decker W, Baker A, Ye X, et al. Development and multi-scale validation of a finite element football helmet model. *Ann Biomed Eng* 2020; 48(1): 258-270.

- [17] National Football League. The NFL Helmet Challenge, <https://www.playsmartplaysafe.com/nfl-helmet-challenge-symposium/> (2019, accessed 19 March 2022).
- [18] Mills NJ, Gilchrist A. Finite-element analysis of bicycle helmet oblique impacts. *Int J Impact Eng* 2008; 35: 1087-1101.
- [19] Forero Rueda MA, Cui L, Gilchrist MD. Finite element modelling of equestrian helmet impacts exposes the need to address rotational kinematics in future helmet designs. *Comput Method Biomec* 2011; 14 (12): 1021-1031.
- [20] Tan LB, Tse KM, Lee HP, et al. Performance of an advanced combat helmet with different interior cushioning systems in ballistic impact: Experiments and finite element simulations. *Int J Impact Eng* 2012; 50: 99-112.
- [21] Shuaeib FM, Hamouda AMS, Wong SV, et al. A new motorcycle helmet liner material: The finite element simulation and design of experiment optimization. *Mater Des* 2007; 28: 182-195.
- [22] Schwizer P, Demierre M, Smith LV. An experimental and numerical study of softball to facemask impacts. *J Sports Engineering and Technology* 2017; 23 (4): 336-343.
- [23] Johnson KL, Chowdhury S, Lawrimore WB, et al. Constrained topological optimization of a football helmet facemask based on brain response. *Mater Des* 2016; 111: 108-118.
- [24] Hernandez F, Wu LC, Yip MC, et al. Six Degree-of-Freedom Measurements of Human Mild Traumatic Brain Injury. *Ann Biomed Eng* 2015; 43 (8): 1918-1934.
- [25] Miller LE, Urban JE, Kelley ME, et al. Evaluation of Brain Response during Head Impact in Youth Athletes Using an Anatomically Accurate Finite Element Model. *J Neurotraum* 2019; 36: 1561-1570.
- [26] Viano DC, Casson IR, Pellman EJ, et al. Concussion in professional football: brain responses by finite element analysis: part 9. *Neurosurgery* 2005; 57(5): 891-916.
- [27] Taha Z, Arif Hassan MH. Parametric analysis of the influence of elastomeric foam on the head response during soccer heading maneuver. *Procedia Engineer* 2016; 47: 139-144.
- [28] Ferriell WD, Batt GS, DesJardins JD. Finite element validation of 3D American football faceguard structural stiffness models. *J Sports Engineering and Technology* 2021; 235 (3): 201-211.

- [29] Riddell, Inc., "Team Catalog," 2020. [Online]. Available: <http://www.riddell.com/team-catalog/>. [Accessed 21 4 2020].
- [30] National Operating Committee on Standards for Athletic Equipment, "Standard Method of Impact Test and Performance Requirements for Football Faceguards - NOCSAE DOC ND087 - 18m18," February 2018. [Online]. Available: <https://nocsae.org/wp-content/uploads/2018/05/1521576803ND08718m18FootballFGStandard.pdf>. [Accessed 4 March 2020].
- [31] Joseph VR. Space-filling designs for computer experiments: A review. *Qual Eng* 2016; 28 (1): 28-35.
- [32] Sobester A, Leary SJ, Keane AJ. On the Design of Optimization Strategies Based on Global Response Surface Approximation Models. *J Global Optim* 2005; 33: 31-59.
- [33] McKay MD, Beckman RJ, Conover WJ. A comparison of three methods for selecting Values of Input Variables in the Analysis of Output from a Computer Code. *Technometrics* 1979; 21 (2): 239-245.
- [34] Mukaka MM. Statistics Corner: A guide to appropriate use of Correlation coefficient in medical research. *Malawi Med J* 2012; 23 (3): 69-71.
- [35] Schmidt JD, Phan TT, Courson RW, et al. The Influence of Heavier Football Helmet Faceguards on Head Impact Location and Severity. *Clin J Sport Med* 2018; 28 (2): 106-110.

CHAPTER FIVE

ANALYSIS OF PARAMETRIC DESIGN METHODS TO AFFECT PERFORMANCE RESPONSES IN VALIDATED AMERICAN FOOTBALL FACEGUARD STRUCTURAL STIFFNESS MODELS

Introduction

In recent years, American football headgear design innovations have influenced sport equipment standards. As new information has become available through research or novel design methods, standards—like those enforced by the National Operating Committee on Standards for Athletic Equipment (NOCSAE)—have been updated to reflect the latest accurate safety-related data. For example, the linear impactor test method for helmet system analysis [1] and brain injury metrics that utilize measured rotational accelerations [2, 3] have resulted in updated standards for athletic equipment and improved athlete agency through communication of results—like the Virginia Tech Helmet ratings [4] and the National Football League (NFL) Helmet Challenge [5].

One design innovation that has not been explicitly addressed in sport equipment standards is the investment casting of American football faceguards. Currently, non-traditional faceguards are banned by the NFL and National Collegiate Athletics Association (NCAA) [6]. Most faceguards are manufactured using proprietary steel wires of approximately 4-6.5 mm diameter. These bars are then welded and coated with a polyethylene powder coating. Standards exist that address requirements for the manufacture of American football faceguards, such as the requirement that welds fixing two wires must occur outside the ocular area [7]. Although research has not proven the extent to which design innovations using this manufacturing method can increase athlete

safety, the results in Chapters 3 and 4 have proven altering faceguard parameters can influence faceguard performance responses such as mass, structural stiffness, and visibility. With increased design capabilities of investment casting faceguards, manufacturers may be able to alter parameter values to influence faceguard performance metrics according to specific athlete preferences; however, athlete preferences for faceguard performance metrics are not clear, as athlete position and personal preferences may influence these choices.

Overbuilt faceguards, a category of faceguards with a greater number of horizontal and/or vertical bars within the design space than traditional faceguards, are banned for use. Work performed by researchers for the NFL and NCAA have suggested a few reasons for banning overbuilt faceguards [6, 8, 9]. Research has shown that an increased mass of a faceguard can increase the frequency of impacts to the top of the head [6]. Since impacts to the top of the head can lead to catastrophic injury of the head, neck, or spine [6], the researchers suggested increased mass of faceguards should be approached with caution; however, the results were not statistically significant, and there were minimal differences in head injury metrics. Although the researchers hypothesized different reasons why there would be a lack of difference in head injury metrics, the theoretical basis for decreasing the weight of faceguards is sound, since increased strain on neck muscles may lead to fatigue and predispositions to lowering the head.

Other research investigating the use of overbuilt faceguards has suggested that it may lead to a false sense of security or may lead to overly aggressive behavior [8]. Leveraging risk compensation theory, the researchers suggest that athletes are more likely

to feel safe when wearing overbuilt faceguards—when safety may or may not be improved. This misconception is likely to alter athlete behavior and may lead to increased risk of injury. Furthermore, the study reports that athletes would feel more intimidating on the field while using an overbuilt faceguard; however, the article discusses the challenge of quantifying the risk of injury due to altered behavior from feeling intimidating. Lastly, the article suggests that opposing athletes' fingers may be predisposed to getting caught within the gaps of an overbuilt faceguard. Other work attempting to quantify the degree to which faceguards may affect peripheral visuomotor ability states the reason the NCAA banned overbuilt faceguards was due to the increased mass and likelihood of leading with the crown of the helmet [9].

Chapter 4 demonstrated the ability of parametric modeling to influence faceguard performance responses. The results demonstrated the high degree of correlation between structural stiffness response, mass response, and the large diameter parameter of the steel wires. One hypothesized innovation that is not explicitly addressed in NOCSAE standards is the shape, or cross-section, of the steel wires which may influence the mass and structural stiffness of the faceguard. Considering overbuilt faceguards are banned, in part, due to their excess mass, an altered cross section of an overbuilt faceguard manufactured using investment casting may result in a viable and safer design.

Other concerns regarding structural stiffness of faceguards have been raised in the literature. Research has shown that the faceguard can stiffen the helmet system; however, minimal changes to head injury metrics were measured [10]. It is not clear what the ideal stiffness of a faceguard should be considering the original intent of the faceguard was to

protect facial structures and a faceguard should aid in the impact energy attenuation of the helmet system. One method of altering the stiffness and the mass of a structure is to change the material. Typical materials used for faceguard wires include proprietary steels, titanium alloys, and aluminum tubing [11, 12]; therefore, using a lighter and less stiff material in the investment casting of a football faceguard will decrease the mass and structural stiffness for the same geometric conformation; however, the extent to which the lighter and less stiff material will decrease mass and structural stiffness is not clear.

The goal of this study is three-fold: to evaluate a parameterized cross-section for the bars of an overbuilt faceguard by minimizing the mass response; to reevaluate the same reverse engineered faceguard models previously reported in the literature using an alternate material; and to compare the mass and structural stiffness responses of the overbuilt faceguard model, alternative material models, and the reverse engineered faceguard models previously reported in the literature. Collectively, these three tasks will elucidate the degree to which parameters—namely, geometric parameters that define the cross section of the bars or material properties—will affect the structural stiffness and mass of a faceguard. These results and methods can be used by headgear manufacturers, equipment safety standards organizations, and athletes to better understand faceguard performance characteristics for improved faceguard design.

Methods

Overbuilt Faceguard

To investigate the exclusion of overbuilt faceguards from use in American football, the BrickhouZe—a banned overbuilt faceguard from Zuti Facemasks (Shelby

Township, MI)—was reverse engineered and modeled using a method previously validated and reported in the literature [12]. The BrickhouZe model, which is compatible with the SpeedFlex helmet (Riddell), is shown in Fig. 5.1.

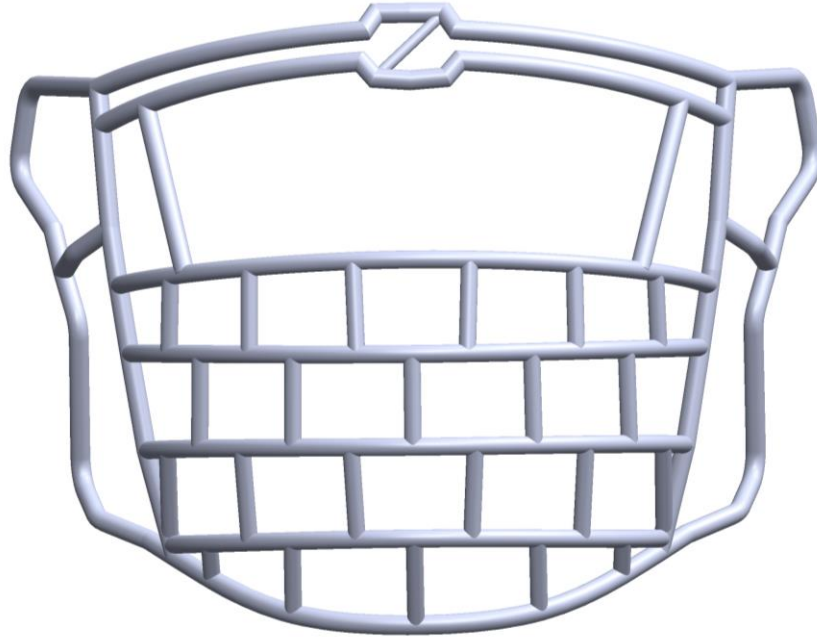


Figure 5.1. Reverse engineered model of the BrickhouZe faceguard manufactured by Zuti Facemasks.

The results of the mass and structural stiffness [13] performance metrics were then compared to results from Chapter 4 to evaluate the exclusion of the overbuilt faceguard category from use.

Cross-section Parameterization and Mass Minimization

Results from Chapters 3 and 4 have proven the cross-sectional area of the faceguard bars—or large diameter parameter—is highly correlated to faceguard mass and structural stiffness, whereas other parameters are much less correlated to these responses; therefore, only the cross-sectional areas of the bars were parameterized in this study. The

cross section of the bars was parameterized as an ellipse with a major axis, minor axis, and angular displacement of the major axis from a reference position. The reference positions were defined by approximating the direction of compression used in the finite element simulation. Since an exact direction was not possible for some of the bars (i.e., the planes did not align so that a parallel reference line could be defined), the bounds on the angle parameters were increased based upon the confidence in the placement of the reference position. The parameter groups were defined based upon the baseline parameter values used to model the reverse engineered original manufacturer's design. The reference positions in each of the parameter groups were free to converge to optimal values that reflect the optimization approach discussed below. The five parameter groups—designated as column vectors in X (5.1)—are organized in Table 5.1 by the baseline parameter values. Parameter groups 1-5 define one, four, three, four, and 22 metal wire cross sections, respectively.

The constrained optimization approach attempted to minimize the mass of the overbuilt faceguard subject to the constraints that the structural stiffness be greater than or equal to 70 N/mm (5.2) and the Von Mises Stress not exceed the ultimate tensile strength of a generic stainless steel (5.3). These constraints provide structural limits on the viability of the design. Considering the mass and structural stiffness are highly correlated, a lack of a structural stiffness constraint would enable unrealistic results; thus, the constraint value for structural stiffness was chosen as it is the lowest value of structural stiffness for the faceguards analyzed in Chapter 4. The three groups of parameters include the major axis (5.4), the minor axis (5.5), and the angle between the

major axis and the reference position (5.6) for each of the faceguard metal wires. The bounds for each of these values are detailed in Table 5.1.

The general optimization approach employed in this study was:

$$\text{Min } f_{mass}(X) \quad (5.1)$$

Subject to:

$$g_1(X) \geq 70 \frac{N}{mm} \quad (5.2)$$

$$g_2(X) \leq 586 \text{ MPa} \quad (5.3)$$

Where:

$$X_1 = [X_{11} X_{12} \dots X_{15}] \quad (5.4)$$

$$X_2 = [X_{21} X_{22} \dots X_{25}] \quad (5.5)$$

$$X_3 = [X_{31} X_{32} \dots X_{35}] \quad (5.6)$$

Table 5.1. The parameter values for the baseline reverse engineered model and the bounds on the parameters used in the optimization approach.

Parameters		Baseline Model Values	Lower Bound	Upper Bound	Units
Major Diameter	$X_{11} - X_{13}$	6.35	4.00	6.50	mm
	X_{14}	5.77	3.50	6.00	
	X_{15}	5.52	3.00	5.75	
Minor Diameter	$X_{21} - X_{23}$	6.35	2.50	6.40	
	X_{24}	5.77	2.25	5.90	
	X_{25}	5.52	2.25	5.60	
Angle	$X_{31} - X_{33}$	90	80	100	degrees
	X_{34}	90	70	110	
	X_{35}	90	70	110	

All elements of the optimization approach detailed above were integrated with ModeFrontier 2020 (ESTECO, Trieste). The Non-dominated Sorting Genetic Algorithm – II (NSGA-II) [14] was used with self-initialization to implement the minimization of the mass response. The NSGA-II was selected due to its preferred performance with non-linear responses and previous use in the literature [11]. Since each design simulation takes approximately three minutes, the experiment was limited to 500 design samples. The results from the optimization approach were then compared to the original manufacturer’s model, as well as previously reverse engineered models, to evaluate the appropriateness of the general overbuilt category’s exclusion from use. Coupled with the results that compared the original design model to previously reverse engineered models, this experiment will clarify whether it is appropriate to exclude the entire overbuilt faceguard category or whether values for mass and structural stiffness responses are most important when considering the exclusion of faceguard technology.

Material Selection

In addition to the investigation of the overbuilt faceguard, the same reverse engineered faceguard models from Chapter 4 were used in this study; however, the material was replaced with a general titanium alloy from ANSYS® Workbench™ 19.0 (ANSYS, Inc., Canonsburg, PA). The material used for the analyses performed previously was a general isotropic stainless steel ($E = 193 \text{ GPa}$, Poisson’s Ratio = 0.31)—this decision was justified following a validation procedure in which the stainless steel achieved reasonable results [12]. In this present study, the manufacturer’s original reverse engineered models were reanalyzed using a general isotropic titanium alloy ($E =$

96 GPa, Poisson's Ratio = 0.36) and compared to the results previously obtained using the general stainless steel. The change in mass and structural stiffness responses was measured to indicate the degree to which changing material affects faceguard performance responses.

Results

Overbuilt Faceguard

The results from the original manufacturer's reverse engineered model reflect large differences in mass and structural stiffness from the faceguard models currently allowed for use. The computational mass was 0.697 kg, which is 46% greater than the next heaviest faceguard modeled in Chapter 4. The computational stiffness was 464 N/mm, which is 65% greater than the next stiffest faceguard modeled in Chapter 4.

Cross-section Parameterization and Mass Minimization

The results from the mass minimization of the BrickhouZe faceguard, an overbuilt style faceguard from Zuti Facemasks, indicate it is possible to decrease the mass when altering elliptical cross-section parameters. In Figs. 5.2 and 5.3, the mass and stiffness responses are plotted as a function of the design evolution. These results demonstrate an approximate convergence within 500 design samples.

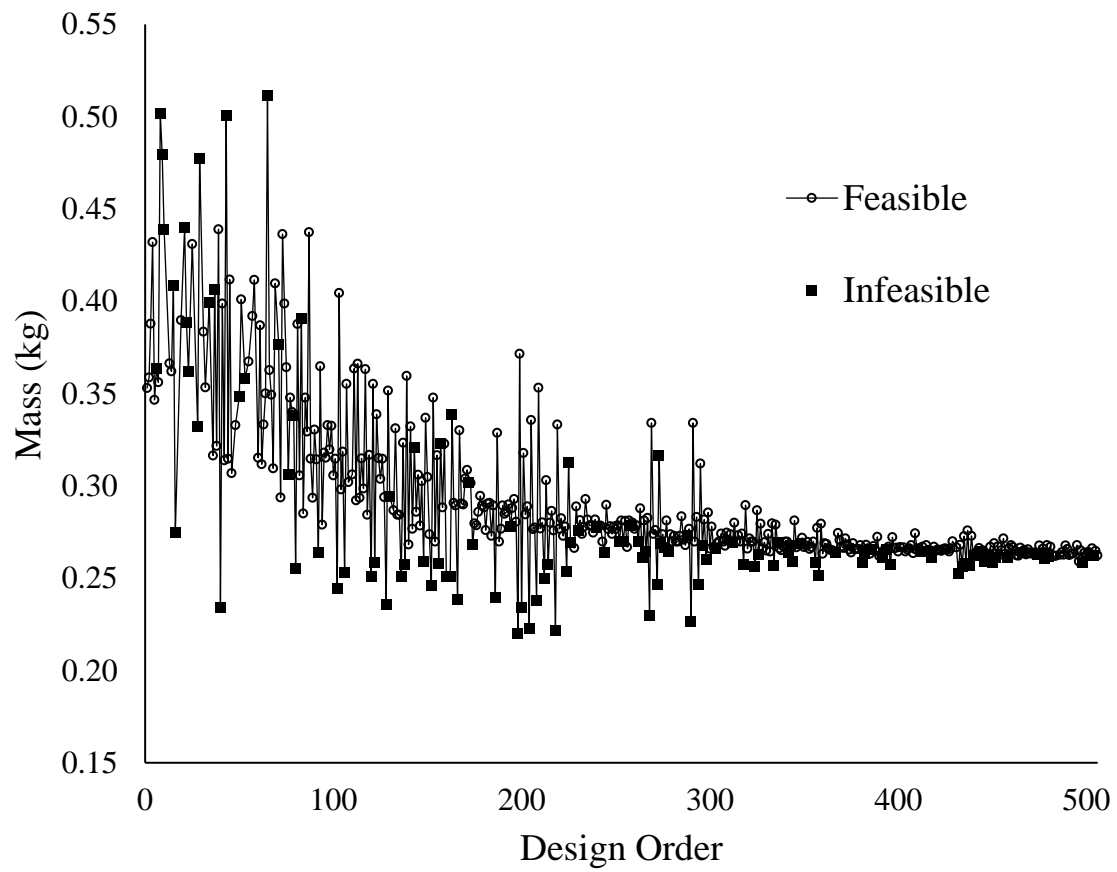


Figure 5.2. Evolution of designs from the minimization approach used in this study demonstrating the decrease in mass.

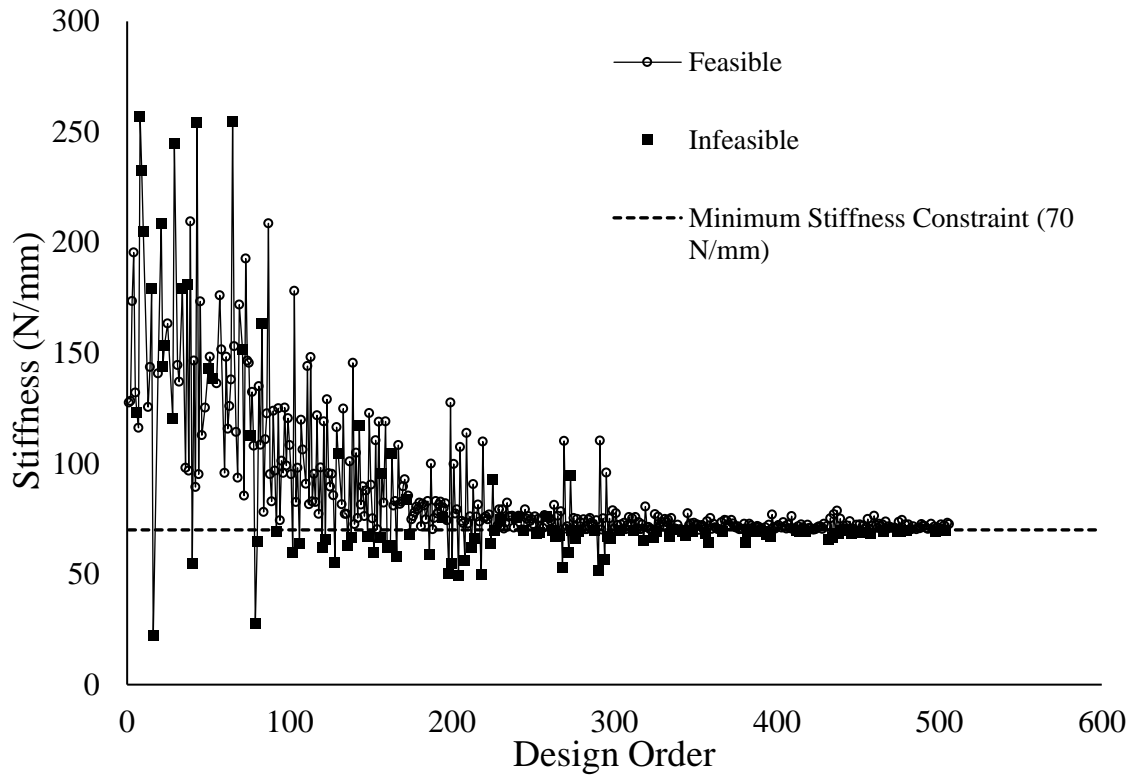


Figure 5.3. Evolution of designs from the minimization approach used in this study demonstrating the decrease in structural stiffness converging around the minimum stiffness constraint (70 N/mm).

Figs. 5.2 and 5.3 show many feasible designs that decrease mass and structural stiffness responses. Table 5.2 compares two of these designs and the respective parameter values to the original reverse engineered model of the manufacturer's design.

Table 5.2. Comparison of two viable designs to the original reverse engineered model of the BrickhouZe faceguard.

	Parameter	Major Axes (X_1), mm					Minor Axes (X_2), mm					Angles (X_3), degrees				
		X_{11}	X_{12}	X_{13}	X_{14}	X_{15}	X_{21}	X_{22}	X_{23}	X_{24}	X_{25}	X_{31}	X_{32}	X_{33}	X_{34}	X_{35}
Design ID	Original	6.35	6.35	6.35	5.77	5.52	6.35	6.35	6.35	5.77	5.52	90	90	90	90	90
	5	4.79	4.67	4.94	5.41	4.78	4.15	4.21	3.05	3.25	3.02	91	95	96	97	80
	500	4.76	4.59	5.06	3.99	3.15	2.87	3.11	3.01	3.56	3.14	86	83	95	79	83

The data in Figs. 5.4 and 5.5 compare two viable designs from the mass minimization experiment to the mass and stiffness ranges of faceguards previously reported in the literature. When compared to faceguards analyzed in Chapter 4, the BrickhouZe model of the original manufacturer's design has a 46% greater mass than the next heaviest faceguard (Schutt F7-compatible ROPO-NB-VC) and is 65% stiffer than the next stiffest faceguard (Schutt Q11-compatible ROPO-SW). Despite this, the minimization approach employed in this study resulted in viable designs that exist within the ranges of mass and stiffness of faceguards currently allowed for use, as proven by comparing the results of this present study to the results in Chapter 4.

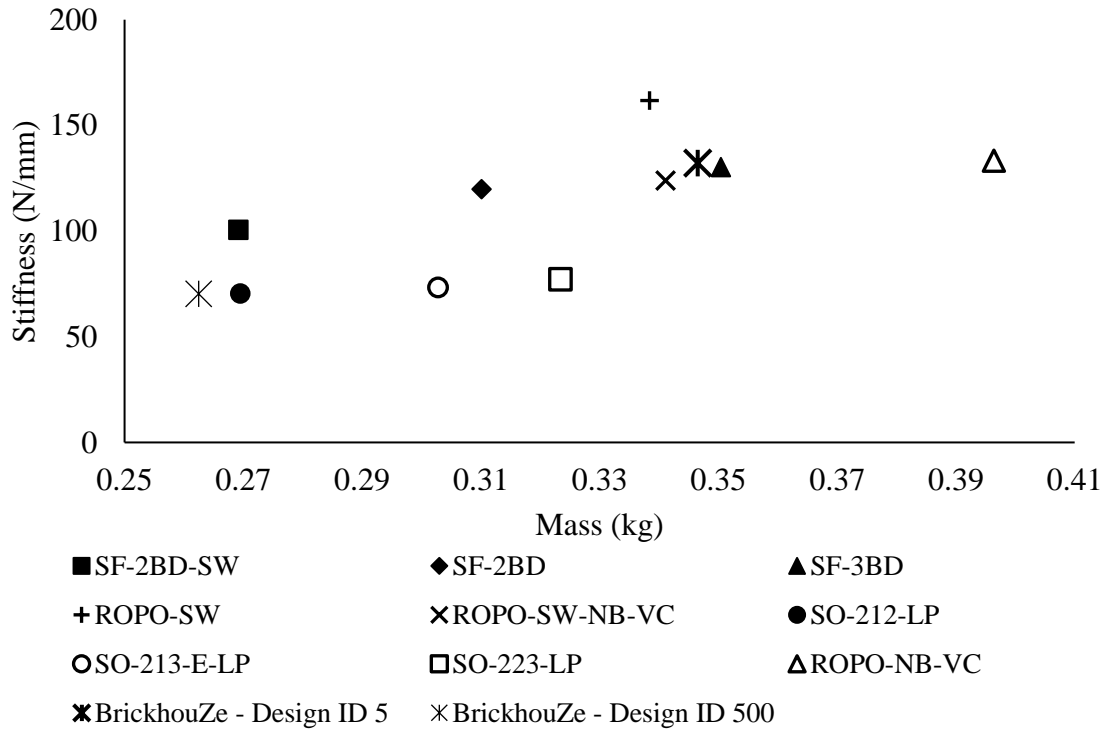


Figure 5.4. Mass and stiffness responses for two viable BrickhouZe designs plotted against results previously reported of original reverse engineered models of manufacturer's designs.

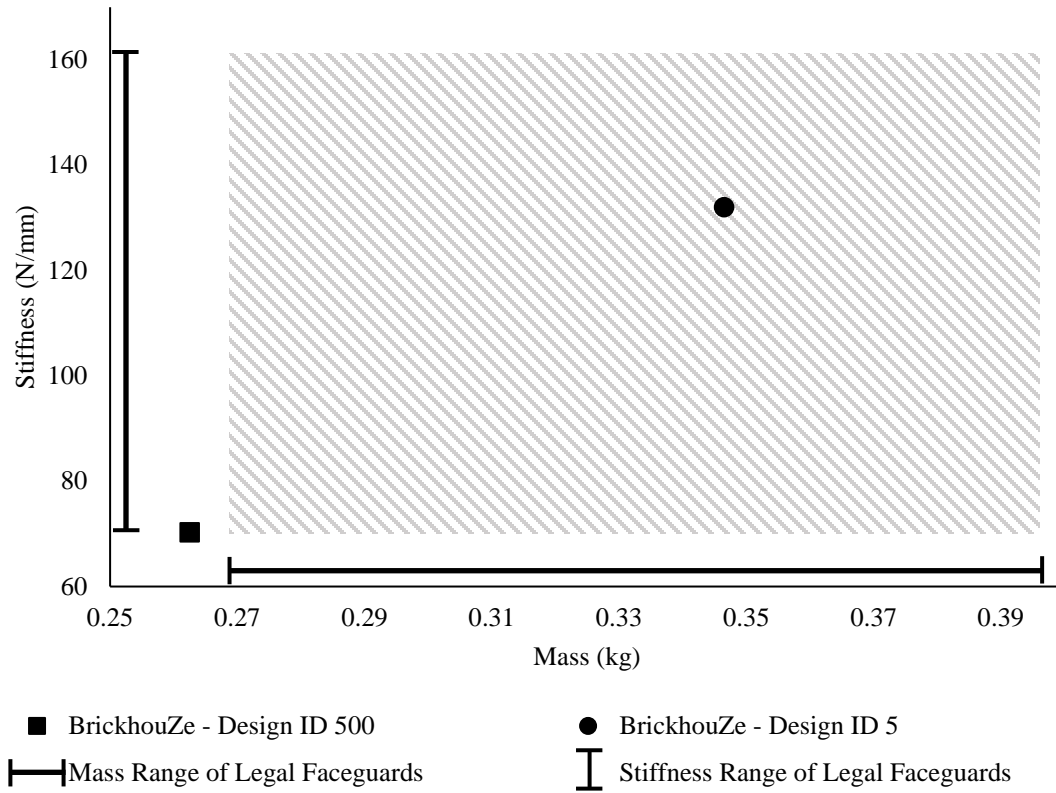


Figure 5.5. Mass and structural stiffness responses for two viable BrickhouZe designs plotted against a gray diagonally striped field representing the ranges for mass and structural stiffness of the legal faceguards analyzed previously in Chapter 4.

Material Selection

The results of changing the material from a stainless steel to a titanium alloy demonstrate decreases in both the mass and structural stiffness responses. The results are shown in Figs. 5.6 and 5.7. Although the reverse engineered model of the original manufacturer's BrickhouZe design decreased in both mass and stiffness, the overbuilt faceguard was slightly greater than the heaviest faceguard analyzed in this study.

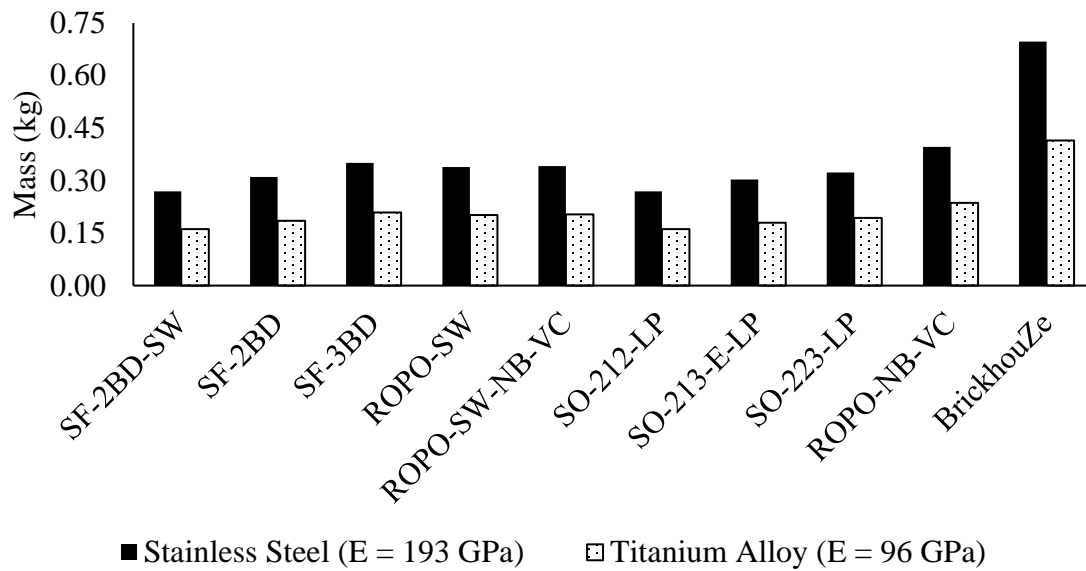


Figure 5.6. Mass responses comparing two materials (stainless steel and titanium alloy) for faceguard models previously reported and the BrickhouZe overbuilt faceguard.

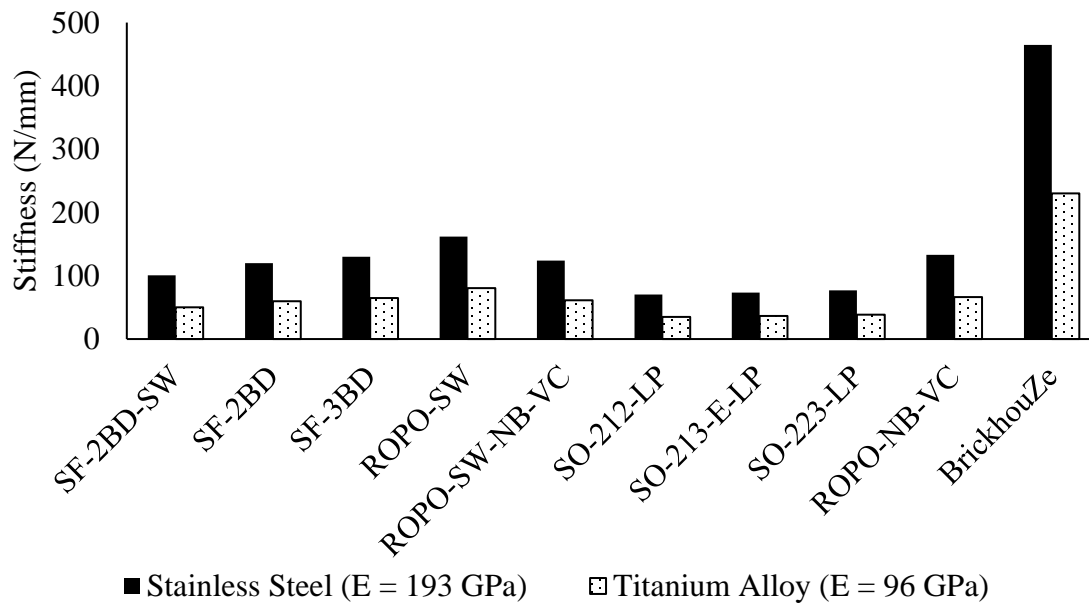


Figure 5.7. Structural stiffness responses comparing two materials (stainless steel and titanium alloy) for faceguard models previously reported and the BrickhouZe overbuilt faceguard.

Discussion

Overbuilt Faceguard

The mass and structural stiffness responses of the original manufacturer's reverse engineered model are much greater than the responses for faceguards currently allowed for use. Considering the primary concern with overbuilt faceguards has been reported to be the increased mass—causing increased likelihood of leading with the crown of the helmet—these results quantify this difference in mass to be 46% greater than the next heaviest faceguard—the ROPO-NB-VC, a Schutt F7-compatible faceguard—as shown in Chapter 4. In each of these models, the large diameter parameters were either as large or larger than most other faceguards. Additionally, the BrickhouZe and ROPO-NB-VC have more metal wires within the design space. Both the increased size of the metal wires and amount of metal wires within the design were the main contributor to the increased mass. For example, the SF-3BD, a Riddell SpeedFlex-compatible faceguard, has more bars than the ROPO-NB-VC; however, the large diameter parameters are much lesser in the SF-3BD model. This comparison indicates the possibility that a more overbuilt faceguard with altered large diameter parameters or cross section shape of the metal wires may decrease the mass.

Cross-section Parameterization and Mass Minimization

The results in Chapter 4 have shown the correlation between the large diameter parameter of American football faceguard metal wires and performance responses such as mass and structural stiffness. The results from the mass minimization approach detailed above—which parameterized only the cross-section shape and size of the metal

wires—demonstrate comparable trends as both the mass and structural stiffness converged similarly as the faceguard design evolved. Figs. 5.4 and 5.5, which compare two designs of the BrickhouZe overbuilt faceguard to reverse engineered models of faceguards currently allowed for use, illustrates the proximity of mass and stiffness responses possible for an overbuilt faceguard due to changes in the cross-section shape and size of the metal wires.

If the entire overbuilt faceguard category is banned from use in American football due to the increased mass compared to other faceguards [9], the results from this study challenge the banning of the entire faceguard style category. Although the manufacturer's original design was much heavier than the next heaviest faceguard modeled, innovations to the cross-section shape and size of the metal wires may improve the faceguard performance response to warrant its use. Despite these findings which challenge the rule being applied to the entire faceguard category based upon mass, this study does not address other concerns with the overbuilt faceguard category being banned. For example, the occlusion to the visual field was not explored. Extensive research has suggested the occlusions to the visual field, particularly the peripheral visual field, can increase the risk of injury to athletes [9, 15, 16]. It is hypothesized overbuilt faceguards occlude the visual field to a greater extent than other faceguards; however, the degree to which the overbuilt faceguard used in this study occluded the visual field was not investigated. Future work should compare the degree of occlusion from overbuilt faceguards and faceguards currently allowed for use. Chapter 4 demonstrated the differences in visual field occlusions between faceguard designs; therefore, those results may provide

manufacturers target ranges of occlusion to the visual field for their overbuilt faceguard designs. In addition to quantifying the degree of occlusion to the visual field, other concerns for allowing the use of overbuilt faceguards that were not addressed in this study include the effects on player attitude while wearing an overbuilt faceguard and the likelihood of opponent fingers becoming entrapped within the smaller geometries of an overbuilt faceguard. Future work should investigate the degree to which these concerns are related to injury on the field since reported data does not clearly indicate there is a relationship [8].

This study used a reverse engineered model of an overbuilt faceguard style in a finite element simulation of a structural stiffness test to perform a mass minimization approach using changes in the cross section of the metal wires to effect mass and structural stiffness responses. This simulation did not account for a dynamic loading condition. Although research has shown the ability to differentiate between faceguard designs using experimental and computational structural stiffness tests [12, 13], it is not clear if the viable designs presented in this study would be viable designs given a dynamic loading condition. Future work should include the development of a validated dynamic finite element simulation that can be used to ensure the viability of the proposed designs in this study. For example, it is possible the size and shape of the cross sections for Design ID 500 may permanently deform subject to a dynamic loading condition. This is likely to occur as faceguards commonly permanently deform after extensive use; however, fracturing or weld separation would render a faceguard design invalid according to NOCSAE standards [17]. Alternatively, future work could include the

manufacture of proposed overbuilt faceguard designs and test each according to NOCSAE standards. The results from the NOCSAE tests, which currently include multiple dynamic loading conditions using a linear drop tower or pneumatic linear impactor [1, 7], may better inform the athletic equipment safety standards community of the viability of overbuilt faceguard designs being used by athletes.

Material Selection

In addition to the decrease in faceguard mass resulting from changes to the large diameter parameter and cross section shape of the metal wires, a change in material can also alter faceguard performance responses. The results, shown in Figs. 5.6 and 5.7, clearly demonstrate the effect material selection can have on the mass and structural stiffness of faceguards. Intuitively, a material with a lesser density and elastic modulus will proportionally affect the mass and structural stiffness of the faceguards. The percent difference of elastic moduli between the general stainless steel and titanium alloy was 50.26%. The average percent difference of the structural stiffness responses between the general stainless steel and titanium alloy models was 50.34%.

Conclusion

Overbuilt faceguards, like the BrickhouZe from Zuti Facemasks, are currently too heavy to be used safely in American football. For example, the BrickhouZe is 46% heavier than the Schutt F7-compatible ROPO-NB-VC, which was the heaviest faceguard analyzed in Chapter 4 that is currently allowed for use. With the vast design capabilities of investment casting, precise parameter values can be manufactured to achieve preferred responses. This study found that changes in the cross-section shape and material can

result in similar mass and structural stiffness values to faceguard designs currently allowed for use. Although not all aspects of the justifications for banning overbuilt faceguards were investigated in this work, this study found that an overbuilt faceguard can achieve similar masses as faceguards currently allowed for use. Additionally, this study found that proportional changes in faceguard mass (density) and structural stiffness (elastic modulus) can be achieved by manufacturing with a different material. Future work should investigate the ability of proposed overbuilt designs to successfully complete NOCSAE standards and withstand dynamic loading conditions. To increase athlete agency in their performance and safety related decisions, standards should be updated to advise manufacturers on the extent of the design innovations viable for safe use.

References

- [1] National Operating Committee on Standards for Athletic Equipment, "Standard Linear Impactor Test Method and Equipment Used in Evaluating the Performance Characteristics of Protective Headgear and Faceguards," June 2021. [Online]. Available: <https://nocsae.org/wp-content/uploads/2018/05/ND081-18am21-Standard-Pneumatic-Ram-Test-Method.pdf>. [Accessed 8 May 2022].
- [2] A. M. Bailey, E. J. Sanchez, G. Park, L. F. Gabler, J. R. Funk, J. R. Crandall, M. Wonnacott, C. Withnall, B. S. Myers and K. B. Arbogast, "Development and Evaluation of a Test Method for Assessing the Performance of American Football Helmets," *Annals of Biomedical Engineering*, vol. 48, no. 11, pp. 2566-2579, 2020.
- [3] L. F. Gabler, J. R. Crandall and M. B. Panzer, "Development of a Second-Order System for Rapid Estimation of Maximum Brain Strain," *Annals of Biomedical Engineering*, vol. 47, no. 9, pp. 1971-1981, 2019.
- [4] S. Rowson and S. M. Duma, "Development of the STAR Evaluation System for Football Helmets: Integrating Player Head Impact Exposure and Risk of Concussion," *Annals of Biomedical Engineering*, vol. 39, no. 8, pp. 2130-2140, 2011.

- [5] National Football League, "The NFL Helmet Challenge," in HeadHealthTech Challenge Symposium, Youngstown, OH, 2019.
- [6] J. D. Schmidt, T. T. Phan, R. W. Courson, F. Reifsteck III, E. D. Merritt and C. N. Brown, "The Influence of Heavier Football Helmet Faceguards on Head Impact Location and Severity," *Clinical Journal of Sports Medicine*, vol. 28, no. 2, pp. 106-110, 2018.
- [7] National Operating Committee on Standards for Athletic Equipment, "Standard Test Method and Equipment Used in Evaluating the Performance Characteristics of Headgear/Equipment," June 2020. [Online]. Available: <https://nocsae.org/wp-content/uploads/2018/05/ND001-17m20.pdf>. [Accessed 8 May 2022].
- [8] E. E. Swartz, J. K. Register-Mihalik, A. Bartlett and K. Guskiewicz, "The Effect of Football Helmet Facemask Style on Perceived Player Behavior: A Pilot Study," *Athletic Training and Sports Health Care*, vol. 11, no. 6, pp. 273-279, 2019.
- [9] J. L. Creamer, R. R. Rogers, C. L. Benjamin, J. P. Marsh, T. D. Williams and C. G. Ballmann, "The Influence of Overbuilt Versus Game-Permitted American Football Facemasks on Peripheral Visuomotor Ability in NCAA Division I Football Athletes," *Topics in Exercise Science and Kinesiology*, vol. 2, no. 1, pp. 1-8, 2021.
- [10] G. A. Rush, G. A. Alston III, N. Sbravati, R. Prabhu, L. N. Williams, J. L. DuBien and H. M. F, "Comparison of shell-facemask responses in American football helmets during NOCSAE drop tower tests," *Sports Engineering*, vol. 20, pp. 199-211, 2017.
- [11] K. L. Johnson, S. Chowdhury, W. B. Lawrimore, Y. Mao, A. Mehmani, R. Prabhu, G. Rush and M. F. Horstemeyer, "Constrained Topological Optimization of a Football Helmet Facemask based on Brain Response," *Materials and Design*, vol. 111, pp. 108-118, 2016.
- [12] W. D. Ferriell, G. S. Batt and J. D. DesJardins, "Finite element validation of 3D American football faceguard structural stiffness models.," *Proceedings of the Institution of Mechanical Engineers, Part P: Journal of Sports Engineering and Technology*, vol. 235, no. 3, pp. 201-211, 2021.
- [13] A. Bina, G. S. Batt and J. DesJardins, "Development of a Non-destructive Method to Measure Football Facemask Stiffness," *Journal of Sports Engineering and Technology*, vol. 233, no. 2, pp. 175-185, 2019.
- [14] K. Deb, A. Pratap, S. Agarwal and T. Meyarivan, "A fast and elitist multiobjective genetic algorithm: NSGA-II," *IEEE transactions on evolutionary computation*, vol. 6, no. 2, pp. 182-197, 2002.

- [15] J. F. Clark, J. K. Ellis, T. M. Burns, J. M. Childress and J. G. Divine, "Analysis of Central and Peripheral Vision Reaction Times in Patients with Postconcussion Visual Dysfunction," *Clinical Journal of Sports Medicine*, vol. 27, no. 5, pp. 457-461, 2017.
- [16] R. A. Miller, R. R. Rogers, T. D. Williams, M. R. Marshall, J. R. Moody, R. W. Hensarling and C. G. Ballmann, "Effects of Protective American Football Headgear on Peripheral Vision Reaction Time and Visual Target Detection in Division I NCAA Football Players," *Sports*, vol. 7, no. 213, pp. 1-8, 2019.
- [17] National Operating Committee on Standards for Athletic Equipment, "Standard Method of Impact Test and Performance Requirements for Football Faceguards - NOCSAE DOC ND087 - 18m18," February 2018. [Online]. Available: <https://nocsae.org/wp-content/uploads/2018/05/1521576803ND08718m18FootballFGStandard.pdf>. [Accessed 4 March 2020].

CHAPTER SIX

CONCLUSION

Summary

This work has presented a reverse engineering, parameterization, and finite element simulation method that can be used to improve the design of American football faceguards. The results have: validated the reverse engineering and finite element simulation protocol; demonstrated preferred sampling of the design space and an ability to differentiate between faceguard designs based upon the parameters defining faceguard structures; compared four faceguard performance responses—mass, structural stiffness, central visual field occlusion, and peripheral visual field occlusion—for models of legal faceguards currently in use; and detailed methods to decrease mass of heavier faceguards using changes in material and altered cross-sections of metal wires constituting faceguard structures.

As presented in Chapter 2, the method of model generation and faceguard validation is important for ensuring accuracy of individual components of headgear systems. The models presented in this study can be used within simulations of the entire headgear system to improve the accuracy of complex headgear computational models. The models and reverse engineering method were then applied to nine total faceguards so that parameterized faceguard models could be developed using structurally validated simulations.

In Chapter 3, the parameterization method was detailed, validated, and verified. This process included iterating parameter bounds, geometric definitions, and modelling

methods to sufficiently sample the design space and appropriately constrain geometry. This methods development chapter detailed the process such that manufacturers that use a traditional manufacturing method (i.e., bend and weld metal wires) may use a similar approach to parameterize according to their manufacturing method. Furthermore, this chapter provided a framework for the parametric model comparison of nine total faceguard styles.

In Chapter 4, the same reverse engineering, finite element validation, and parametric modelling method was used to compare nine faceguards according to four faceguard performance metrics—mass, structural stiffness, Central Visual Field-Occlusion (CVF-O) and Peripheral Visual Field-Occlusion (PVF-O). The results indicated: the most critical design parameter for affecting mass and structural stiffness was the large diameter parameter; the stiffness and mass were highly correlated for each faceguard; the visibility metrics did not correlate to other responses; and the responses varied for each faceguard style and helmet-compatible series. The implications of these results include providing athletes with greater agency in their safety and performance related decisions by comparing these faceguards according to these four metrics. Athletes can use these results to consider the effects that a faceguard may have on their safety and performance when they are deciding which headgear system to use. Manufacturers may be able to use these results to alter the designs that are currently available to have a desired effect on faceguard performance metrics (i.e., increasing or decreasing weight, increasing or decreasing structural stiffness, increasing or decreasing occlusions to the visual field).

As presented in Chapter 5, the BrickhouZe overbuilt faceguard from Zuti Facemasks was modeled. The BrickhouZe is 46% heavier than the Schutt F7-compatible ROPO-NB-VC, which was the heaviest faceguard analyzed in Chapter 4. After parameterizing the cross-section of the BrickhouZe metal wires, this study found that changes in the cross-section shape and material can result in similar mass and structural stiffness values to faceguard designs currently allowed for use. Although not all justifications for banning overbuilt faceguards were investigated in this work, this study found that an overbuilt faceguard can achieve similar masses as faceguards currently allowed for use. Additionally, this study found that proportional changes in faceguard mass (density) and structural stiffness (elastic modulus) can be achieved by manufacturing with a different material. These results challenge the blanket ban of the overbuilt faceguard category based solely on mass. Additionally, the results prove the methods may be used by headgear manufacturers to decrease faceguard mass by altering the faceguard metal wire cross-sections.

Future Work

The methods employed in this study are based upon work completed previously in the laboratory that identified structural stiffness as a unique property of individual faceguard designs. This quasi-static experimental test does not completely describe the faceguard performance. For example, the structural stiffness does not correlate with the visibility metrics developed for this study. Similarly, it is possible the structural stiffness does not correlate to dynamic performance. A major limitation of this study is the lack of a dynamic simulation or experimental verification that the proposed design innovations

(i.e., changing the cross-section shape of an overbuilt faceguard) can produce viable designs within the ranges of mass and structural stiffness of the legal faceguards currently in use.

Although the faceguard is not the primary mechanism for impact attenuation within the headgear system, athlete safety is likely dependent on the faceguard's mass, structural stiffness, and occlusions to the visual the field. Future work should further study the degree to which the visual field can affect athlete safety. Although work has been performed to quantify the effect of a faceguard on reaction time, a direct relationship between occlusions to the visual field from a faceguard and traumatic brain injury risk have not been established. Additionally, the degree to which increased mass affects traumatic brain injury risk during gameplay should be investigated further. Despite this, a decreased mass is hypothesized to be preferred for athlete performance; therefore, manufacturers should continue to develop methods for innovating structure and material such that mass of the faceguard is decreased.

In Chapter 4, two visibility metrics were defined and used to compare currently available faceguard styles. The nine faceguards analyzed were from four helmet-compatible series (i.e., groups of faceguards that can configure with a specific helmet). To configure with the respective helmet, faceguards from different helmet-compatible series have different outer frames. Considering this study did not explicitly investigate the effect of the outer frame on visibility metrics—or other faceguard performance responses—future work should compare the effects of frame design on faceguard performance. Headgear manufacturers should use this body of work to inform integrated

headgear design to optimize player safety and performance considering objective responses from the helmet, faceguard, and other component systems.

APPENDICES

Appendix A

Riddell SpeedFlex SF-2BD-SW Results

Original Manufacturer's Design

Table A1. List of initial parameter values for the reverse engineered SF-2BD-SW.

Solidworks Parameter	ModeFrontier Parameter	Value	Description
ANS_D1	D1	17.6581mm	Nose Visibility (Translation of Nose Bar)
ANS_D2	D2	90.00°	Nose Visibility (Rotation of Nose Bar)
ANS_D3	D3	77.04158955mm	Nose Protection
ANS_D4	D4	39.03082464mm	Cheek Bone Protection
ANS_D5	D5	12.826823mm	Nose Sharpness Index
ANS_D6	D4	39.03082464mm	Upper Mouth Protection
ANS_D7	D7	27.900416mm	Lower Mouth Protection
ANS_D8	D8	90.00°	Left Side Vertical Bar Angle
ANS_D9	D8	90.00°	Right Side Vertical Bar Angle
ANS_D10	D10	38.00697708mm	Left Side Vertical Bar Apex Length
ANS_D11	D11	9.490063mm	Left Side Vertical Bar Apex Height
ANS_D12	D10	38.00697708mm	Right Side Vertical Bar Apex Length
ANS_D13	D11	9.490063mm	Right Side Vertical Bar Apex Height
ANS_Dia1-7	DiaL	4.7625mm	Large Diameter Bars
ANS_Dia8-10	DiaS	3.69mm	Small Diameter Bars

Table A2. Responses for the reverse engineered SF-2BD-SW model.

	Original Manufacturer's Design Response Results			
Faceguard	Mass (kg)	Stiffness (N/mm)	CVF-O	PVF-O
SF-2BD-SW	0.269	101	188	5031

Results from Parametric Analysis

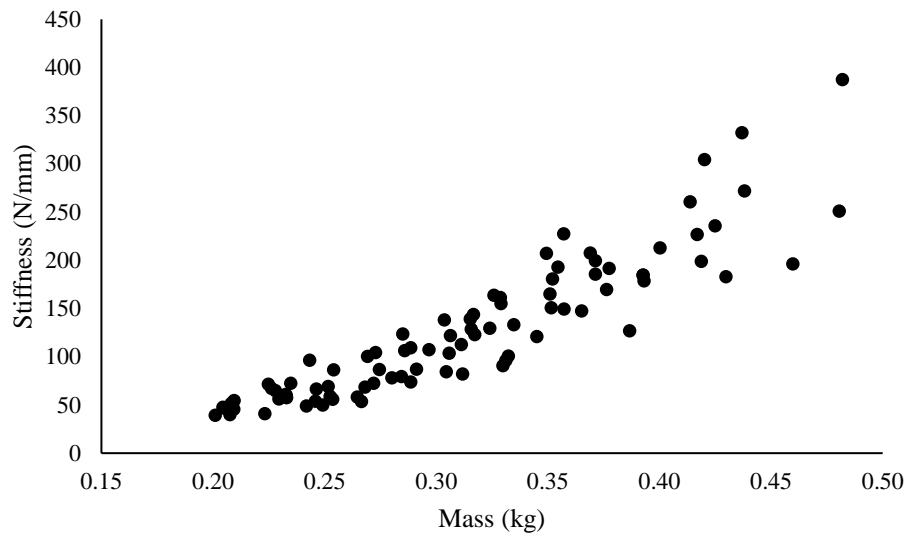


Figure A1. Mass and Stiffness responses for all viable designs for the SF-2BD-SW parametric analysis.

Table A3. Percent change of responses for all viable designs from the SF-2BD-SW parametric analysis.

	Percent Change in Response Among Viable Designs			
Faceguard	Structural Stiffness	Mass	CVF-O	PVF-O
SF-2BD-SW	90%	58%	97%	42%

Appendix B

Riddell SpeedFlex SF-2BD Results

Original Manufacturer's Design

Table A4. List of initial parameter values for the reverse engineered SF-2BD.

Solidworks Parameter	ModeFrontier Parameters	Value	Description
ANS_D1	D1	47.71560mm	Nose Visibility (Translation of Nose Bar)
ANS_D2	D2	90.00°	Nose Visibility (Rotation of Nose Bar)
ANS_D3	D3	82.271592mm	Nose Protection
ANS_D4	D4	40.912219mm	Cheek Bone Protection
ANS_D5	D5	14.220985mm	Nose Sharpness Index
ANS_D6	D4	40.912219mm	Upper Mouth Protection
ANS_D7	D7	28.55469394mm	Lower Mouth Protection
ANS_D8	D8	90.00°	Left Side Vertical Bar Angle
ANS_D9	D8	90.00°	Right Side Vertical Bar Angle
ANS_D10	D10	30.55236655mm	Left Side Vertical Bar Apex Length
ANS_D11	D11	5.66247957mm	Left Side Vertical Bar Apex Height
ANS_D12	D10	30.55236655mm	Right Side Vertical Bar Apex Length
ANS_D13	D11	5.66247957mm	Right Side Vertical Bar Apex Height
ANS_D14	D14	31.63171385mm	Mid Vertical Bar Apex Length
ANS_D15	D15	5.22171906mm	Mid Vertical Bar Apex Height
ANS_D16	D16	17.71410973mm	Secondary Horizontal Bar Offset Distance
ANS_D17	D17	90.00°	Secondary Horizontal Bar Offset Angle
ANS_Dia1-10	DiaL	4.7625mm	Frame/Horizontal Bar Diameter
ANS_Dia11-14	DiaS	3.69mm	Vertical Bar Diameter

Table A5. Responses for the reverse engineered SF-2BD model.

	Original Manufacturer's Design Response Results			
Faceguard	Mass (kg)	Stiffness (N/mm)	CVF-O	PVF-O
SF-2BD	0.310	120	178	4995

Results from Parametric Analysis

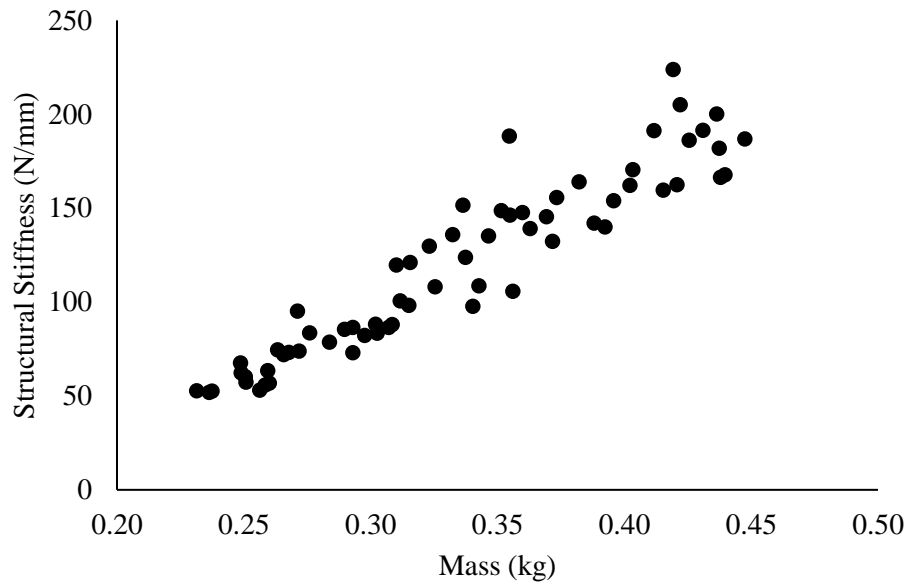


Figure A2. Mass and Stiffness responses for all viable designs for the SF-2BD parametric analysis.

Table A6. Percent change of responses for all viable designs from the SF-2BD parametric analysis.

	Percent Change in Response Among Viable Designs			
Faceguard	Structural Stiffness	Mass	CVF-O	PVF-O
SF-2BD-SW	90%	58%	97%	42%

Appendix C

Riddell SpeedFlex SF-3BD Results

Original Manufacturer's Design

Table A7. List of initial parameter values for the reverse engineered SF-3BD.

Solidworks Parameter	ModeFrontier Parameters	Value	Description
ANS_D1	D1	49.28219mm	Nose Visibility (Translation of Nose Bar)
ANS_D2	D2	90.00 °	Nose Visibility (Rotation of Nose Bar)
ANS_D3	D3	75.32476315mm	Nose Protection
ANS_D4	D4	38.28080751mm	Cheek Bone Protection
ANS_D5	D5	9.72816238mm	Nose Sharpness Index
ANS_D6	D4	38.28080751mm	Upper Mouth Protection
ANS_D7	N/A	N/A	Lower Mouth Protection
ANS_D8	D8	90.00 °	Left Side Vertical Bar Angle
ANS_D9	D8	90.00 °	Right Side Vertical Bar Angle
ANS_D10	D1-	24.28751542mm	Left Side Vertical Bar Apex Length
ANS_D11	D11	4.98779481mm	Left Side Vertical Bar Apex Height
ANS_D12	D10	24.28751542mm	Right Side Vertical Bar Apex Length
ANS_D13	D11	4.98779481mm	Right Side Vertical Bar Apex Height
ANS_D14	D14	23.71168792mm	Mid Vertical Bar Apex Length
ANS_D15	D15	4.45161637mm	Mid Vertical Bar Apex Height
ANS_D16	D16	24.7481694mm	Secondary Horizontal Bar Offset Distance
ANS_D17	D17	90.00 °	Secondary Horizontal Bar Offset Angle
ANS_D18	D18	19.00586243mm	Tertiary Horizontal Bar Offset Distance
ANS_D19	D17	90.00 °	Tertiary Horizontal Bar Offset Angle
ANS_Dia1-14	DiaL	4.7625mm	Frame/Horizontal Bar Diameter
ANS_Dia15-18	DiaS	3.69mm	Vertical Bar Diameter

Table A8. Responses for the reverse engineered SF-3BD model.

	Original Manufacturer's Design Response Results			
Faceguard	Mass (kg)	Stiffness (N/mm)	CVF-O	PVF-O
SF-3BD	0.350	130	195	5230

Results from Parametric Analysis

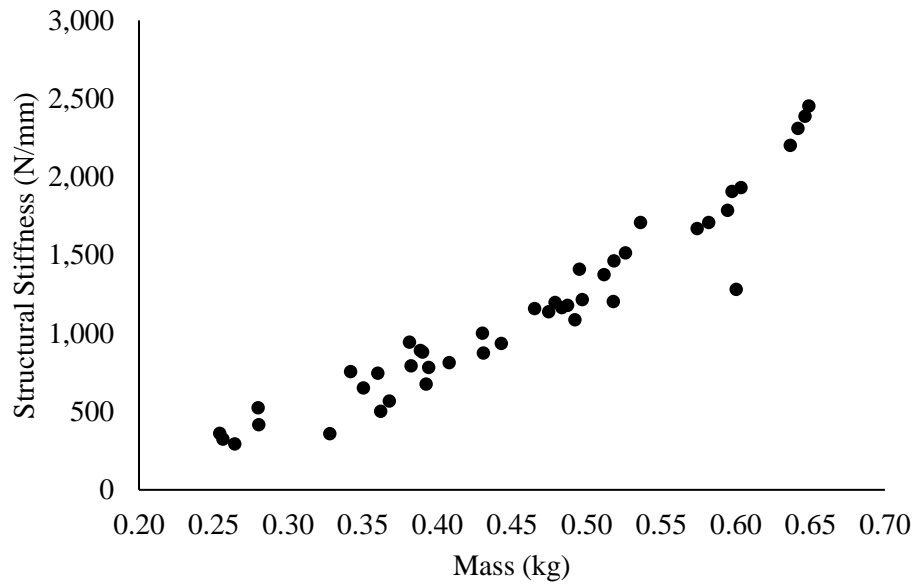


Figure A3. Mass and Stiffness responses for all viable designs for the SF-3BD parametric analysis.

Table A9. Percent change of responses for all viable designs from the SF-3BD parametric analysis.

	Percent Change in Response Among Viable Designs			
Faceguard	Structural Stiffness	Mass	CVF-O	PVF-O
SF-3BD	88%	61%	82%	27%

Appendix D

Schutt Q11 ROPO-SW Results

Original Manufacturer's Design

Table A10. List of initial parameter values for the reverse engineered ROPO-SW.

Solidworks Parameter	ModeFrontier Parameters	Value	Description
ANS_D1	D1	44.11008mm	Nose Visibility (Translation of Nose Bar)
ANS_D2	D2	90.00°	Nose Visibility (Rotation of Nose Bar)
ANS_D3	D3	76.60517315mm	Nose Protection
ANS_D4	D4	41.50000mm	Cheek Bone Protection
ANS_D5	D5	8.58366904mm	Nose Sharpness Index
ANS_D6	D4	41.50000mm	Upper Mouth Protection
ANS_D7	D7	32.24359198mm	Lower Mouth Protection
ANS_D8	D8	90.00°	Left Side Vertical Bar Angle
ANS_D9	D8	90.00°	Right Side Vertical Bar Angle
ANS_D10	D10	19.90582947mm	Left Side Vertical Bar Apex Length
ANS_D11	D11	7.81491764mm	Left Side Vertical Bar Apex Height
ANS_D12	D10	19.90582947mm	Right Side Vertical Bar Apex Length
ANS_D13	D11	7.81491764mm	Right Side Vertical Bar Apex Height
Dia1-5	DiaL	5.55625mm	Large Diameter Parameter
Dia6-8	DiaS	4.7625mm	Small Diameter Parameter

Table A11. Responses for the reverse engineered ROPO-SW model.

	Original Manufacturer's Design Response Results			
Faceguard	Mass (kg)	Stiffness (N/mm)	CVF-O	PVF-O
ROPO-SW	0.338	162	204	5078

Results from Parametric Analysis

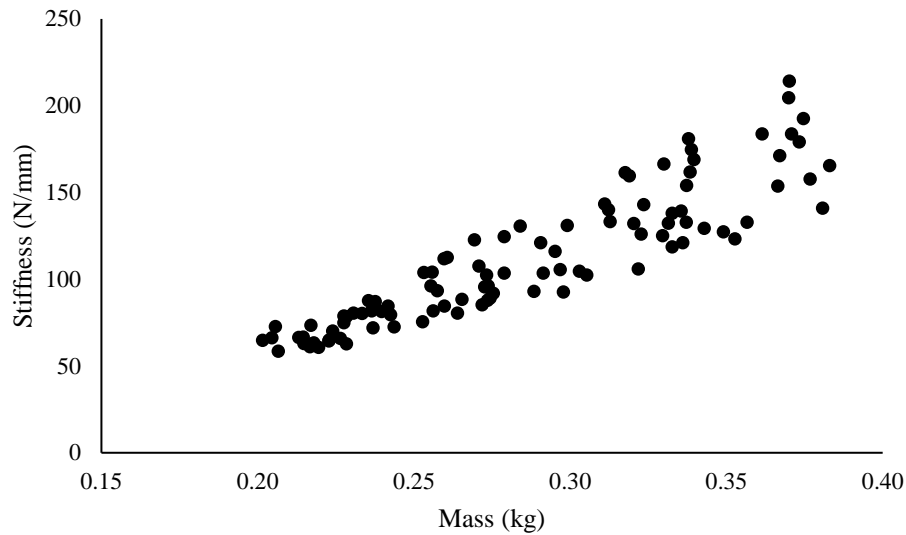


Figure A4. Mass and Stiffness responses for all viable designs for the ROPO-SW parametric analysis.

Table A12. Percent change of responses for all viable designs from the ROPO-SW parametric analysis.

	Percent Change in Response Among Viable Designs			
Faceguard	Structural Stiffness	Mass	CVF-O	PVF-O
ROPO-SW	73%	47%	87%	29%

Appendix E

Schutt F7 ROPO-SW-NB-VC Results

Original Manufacturer's Design

Table A10. List of initial parameter values for the reverse engineered ROPO-SW-NB-VC.

Solidworks Parameter	ModeFrontier Parameters	Value	Description
ANS_D1	D1	38.80406 mm	Nose Visibility (Translation of Nose Bar)
ANS_D2	D2	90.00°	Nose Visibility (Rotation of Nose Bar)
ANS_D3	D3	99.63104251mm	Nose Protection
ANS_D4	D4	43.74764864mm	Cheek Bone Protection
ANS_D5	D5	10.70985656mm	Nose Sharpness Index
ANS_D6	D3	43.74764864mm	Upper Mouth Protection
ANS_D7	D7	26.78173242mm	Lower Mouth Protection
ANS_D8	D8	90.00°	Left Side Vertical Bar Angle
ANS_D9	D8	90.00°	Right Side Vertical Bar Angle
ANS_D10	D10	39.68805915mm	Left Side Vertical Bar Apex Length
ANS_D11	D11	3.29036374mm	Left Side Vertical Bar Apex Height
ANS_D12	D10	39.68805915mm	Right Side Vertical Bar Apex Length
ANS_D13	D11	3.29036374mm	Right Side Vertical Bar Apex Height
ANS_Dia1-4	DiaL	5.55625mm	Large Diameter Parameter
ANS_Dia5-9	DiaS	4.7625 mm	Small Diameter Parameter

Table A11. Responses for the reverse engineered ROPO-SW-NB-VC model.

	Original Manufacturer's Design Response Results			
Faceguard	Mass (kg)	Stiffness (N/mm)	CVF-O	PVF-O
ROPO-SW-NB-VC	0.341	124	174	4766

Results from Parametric Analysis

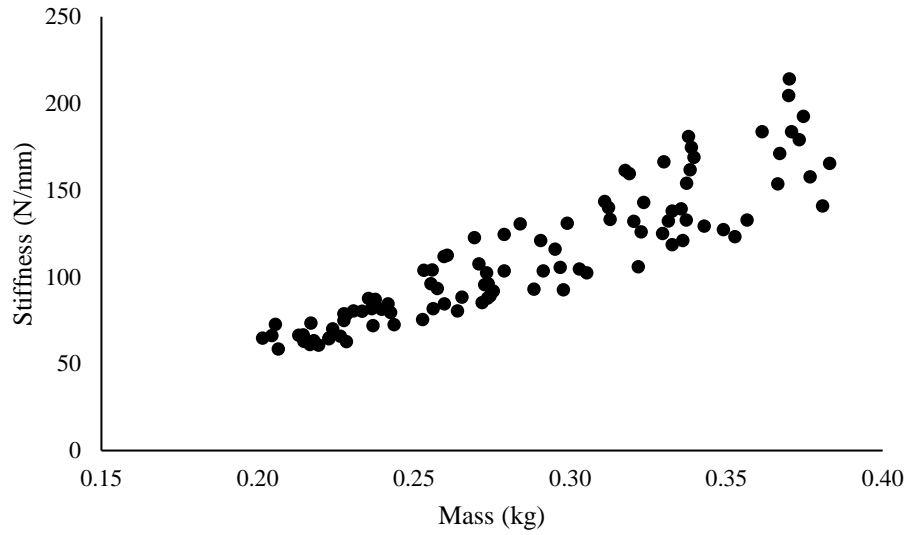


Figure A4. Mass and Stiffness responses for all viable designs for the ROPO-SW-NB-VC parametric analysis.

Table A12. Percent change of responses for all viable designs from the ROPO-SW-NB-VC parametric analysis.

	Percent Change in Response Among Viable Designs			
Faceguard	Structural Stiffness	Mass	CVF-O	PVF-O
ROPO-SW-NB-VC	96%	55%	91%	45%

Appendix F

Schutt F7 ROPO-NB-VC Results

Original Manufacturer's Design

Table A10. List of initial parameter values for the reverse engineered ROPO-NB-VC.

Solidworks Parameter	ModeFrontier Parameters	Value	Description
ANS_D1	D1	44.93791mm	Nose Visibility (Translation of Nose Bar)
ANS_D2	D2	90.00°	Nose Visibility (Rotation of Nose Bar)
ANS_D3	D3	99.28586188mm	Nose Protection
ANS_D4	D4	44.95483886mm	Cheek Bone Protection
ANS_D5	D5	8.72928834mm	Nose Sharpness Index
ANS_D6	D4	44.95483886mm	Upper Mouth Protection
ANS_D7	D7	30.49094474mm	Lower Mouth Protection
ANS_D8	D8	90.00°	Left Side Vertical Bar Angle
ANS_D9	D8	90.00°	Right Side Vertical Bar Angle
ANS_D10	D10	27.61301742mm	Left Side Vertical Bar Apex Length
ANS_D11	D11	4.25048583mm	Left Side Vertical Bar Apex Height
ANS_D12	D10	27.61301742mm	Right Side Vertical Bar Apex Length
ANS_D13	D11	4.25048583mm	Right Side Vertical Bar Apex Height
ANS_D14	N/A	N/A	Mid Vertical Bar Apex Length
ANS_D15	N/A	N/A	Mid Vertical Bar Apex Height
ANS_D16	D16	18.97799955mm	Secondary Horizontal Bar Offset Distance
ANS_D17	D17	90.00°	Secondary Horizontal Bar Offset Angle
ANS_Dia1-5	DiaL	5.55625mm	Large Diameter Parameter
ANS_Dia6-10	DiaS	4.7625mm	Small Diameter Parameter

Table A11. Responses for the reverse engineered ROPO-NB-VC model.

	Original Manufacturer's Design Response Results			
Faceguard	Mass (kg)	Stiffness (N/mm)	CVF-O	PVF-O
ROPO -NB-VC	0.396	133		

Results from Parametric Analysis

Figure A4. Mass and Stiffness responses for all viable designs for the ROPO-NB-VC parametric analysis.

Table A12. Percent change of responses for all viable designs from the ROPO-NB-VC parametric analysis.

	Percent Change in Response Among Viable Designs			
Faceguard	Structural Stiffness	Mass	CVF-O	PVF-O
ROPO-SW-NB-VC				

Appendix G

Vicis Zero1 SO-212-LP Results

Original Manufacturer's Design

Table A10. List of initial parameter values for the reverse engineered SO-212-LP.

Solidworks Parameter	ModeFrontier Parameters	Value	Description
ANS_D1	D1	40.73844mm	Nose Visibility (Translation of Nose Bar)
ANS_D2	D2	90.00°	Nose Visibility (Rotation of Nose Bar)
ANS_D3	D3	85.50443741mm	Nose Protection
ANS_D4	D4	47.19678526mm	Cheek Bone Protection
ANS_D5	D5	15.44005207mm	Nose Sharpness Index
ANS_D6	D4	47.19678526mm	Upper Mouth Protection
ANS_D7	D7	36.51900571mm	Lower Mouth Protection
ANS_D8	D8	90.00°	Left Side Vertical Bar Angle
ANS_D9	D8	90.00°	Right Side Vertical Bar Angle
ANS_D10	D10	40.78771751mm	Left Side Vertical Bar Apex Length
ANS_D11	D11	6.0755859mm	Left Side Vertical Bar Apex Height
ANS_D12	D10	40.78771751mm	Right Side Vertical Bar Apex Length
ANS_D13	D11	6.0755859mm	Right Side Vertical Bar Apex Height
ANS_Dia1-3	DiaL	4.7625mm	Large Diameter Parameter
ANS_Dia4-7	DiaS	3.69mm	Small Diameter Parameter

Table A11. Responses for the reverse engineered SO-212-LP model.

	Original Manufacturer's Design Response Results			
Faceguard	Mass (kg)	Stiffness (N/mm)	CVF-O	PVF-O
SO-212-LP	0.296	70	161	4070

Results from Parametric Analysis

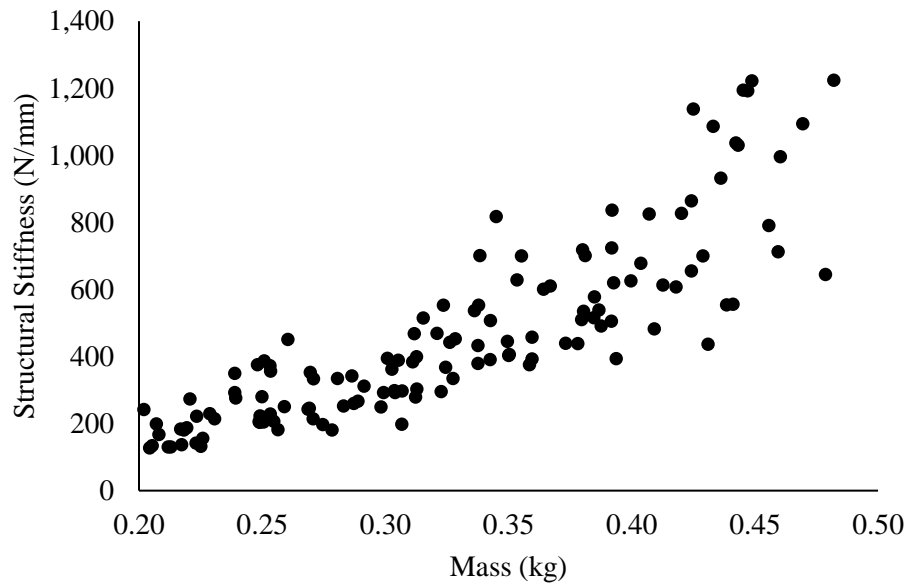


Figure A4. Mass and Stiffness responses for all viable designs for the SO-212-LP parametric analysis.

Table A12. Percent change of responses for all viable designs from the SO-212-LP parametric analysis.

	Percent Change in Response Among Viable Designs			
Faceguard	Structural Stiffness	Mass	CVF-O	PVF-O
ROPO-SW-NB-VC	90%	61%	86%	40%

Appendix H

Vicis Zero1 SO-213-E-LP Results

Original Manufacturer's Design

Table A10. List of initial parameter values for the reverse engineered SO-213-E-LP.

Solidworks Parameter	ModeFrontier Parameters	Value	Description
ANS_D1	D1	41.28047mm	Nose Visibility (Translation of Nose Bar)
ANS_D2	D2	90.00°	Nose Visibility (Rotation of Nose Bar)
ANS_D3	D3	86.64993935mm	Nose Protection
ANS_D4	D4	48.77464734mm	Cheek Bone Protection
ANS_D5	D5	17.18061091mm	Nose Sharpness Index
ANS_D6	D4	48.77464734mm	Upper Mouth Protection
ANS_D7	D7	39.24725482mm	Lower Mouth Protection
ANS_D8	D8	90.00°	Left Side Vertical Bar Angle
ANS_D9	D8	90.00°	Right Side Vertical Bar Angle
ANS_D10	D10	39.23600265mm	Left Side Vertical Bar Apex Length
ANS_D11	D11	4.46560302mm	Left Side Vertical Bar Apex Height
ANS_D12	D10	39.23600265mm	Right Side Vertical Bar Apex Length
ANS_D13	D11	4.46560302mm	Right Side Vertical Bar Apex Height
ANS_D14	D14	40.99271438mm	Middle Vertical Bar Apex Length
ANS_D15	D15	6.97441553mm	Middle Vertical Bar Apex Length
ANS_D16	D16	77.22936924mm	Lower Eye Protection
ANS_D17	D17	72.89241544mm	Upper Eye Protection
ANS_Dia1-3	DiaL	4.7625mm	Large Diameter Parameter
ANS_Dia4-10	DiaS	3.69mm	Small Diameter Parameter

Table A11. Responses for the reverse engineered SO-213-E-LP model.

	Original Manufacturer's Design Response Results			
Faceguard	Mass (kg)	Stiffness (N/mm)	CVF-O	PVF-O
SO-213-E-LP	0.303	73	159	4751

Results from Parametric Analysis

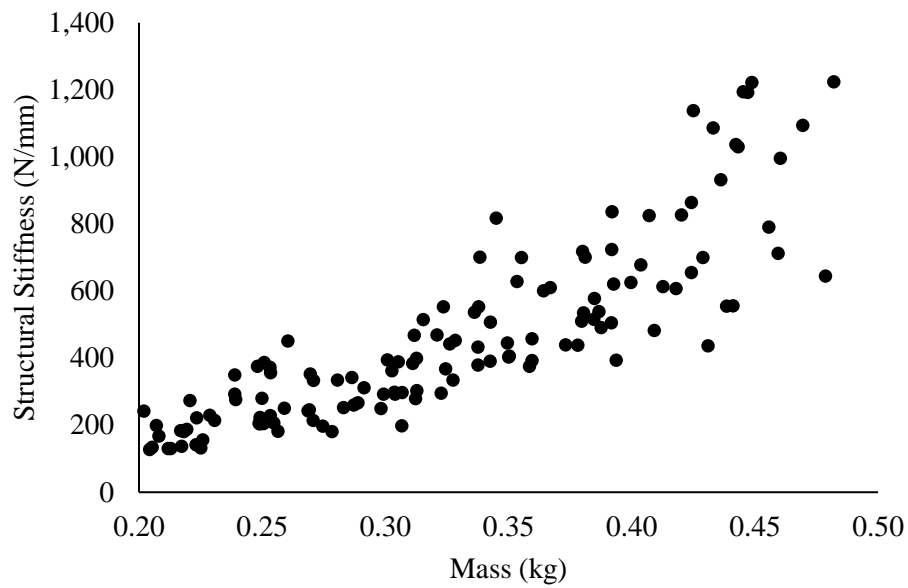


Figure A4. Mass and Stiffness responses for all viable designs for the SO-213-E-LP parametric analysis.

Table A12. Percent change of responses for all viable designs from the SO-213-E-LP parametric analysis.

	Percent Change in Response Among Viable Designs			
Faceguard	Structural Stiffness	Mass	CVF-O	PVF-O
SO-213-E-LP	91%	60%	95%	40%

Appendix I

Vicis Zero1 SO-223-LP Results

Original Manufacturer's Design

Table A10. List of initial parameter values for the reverse engineered SO-223-LP.

Solidworks Parameter	ModeFrontier Parameters	Value	Description
ANS_D1	D1	45.47278mm	Nose Visibility (Translation of Nose Bar)
ANS_D2	D2	90.00°	Nose Visibility (Rotation of Nose Bar)
ANS_D3	D3	86.70176341mm	Nose Protection
ANS_D4	D4	49.69328721mm	Cheek Bone Protection
ANS_D5	D5	16.21084781mm	Nose Sharpness Index
ANS_D6	D4	49.69328721mm	Upper Mouth Protection
ANS_D7	D7	38.44452571mm	Lower Mouth Protection
ANS_D8	D8	90.00°	Left Side Vertical Bar Angle
ANS_D9	D8	90.00°	Right Side Vertical Bar Angle
ANS_D10	D10	29.32373644mm	Left Side Vertical Bar Apex Length
ANS_D11	D11	4.12356245mm	Left Side Vertical Bar Apex Height
ANS_D12	D10	29.32373644mm	Right Side Vertical Bar Apex Length
ANS_D13	D11	4.12356245mm	Right Side Vertical Bar Apex Height
ANS_D14	D14	31.55406077mm	Mid Vertical Bar Apex Length
ANS_D15	D15	4.52755749mm	Mid Vertical Bar Apex Height
ANS_D16	D16	13.51064307mm	Secondary Horizontal Bar Offset Distance
ANS_D17	D17	90.00°	Secondary Horizontal Bar Offset Angle
ANS_Dia1-4	DiaL	4.7625mm	Large Diameter Parameter
ANS_Dia5-9	DiaS	3.69mm	Small Diameter Parameter

Table A11. Responses for the reverse engineered SO-223-LP model.

	Original Manufacturer's Design Response Results			
Faceguard	Mass (kg)	Stiffness (N/mm)	CVF-O	PVF-O
SO-223-LP	0.323	77	107	5013

Results from Parametric Analysis

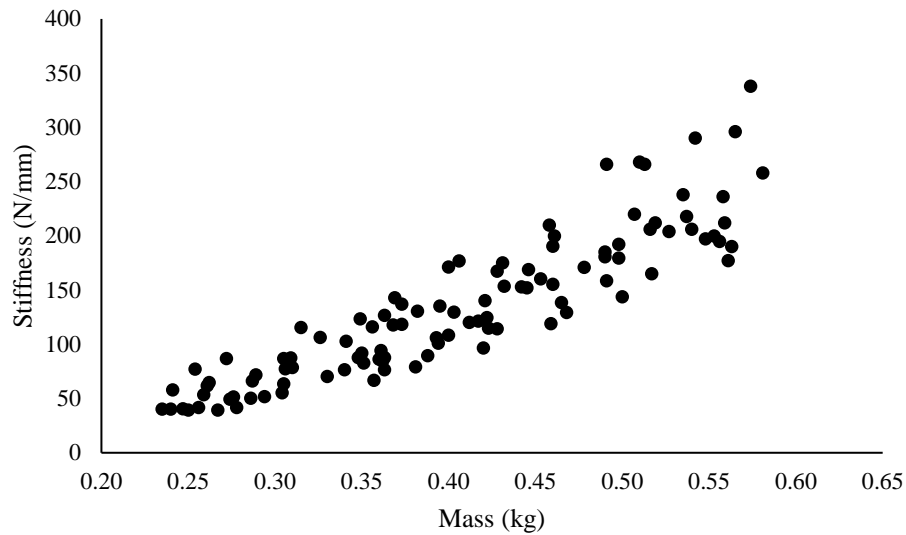


Figure A4. Mass and Stiffness responses for all viable designs for the SO-223-LP parametric analysis.

Table A12. Percent change of responses for all viable designs from the SO-223-LP parametric analysis.

	Percent Change in Response Among Viable Designs			
Faceguard	Structural Stiffness	Mass	CVF-O	PVF-O
SO-223-LP	88%	60%	76%	41%

Appendix I

Visibility Calculations Documentation

Central Visual Field—Occlusion Metric

Quantifies obstructions to the central visual field caused by the faceguard but omitting obstructions of the helmet-compatible frame

This was done to analyze the faceguard within the design space which does not include the outer frame since the helmet-compatible frame changes with each helmet.

Process:

Using image analysis, approximate location of eyes with respect to the frame of the faceguard. This is performed once per helmet.

Place the location of the eyes on the reverse engineered Solidworks part file of each faceguard. This should be placed on the median plane. Considering the parametric method includes mirroring the side that is structurally most similar to the experimental (i.e. the computational stiffness of each side was analyzed and then compared to the experimental; the side with the computational stiffness closest to experimental stiffness was considered to be the most accurate computational model), the point will be placed in the middle of the sides of the frame and/or on the same plane as a central vertical bar.

Create a plane at the arc apex parallel to Plane 7 (used for attachment location of horizontal bar and frame)

Draw a line perpendicular from new plane to center of eyes point and draw a circle. This line should be D3 plus some.

Measure the distance of this line as a function of D3 (i.e. D3+12)

Draw lines that represent opposite sides of circle and make them 60 degrees apart. That will define the diameter of the CVF circle.

Draw a line from the center of circle to bottom of circle. Should be perpendicular to planes, etc to make sure it is vertical.

This distance is the radius of the circle. It should be slightly less than from where D1 is measured. Measure this distance to D1's reference (i.e. if the offset is 2mm, then a D1=2mm would have the arc tangent to the circle)

$$CVF - O = \theta_H * \theta_V \quad (A1)$$

Where:

$$\theta_H = 2 * \alpha \quad (A2)$$

$$\theta_V = \tan^{-1} \frac{DiaL}{D3 + Offset \ D3} \quad (A3)$$

$$\alpha = \tan^{-1} \frac{x}{\sqrt{y^2 + (D3 + Offset \ D3)^2}} \quad (A4)$$

$$x = \sqrt{r^2 - y^2} \quad (A5)$$

$$y = Offset \ D1 - D1 - D3 * \sin(90^\circ - D2) \quad (A6)$$

$$r = (D3 + Offset \ D3) * \tan(30^\circ) \quad (A7)$$

DiaL is the large diameter parameter

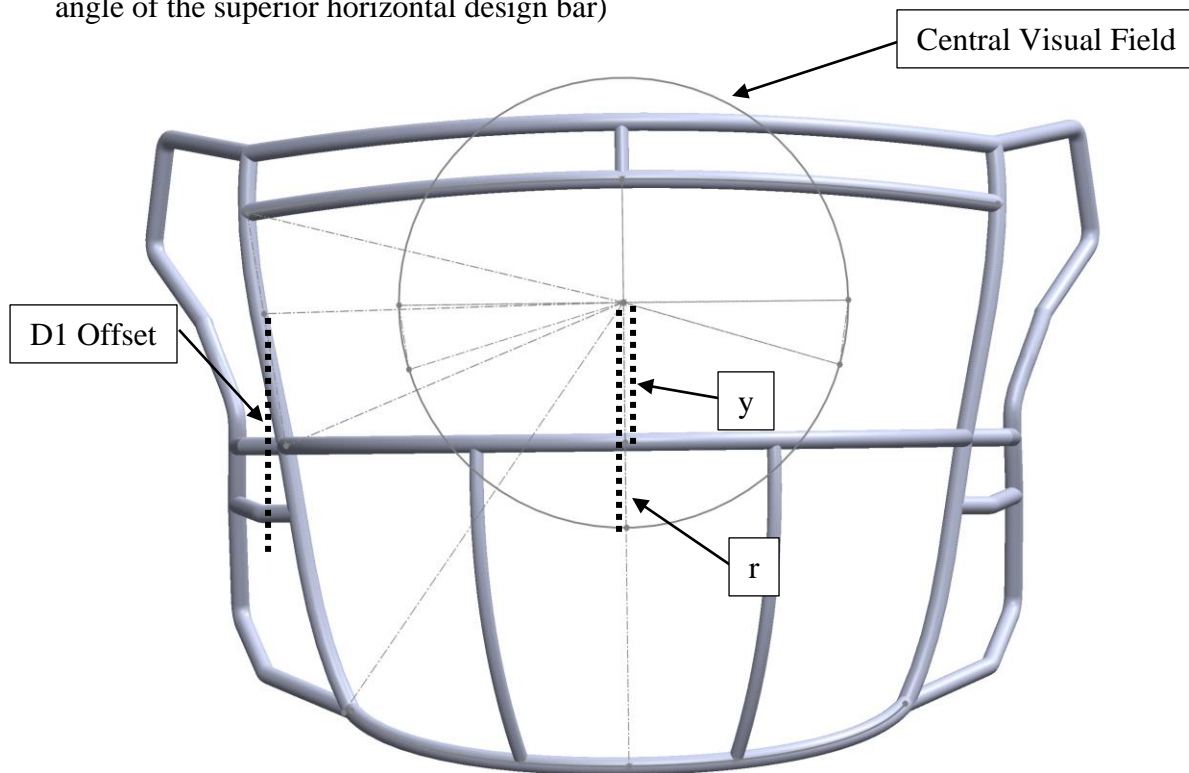
D3 is the distance from a point centered between the attachment locations of the superior horizontal design bar to the apex of the superior horizontal design bar

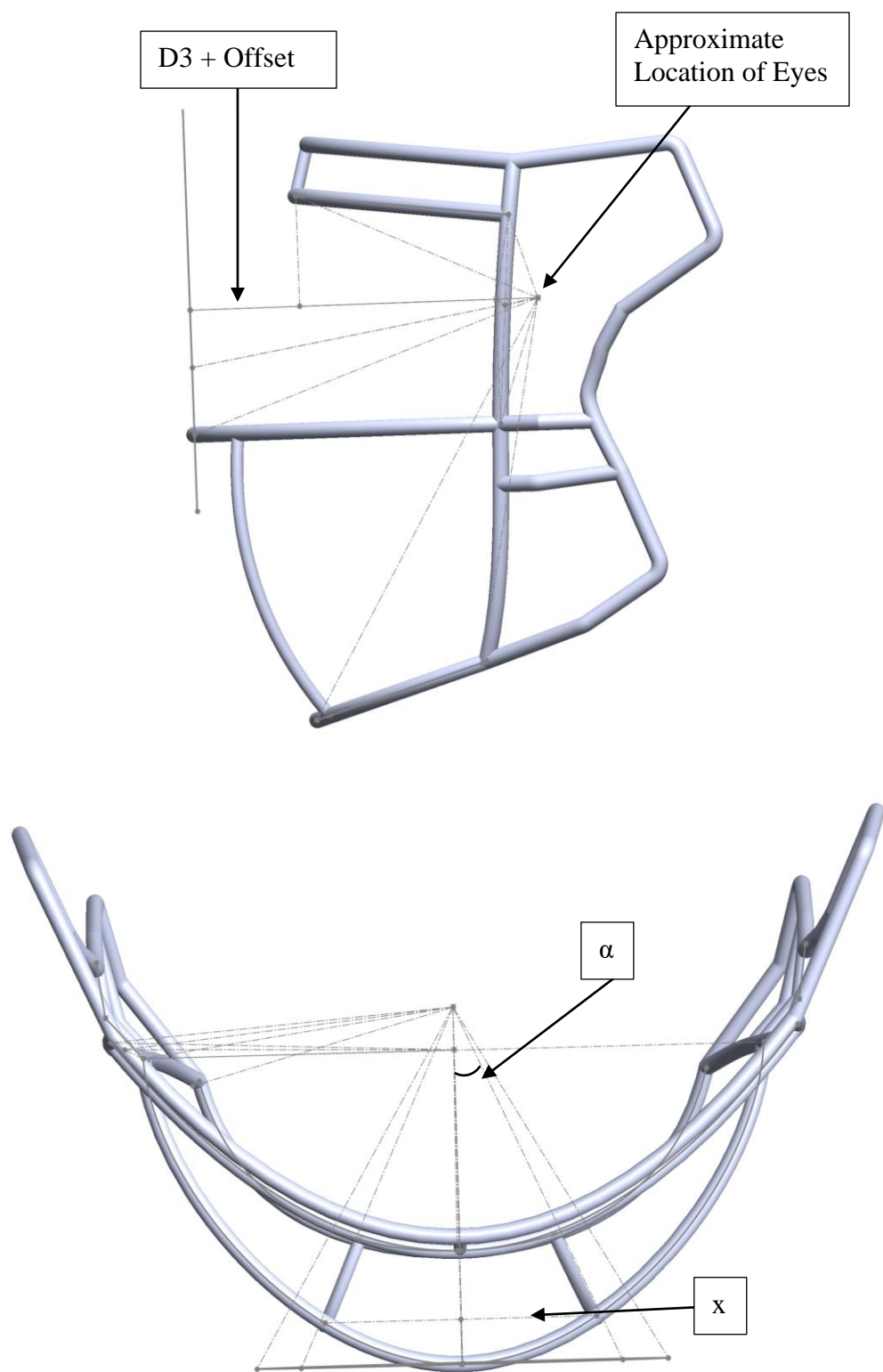
Offset D3 is a constant value for each individual faceguard that measures the horizontal distance from the approximate location of the eyes to the point centered between the attachment locations of the superior horizontal design bar (i.e. the reference location from which D3 is measured)

Offset D1 is the vertical distance measured from the approximate location of the eyes to the reference location from which D1 is measured

D1 is the vertical distance from a reference location (Offset D1) where the superior horizontal design bar attaches to the outer frame

D2 is the angle of the superior horizontal design bar measured with respect to the original manufacturer's angle (i.e. $D2 = 90^\circ$ is the reverse-engineered original manufacturer's angle of the superior horizontal design bar)





Peripheral Visual Field—Occlusion Metric

Quantifies obstructions to the peripheral visual field caused by the faceguard but omitting obstructions of the helmet-compatible frame

This was done to analyze the faceguard within the design space which does not include the outer frame since the helmet-compatible frame changes with each helmet.

Assumptions:

The peripheral visual field is limited to 180° laterally. This is incorrect because the location of the eyes may be anterior or posterior to the outer frames; however, this is dependent upon the helmet. This design parameter is a function of helmet and faceguard frame so it was not considered in this study.

The peripheral visual field, intending to calculate independently from the central visual field, is only considering the occlusions to the peripheral visual field due to the superior horizontal bar and categorical variables such as eye guards outside of the central visual field. To do this, only the portion of the design area from 0°-60° and 120°-180° will be considered occlusions to the peripheral visual field. This assumption is justified by calculating for independent responses.

Process:

$$PVF - O = (180^\circ - 60^\circ) * \beta + \theta_1 * \gamma \quad (A8)$$

Where:

$$\beta = \left(\frac{\text{Max Far Peripheral Visual Field} + \text{Max Peripheral Visual Field}}{2} \right) - \left(\text{Max Upper Far Peripheral Visual Field} + \tan^{-1} \left(\frac{\text{Offset D1} - D1 - \frac{\text{Dial}}{2}}{\text{Offset Lateral}} \right) \right) \quad (\text{A9})$$

$$\theta_1 = \tan^{-1} \left(\frac{\text{Dial}}{\text{Offset Lateral}} \right) \quad (\text{A10})$$

$$\gamma = \tan^{-1} \left(\frac{\text{length of eye guard}}{D3} \right) * 2 \quad (\text{A11})$$

$$\text{length of eye guard} = \sqrt{(D17 - D16)^2 + (\text{Offset D1} + \text{Vertical Eye Location} - D1)^2} \quad (\text{A12})$$

The max far peripheral visual field is the angle between the upper and lower limits of the design space at the lateral most point of the design space (at 0° and 180°) as measured with respect to the approximate location of the eyes. This value does not change for each faceguard model because it is measuring the limits of the design space—which is defined by the outer frame.

The max peripheral visual field is the angle between the upper and lower limits of the design space on the median plane as measured with respect to the approximate location of the eyes. This value does not change for each faceguard model because it is defined by the outer frame.

The lateral offset measures the distance from the approximate location of the eyes (median plane) to the attachment location of the superior horizontal design bar and frame. This distance is measured laterally from the median plane.

Eq. 12 calculates the length of the eye guard section which is measured as the square root of the approximate horizontal distance difference between the upper and lower attachment location squared plus the vertical distance in the periphery between the upper attachment location and the lower attachment location squared. This assumes the location of the lower attachment will not be affected by D2 (angle of the primary horizontal design bar). This is known to be false; however, the approximation is close.

Eq. 11 measures the angle from the approximate location of the eye of the vertical obstruction to the peripheral visual field by the eye guard multiplied by two eye guards on either side of the faceguard.

Eq. 10 measures the horizontal obstruction due to the diameter of the eye guard.

Therefore, the second term in Eq. 8 quantifies the obstruction of an eye guard. In this project, the only faceguard with eye guards was the Vicis Zero 1 SO-213-E-LP faceguard.

Eq. 9 averages the maximum possible peripheral and far peripheral visual fields which is constant for each frame. This value represents the maximum possible occlusion; therefore, any terms subtracted from this value should be greater for less occlusions and lesser for more occlusions. Since the PVF-O metric calculates occlusions to the visual field, a larger β will increase the amount of occlusion to the peripheral visual field. The second term in Eq. 9 subtracts the visible space above the superior horizontal design bar from the maximum occlusion term such that the remainder quantifies the maximum amount of occlusion minus the amount that is not occluded.

The average of the max peripheral and far peripheral visual fields was justified by the approximate linearity of these bars. Although the differences between the maximum visual field extending radially from the outer frame at any one point is not linear, this approximation aids in simplifying the quantification of the differences between the maximum possible visibility (or obstruction) that is possible. This quantification is the only term in the visibility calculations intended to bias for the design of the frames. Since multiple errors could exacerbate this bias (i.e. image analysis for location of eyes), using this measurement only once was important. Despite this, the location of the eyes was varied to see how sensitive the metric was to the location. Since the angle does not change substantively with large changes in the approximate location of the eyes, the bias is minimal and considered negligible.